Conversion of real-world Plastic Waste into Fuel Grade Hydrocarbon by Pyrolysis: Thermal and Catalytic route

Doctoral Thesis

by **Subhashini**(2018chz0004)



DEPARTMENT OF CHEMICAL ENGINEERING INDIAN INSTITUTE OF TECHNOLOGY ROPAR

August, 2024

Conversion of real-world Plastic Waste into Fuel Grade Hydrocarbon by Pyrolysis: Thermal and Catalytic route

A Thesis Submitted
In Partial Fulfillment of the
Requirements for the Degree of

DOCTOR OF PHILOSOPHY

by

Subhashini (2018chz0004)



DEPARTMENT OF CHEMICAL ENGINEERING INDIAN INSTITUTE OF TECHNOLOGY ROPAR

August, 2024

| Subhashini: Conversion of real-world Plastic Waste into Fuel Grade Hydrocarbon by Pyrolysis: Thermal and Catalytic route |
|--|
| Copyright © 2024, Indian Institute of Technology Ropar |
| All Rights Reserved |
| |
| |

DEDICATED TO FAMILY & FRIENDS

Declaration of Originality

I hereby declare that the work which is being presented in the thesis entitled 'Conversion of real-world Plastic Waste into Fuel Grade Hydrocarbon by Pyrolysis: Thermal and Catalytic route' has been solely authored by me. It presents the result of my own independent investigation/research conducted during the period from July 2018 to June 2024 under the supervision of Dr. Tarak Mondal, Assistant Professor at Indian Institute of Technology Ropar. To the best of my knowledge, it is an original work, both in terms of research content and narrative, and has not been submitted or accepted elsewhere, in part or in full, for the award of any degree, diploma, fellowship, associateship, or similar title of any university or institution. Further, due credit has been attributed to the relevant state-of-the-art and collaborations (if any) with appropriate citations and acknowledgments, in line with established ethical norms and practices. I also declare that any idea/data/fact/source stated in my thesis has not been fabricated/ falsified/ misrepresented. All the principles of academic honesty and integrity have been followed. I fully understand that if the thesis is found to be unoriginal, fabricated, or plagiarized, the Institute reserves the right to withdraw the thesis from its archive and revoke the associated Degree conferred. Additionally, the Institute also reserves the right to appraise all concerned sections of society of the matter for their information and necessary action(if any). If accepted, I hereby consent for my thesis to be available online in the Institute's Open Accessrepository, inter-library loan, and the title & abstract to be made available to outside organizations.

Signature:

Name: Subhashini

Entry Number: 2018CHZ0004

Program: Ph.D.

Department: Chemical Engineering

Indian Institute of Technology

RoparRupnagar, Punjab 140001

Date: 02/08/2024

Acknowledgments

I would like to express my sincere gratitude towards my supervisor Dr. Tarak Mondal for excellent guidance, support and believe towards me in every stage of my research work. His motivation to persevere through the challenges of research has been instrumental in my growth as an independent researcher.

I am also grateful to Doctoral committee members, Dr. Asad H Sahir, Dr. Arghya Banerjee, Dr. Durba Pal, and chairperson Dr. Vishwajeet Mehandia for providing their feedback, insightful suggestions, and assisting throughout the journey. I wish to convey my sincere thanks to Dr. Swati A. Patel and Dr. Himanshu Paliwal for fruitful academic and non-academic discussions, suggestions, and motivation. I am also thankful to all faculty and staff members of Chemical Engineering department for their constant support during my tenure.

I would like to thank the department office staff, Mrs. Sunpreet Kaur for her assistance. I also thank my research group members, colleagues, and friends (Dr. Pawan Chauhan, Neha Baranwal, Kumari Neha, Deepali Jha, Tanvi Shah, and Praveen) for their support.

My deepest gratitude, appreciation, and love to my parents (Mr. Jitendra Kumar Amit and Mrs. Munni), husband (Mr. Sai Sundara Madhava Prasad), sister (Payal Malik) and parents-in-law for their unconditional support, attachment, understanding, and warmth towards me. Without their encouragement, this endeavor would not have been possible. My most special and most important of all – my pet, Bhooru had been the pillar of my strength and showered me with its unconditional love in the most challenging situations.

Finally, I sincerely thank all those, who have helped me directly or indirectly at different stages of my research work.

Subhashini

Certificate

This is to certify that the thesis entitled 'Conversion of real-world Plastic Waste into Fuel

Grade Hydrocarbon by Pyrolysis: Thermal and Catalytic route,' submitted by

Subhashini (2018CHZ0004) for the award of the degree of Doctor of Philosophy of Indian

Institute of Technology Ropar, is a record of bonafide research work carried out under my

guidance and supervision. To the best of my knowledge and belief, the work presented in this

thesis is original and has not been submitted, either in part or full, for the award of any other

degree, diploma, fellowship, associateship or similar title of any university or institution.

In my opinion, the thesis has reached the standard fulfilling the requirements of the

regulations relating to the Degree.

Signature of the Supervisor

Name: Dr. Tarak Mondal

Department: Chemical Engineering

Indian Institute of Technology Ropar

Rupnagar, Punjab 140001

Date: 02/08/2024

Lay Summary

Billion tons of plastic waste has been a crucial and sweeping root to environmental hazard as well as human health. Since, plastics are non-biodegradable, these take thousands and thousands of years to break down and until then keeps damaging the soil, poisoning the groundwater, chokes the marine wildlife and cause serious health impacts like developmental, reproductive, neurological, and immune disorders due to carcinogenic chemicals present in them. Consequently, an efficient and cost-effective plastic waste management technique is the need of the hour. Pyrolysis of plastic waste is the most suitable solution that comes to the rescue. Plastics are petro derived materials with high hydrocarbon resource able to generate H₂-enriched syngas, higher quality fuel grade oil, chemicals, and high-value carbon materials. Hence, thermal, and catalytic pyrolysis of plastic waste performed under optimum parameter conditions, provides an alternative and sustainable route to convert them into rich fuel grade hydrocarbon liquid oil. In this manner, pyrolysis technique successfully converts the plastic waste into energy and aids in meeting the global energy requirement.

In the present work, thermal and catalytic pyrolysis technique is used to convert the real-world plastic waste into aromatic rich fuel grade hydrocarbon liquid oil in a fixed-bed reactor set-up. The liquid oil obtained were characterized by various scientific techniques such as; FT-IR, GCMS, ¹H NMR, bomb calorimeter, and parallel-plate rheometer to obtain various chemical and fuel properties. It was found evident that the catalytic pyrolysis process outdoes the thermal pyrolysis of real-world plastic waste to provide enhanced selectivity and yield of the desired liquid oil.

Abstract

With ever-increasing plastic waste, a robust and sustainable methodology to valorize the waste and modification of the composition of the value-added product is the need of the hour. The present study describes the effect of thermal and heterogeneous catalytic pyrolysis system on the yield, composition and the nature of the pyrolytic oil produced from various real-world plastic wastes like high-density polyethylene (HDPE), low-density polyethylene (LDPE), polypropylene (PP), and polystyrene (PS). These wastes were subjected to thermal as well as catalytic pyrolysis. Liquid, gas, and solid products were obtained during the pyrolysis. Pyrolysis liquid products were analyzed using gas chromatography- mass spectroscopy (GC-MS), nuclear magnetic resonance (NMR), Fouriertransform infrared spectroscopy (FT-IR), parallel plate rheometer and bomb calorimeter. In thermal pyrolysis the reaction temperature range of 450 – 480 °C favored the liquid oil yield. Compared with other wastes, PS waste produced the maximum liquid oil yield of 52%. Furthermore, kinetic study was carried out to understand the kinetic triplets i.e., activation energy (E_{α}) , frequency factor (A_0) and reaction mechanism ($f(\alpha)$) of complex thermal pyrolysis process of plastic waste. A combined strategy of employing model-free (OFW, KAS, Starink, Tang and Boswell) isoconversional methods and model-fitting (Criado and Coats-Redfern) methods was used to study kinetics of thermal pyrolysis process.

Hierarchical ZSM-5 (zeolite) catalyst was synthesized by hydrothermal method using organic template for inducing the mesoporous framework network and was used in catalytic pyrolysis in a fixed bed tubular reactor. A wide array of techniques such as XRD, BET, FE-SEM and FT-IR were used to analyze the material properties of the synthesized catalysts. The results of these analyses verified the successful formation of the mesoporous ZSM-5 framework with high surface area (approx. 295 m²/g). Usage of catalyst has reduced the temperature of the pyrolysis reaction from 450 to 420 °C with better product yield. In catalytic pyrolysis also, PS waste generated higher liquid yield as compared to PP, HDPE, and LDPE waste. The highest liquid yield of 63% was achieved with PS waste. However, 59%, 54%, and 45% yield of liquid oil were obtained from LDPE, HDPE, and PP wastes. The obtained liquid products consist of paraffin, naphthalene, olefin, and aromatic components. It was observed that the viscosity of the obtained liquid oil was in good relevance with that of the commercial grade diesel and kerosene oil. Also, the HHV values of the obtained liquid oils were as good as that of the petro fuels.

Keywords: Real-world plastic waste; Chemical recycling; Thermal pyrolysis; Kinetic study; Hierarchical ZSM-5 zeolite; Catalytic pyrolysis; Waste management.

TABLE OF CONTENTS

| CHAPTER 1: INTRODUCTION | 1 |
|--|------|
| 1.1. Background | 1 |
| 1.2. Plastic | 2 |
| 1.2.1. Types of plastic | 3 |
| 1.2.2. Plastic and plastic waste generation | 4 |
| 1.2.3. Plastic waste management techniques: | 6 |
| 1.2.3.1 Pyrolysis process | 6 |
| 1.2.3.2 Catalytic pyrolysis | 7 |
| 1.2.3.3 Various factors affecting pyrolysis proces | ss8 |
| 1.2.3.4 Kinetic modelling of pyrolysis process | 10 |
| 1.3. Motivation and thesis content | 11 |
| 1.3.1. Objectives of the research work | 11 |
| 1.3.2. Thesis outline | 11 |
| 1.4. References | 14 |
| CHAPTER 2: LITERATURE REVIEW | 16 |
| 2.1. Introduction | 16 |
| 2.2. Thermal pyrolysis of plastic waste | 16 |
| 2.3. Kinetic study of thermal pyrolysis of plastic | 18 |
| 2.4. Catalytic pyrolysis of plastic waste | |
| 2.5. References | 22 |
| CHAPTER 3: MATERIALS AND METHODOLOG | GY29 |
| 3.1. Introduction | 29 |

| 3.2. | Preparation of raw material | 29 |
|--------|---|----|
| 3.2 | 2.1 Feedstock used | 29 |
| 3.2 | 2.2 Procedure of raw material preparation | 29 |
| 3.3 | Synthesis of catalyst | 30 |
| 3.3 | 3.1 Materials used | |
| | 3.2 Preparation of catalyst | |
| 3.4 | Various analytical characterization techniques used | 31 |
| 3.4 | 4.1 Fourier transform infrared spectroscopy (FTIR) | 32 |
| 3.4 | 4.2 BET- surface area | 33 |
| 3.4 | 1.3 Thermogravimetric analysis (TGA) | 33 |
| 3.4 | 1.4 X-ray diffraction (XRD) | 33 |
| 3.4 | 4.5 Scanning electron microscopy (SEM) | 34 |
| 3.4 | 4.6 RAMAN spectroscopy | 34 |
| 3.4 | 1.7 Nuclear magnetic resonance spectroscopy (NMR) | 35 |
| 3.4 | 4.8 Gas chromatography mass spectroscopy (GC-MS) | 35 |
| 3.5 | Experimental set-up for thermal pyrolysis process | 36 |
| 3.6.1 | | 38 |
| 3.7 | Theoretical considerations for kinetic study of thermal pyrolysis | 39 |
| 3.7 | 7.1 Evaluation of kinetic parameters by isoconversional or model-free methods | 41 |
| 3 | 3.7.1.1 Ozawa-Flynn-Wall (OFW) method | 41 |
| 3 | 3.7.1.2 Kissinger-Akahira- Sunose (KAS) method | 42 |
| 3 | 3.7.1.3 Starink method | 42 |
| 3 | 3.7.1.4 Tang method | 42 |
| 3 | 3.7.1.5 Boswell method | 42 |
| 3.7 | 7.2 Prediction of decomposition model | 43 |
| 3.8 | References | 45 |
| СНА | APTER 4: THERMAL PYROLYSIS OF REAL-WORLD PLASTIC WASTE | 47 |
| 4.1 Iı | ntroductionntroduction | 47 |

| 4.2 I | Results and discussion | 47 |
|--|--|--------------------|
| 4.2 | 2.1 Raw material characterizations | 47 |
| | 4.2.1.1 Proximate and Ultimate analysis of the raw material | 48 |
| | 4.2.1.2 FT-IR | 49 |
| | 4.2.1.3 Thermogravimetric analysis | 51 |
| 4. | 2.2 Distribution of pyrolysis products | 58 |
| | 4.2.2.1 Product yield | 58 |
| 4.2 | 2.3 Liquid oil characterizations | 60 |
| | 4.2.3.1 Viscosity and HHV | 60 |
| | 4.2.3.2 FT-IR | 61 |
| | 4.2.3.3 GC-MS | 62 |
| | 4.2.3.4 ¹ H NMR | 65 |
| 4.3 (| Conclusion: | 66 |
| 4.4 I | Reference | 68 |
| | | |
| | APTER 5: KINETIC STUDY OF THERMAL PYROLYSIS OF REAL-WORLD | |
| | APTER 5: KINETIC STUDY OF THERMAL PYROLYSIS OF REAL-WORLD STE | |
| | | 71 |
| WA | STE | 71 71 |
| WA: 5.1 5.2 | STE | 71 71 71 |
| WA 5 5.1 5.2 5.3 | Introduction | 71717171 |
| WA 3 5.1 5.2 5.3 5.3 | Introduction Results and discussions 2.1 Feedstock characteristics | 7171717171 |
| 5.1 5.2 5.3 5.3 5.3 | Introduction Results and discussions 2.1 Feedstock characteristics 2.2 Thermogravimetric (TG)/ Derivative thermogravimetric (DTG) analysis. | 717171717172 |
| 5.1 5.2 5.3 5.3 5.3 | Introduction Results and discussions 2.1 Feedstock characteristics 2.2 Thermogravimetric (TG)/ Derivative thermogravimetric (DTG) analysis 2.3 Kinetic parameters estimation using isoconversional methods | 7171717171727676 |
| WA 3 5.1 5.2 5.3 5.3 5.3 | Introduction Results and discussions 2.1 Feedstock characteristics 2.2 Thermogravimetric (TG)/ Derivative thermogravimetric (DTG) analysis 2.3 Kinetic parameters estimation using isoconversional methods 2.4 Model-fitting methods | 71717171727680 |
| WA 3 5.1 5.2 5.3 5.3 5.3 | Introduction Results and discussions 2.1 Feedstock characteristics 2.2 Thermogravimetric (TG)/ Derivative thermogravimetric (DTG) analysis 2.3 Kinetic parameters estimation using isoconversional methods 2.4 Model-fitting methods 5.2.4.1 Coats-Redfern Method | 71717172768080 |
| WA (5.1 5.2 5 5 5 5 | Introduction Results and discussions 2.1 Feedstock characteristics 2.2 Thermogravimetric (TG)/ Derivative thermogravimetric (DTG) analysis 2.3 Kinetic parameters estimation using isoconversional methods 2.4 Model-fitting methods 5.2.4.1 Coats-Redfern Method 5.2.4.2 Master plots of Criado Method to determine the reaction mechanism | 717171717276808081 |

| 6.1 Introduction | 88 |
|---|-----|
| 6.2. Results and discussion | 88 |
| 6.2.1. Raw material characterizations | 88 |
| 6.2.1.1 Proximate and ultimate (elemental) analysis | 88 |
| 6.2.1.2 FT-IR | 89 |
| 6.2.2 Catalyst characterizations | 90 |
| 6.2.2.1 Scanning electron microscope (SEM) | 90 |
| 6.2.2.2 X-ray diffraction (XRD) | 91 |
| 6.2.2.3 FT-IR | 91 |
| 6.2.2.4 N ₂ adsorption-desorption | 92 |
| 6.2.3 Catalytic cracking test and product analysis | 93 |
| 6.3 Conclusion | 99 |
| 6.4 References: | 101 |
| CHAPTER 7: CONCLUSIONS AND FUTURE RECOMMENDATIONS | 106 |
| 7.1 Conclusions | 106 |
| 7.2 Recommendation for future work | 107 |

List of Figures

| Figure1.1 | Fossil fuel consumption of the world (Holechek, J.L., Geli, H.M.E., Sawalhah, M.N., | |
|--------------|---|------------|
| Valdez, R., | 2022. A Global Assessment: Can Renewable Energy Replace Fossil Fuels by 2050? | |
| Sustain. 14) | | . 1 |
| Figure 1.2 | Different types of plastic | . 3 |
| Figure 1.3 | Various plastic types with their codification and application | . 4 |
| Figure 1.4 | World-wide production of plastic and plastic waste since 1950 (Geyer, R., Jambeck, | |
| J.R., Law, I | K.L., 2017. Production, use, and fate of all plastics ever made. Sci. Adv. 3, 25–29.) | . 5 |
| Figure 1.5 | Various factors affecting the pyrolysis process of plastic waste | . 8 |
| Figure 1.6 | Types of catalysts used in the catalytic pyrolysis of plastic waste | 10 |
| Figure 3.1 | Depicting the procedure of raw material preparation for pyrolysis process | 30 |
| Figure 3.2 | Catalyst preparation method for catalytic pyrolysis process | 31 |
| Figure 3.3 | Fixed -bed reactor set-up for thermal pyrolysis of different plastic waste | 37 |
| Figure 3.4 | Schematic diagram of catalytic pyrolysis process of different plastic wastes in a fixed | ı – |
| bed reactor | set-up3 | 38 |
| Figure 4.1 | FT-IR spectra of (a) modal plastic and (b) real-world plastic waste compounds 5 | 51 |
| Figure 4.2 | (a) TG plot and (b) DTG plot for PP, HDPE, and LDPE modal compounds at | |
| 15°C/min; (| c), (d), (e), and (f) are showing the TG plots with inset DTG plots at four different | |
| heating rate | s for HDPE, LDPE, PP and PS waste compounds respectively | 56 |
| Figure 4.3 | (a), (b), and (c) depicts TG and DTG (inset) plots for HDPE, LDPE, and PP modal | |
| compounds | at four different heating rates respectively | 57 |
| Figure 4.4 | Percentage yield (by wt.) of the liquid oil, wax, gas, and residue (char) during the | |
| thermal pyr | olysis experiment of PS, PP, LDPE, and HDPE5 | 59 |
| Figure 4.5 | Liquid oil product obtained from thermal pyrolysis of different plastic wastes | 50 |

| Figure 4.6 | FT-IR of liquid oils obtained from different plastic wastes |
|--------------|--|
| Figure 4.7 | Compounds present in the liquid oil obtained from different plastic wastes 64 |
| Figure 4.8 | Hydrocarbon distribution in liquid oils obtained from different plastic wastes 65 |
| Figure 4.9 | 1H NMR of liquid oil obtained from different real-world plastic wastes |
| Figure 5.1 | TG/DTG curves of (a)HDPE, (b)LDPE, (c)PP, and (d)PS waste at different heating |
| rates | 74 |
| Figure 5.2 | The calculated values of activation energies for (a) HDPE, (b) LDPE, (c) PP, and (d) |
| PS plastic w | rastes obtained from model-free methods |
| Figure 5.3 | Determination of reaction mechanism for (a) HDPE, (b) LDPE, (c) PP, and (d) PS |
| wastes from | master plots of Criado method |
| Figure 6.1 | FT-IR spectrum of HDPE, PP, LDPE, and PS plastic wastes (raw materials) |
| Figure 6.2 | SEM images showing the surface morphology of the synthesized hierarchical ZSM-5 |
| catalyst | 9 |
| Figure 6.3 | XRD pattern of the synthesized hierarchical ZSM-5 catalyst |
| Figure 6.4 | FT-IR spectra of synthesized hierarchical ZSM-5 catalyst |
| Figure 6.5 | Nitrogen adsorption-desorption isotherm for synthesized hierarchical ZSM-5 with |
| inset BJH po | ore size distribution result |
| Figure 6.6 | The thermal degradation trends of PP, HDPE, LDPE, and PS along with their inset |
| DTG curves | 94 |
| Figure 6.7 | Product distribution of catalytic process of different plastic wastes |
| Figure 6.8 | (a) FT-IR of liquid oil and (b) liquid oil composition obtained from GCMS results 98 |

List of tables

| Table 1.1 Various operating parameters of different type of pyrolysis process |
|---|
| Table 3.1 Most commonly used reaction mechanism for the solid-state thermal degradation43 |
| Table 4.1 Proximate and ultimate analysis of modal plastic and real-world plastic waste49 |
| Table 4.2 Providing the temperature interval of thermal degradation process, the maximum wt. loss |
| temperature (T max), and the maximum wt. loss of real-world waste and modal compounds of HDPE, |
| PP, LDPE, and PS at different heating rates |
| Table 4.3 Viscosity and HHV of pyrolytic oils obtained from different plastic wastes60 |
| Table 5.1 Thermal degradation interval, maximum weight loss temperature (T _{max}) and maximum |
| weight loss at different heating rates for HPDE, PP, LDPE, and PS waste75 |
| Table 5.2 The evaluated values of Eα for LDPE, PS, PP and HDPE at 15 °C·min−1 by Coats-Redfern |
| method80 |
| Table 6.1 Textural properties of the synthesized hierarchical ZSM-5 catalyst93 |
| Table 6.2 Different compounds constituting the composition of PP oil, HDPE oil, LDPE oil, and PS |
| oil97 |
| Table 6.3 Comparison of product distribution obtained from catalytic cracking of waste plastics99 |

List of abbreviations, and symbols

| | Abbreviations | Symbols | |
|--------|---|--------------|-----------------------------|
| ВЈН | Barrett-Johner-Halenda | α | Extent of conversion |
| BET | Brunauer-Emmett-Teller | β | Heating rate |
| BIS | Bureau of Indian Standards | A_0 | Pre-exponential factor or |
| | | | frequency factor |
| CSBR | Conical spouted bed reactor | E_{α} | Activation Energy |
| ID | Inner diameter | f(a) | Reaction mechanism |
| FID | Flame ionization detector | g(a) | Reaction mechanism function |
| FTIR | Fourier transform infrared spectroscopy | T | Temperature |
| FE-SEM | Field emission – scanning electron | (d\alpha/dt) | Rate of conversion |
| | microscopy | | |
| GCMS | Gas chromatography mass spectroscopy | | |
| HDPE | High density polyethylene | | |
| HHV | Higher heating value | | |
| LDPE | Low density polyethylene | | |
| KAS | Kissinger- Akahira-Sunose | | |
| MOF | Metal organic framework | | |
| MSW | Municipal solid waste | | |
| OFW | Ozawa Flynn Wall | | |
| PE | Polyethylene | | |
| PP | Polypropylene | | |
| PS | Polystyrene | | |
| TGA | Thermal gravimetric analysis | | |
| UNEP | United Nations Environment Programme | | |
| XRD | X-ray diffraction | | |

1.1. Background

Global industrialization and urbanization have attributed to increasing energy demand and consumption in last few decades, which have been solemn disquiet of world leaders and researchers. To overcome these demands, an astonishing rise in the dependency on fossil fuels has been observed since 1965. Utilization of coal, oil and gas have increased exponentially at a rate of 176%, 184%, and 540% respectively since then (Fig. 1.1) (Holechek et al., 2022). However, these conventional fossil fuel reserves are rapidly diminishing, thus demanding for an alternative sustainable technology. Also,

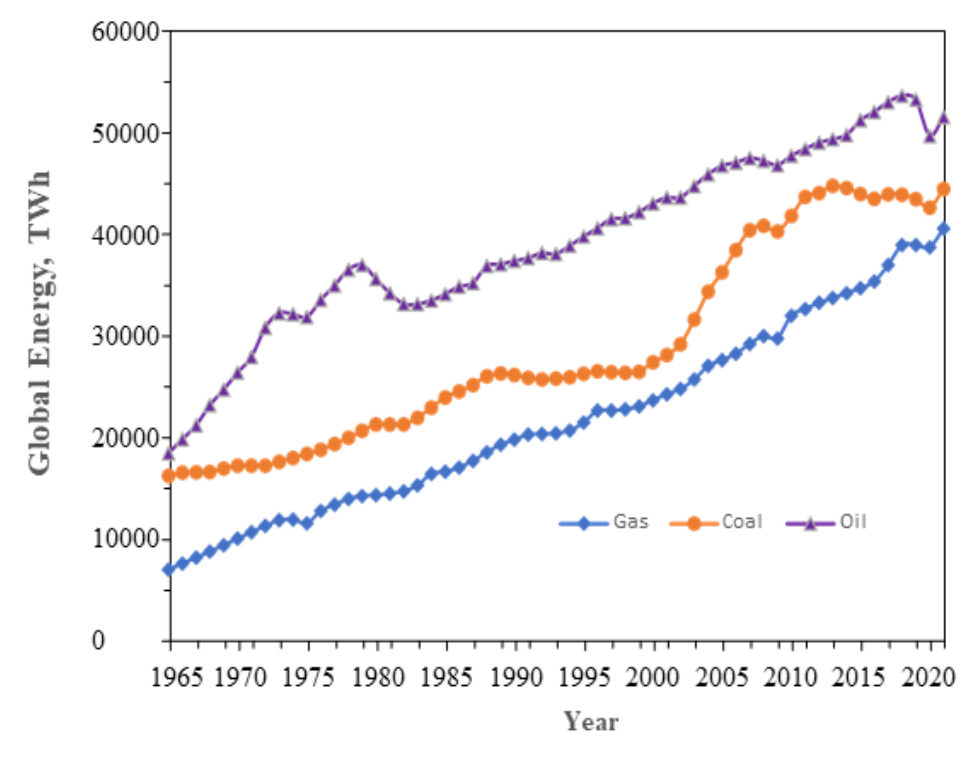


Figure 1.1 Fossil fuel consumption of the world (Holechek, J.L., Geli, H.M.E., Sawalhah, M.N., Valdez, R., 2022. A Global Assessment: Can Renewable Energy Replace Fossil Fuels by 2050?

Sustain. 14)

is it being forecasted that the oil reserves will get depleted by the year 2050 (Mohseni-Roodbari et al., 2022). Furthermore, twin environmental issues, global warming and climate change arise from

excessive dependence on fossil fuels. Consequently, the need for an alternative sustainable source of energy to meet the global energy demand has become essential.

Exponentially increasing population has not only contributed in challenging environmental issues like global warming and climate change, but also has attributed to generation of million tons of municipal solid waste (MSW). According to UN environment reports, 11.2 billion tons of solid waste is collected worldwide per annum of which plastic solid waste constitutes around 13% of it (Subhashini and Mondal, 2023). Hence the world is struggling by mounting huge heaps of plastic waste (N., 2021). Hence, to meet the increasing energy demands and save the fossil fuel reserves, researchers are working persistently to develop more economic, sustainable, advanced, and environment-friendly alternative fuels. The best solution to this alarming problem can be developing a process that can convert the plastic waste back into a valuable source of energy that can be used as an alternative to fossil fuels. Consequently, using waste plastic as source for retrieving valuable products and energy has become a significant field of research. The higher calorific value associated with the plastics due to their origin from fossil fuels favours the process of their conversion into valuable energy products (Anuar Sharuddin et al., 2016). Pyrolysis appears to be the significant solution to this. The end products of pyrolysis process are liquid hydrocarbon fuel and value-added chemicals. Therefore, it is a valuable hydrocarbon reenergizing process (Thahir et al., 2021a).

Therefore, this PhD thesis aims to explore the potential of thermal and catalytic pyrolysis of real-world plastic waste as a sustainable and resilient solution. A comprehensive study of various aspects of complex pyrolysis reaction of waste plastic contributes towards the better understanding of various plastics' role in providing an alternative sustainable energy resource as well as effective waste management technique. Through the implementation of this study, valuable insights can be gained to support the development and implementation of effective waste minimization and management policies and strategies for a more sustainable and greener future.

1.2. Plastic

Plastics are made up of polymers resulting in a wide range of synthetic or semi-synthetic materials. Plastic invention has contributed in uplifting the living standard of mankind (Thahir et al., 2021b).

Several intrinsic properties of plastics such as durability, pressure resistance, chemical inertness, flexibility, versatility, cheap production cost, and better thermal stability (attained by addition of stabilizers and additives) makes them the first choice of human beings in different applications (Al-Salem et al., 2009; Xu et al., 2018). However, modern plastics are polymers resulting from 'n' degree polymerization of petroleum derived hydrocarbon monomers. Hence, the complete degradation of these plastics can take centuries of time. However, the rate of disposing of waste plastic has risen remarkably and thereby imposing a negative impact on public health and environment (Osman et al., 2020).

1.2.1. Types of plastic

The first manmade plastic called "Bakelite" was developed in the year 1907. Later, plastics were modified and developed by varying the degree of chemical processes used to make them. Two broad classes of plastics can be categorized into (i) thermosets and (ii) thermoplastics. Thermosets are those kinds of plastics which do not melt upon heating rather undergo decomposition. Thermosets change their chemical composition when exposed to higher temperatures. In thermosetting an irreversible chemical reaction occur. Whereas, in thermoplastics, these do not undergo any chemical change when exposed to the higher temperatures, and end up in melting. These can be molded repeatedly. For example, polyethylene (PE), polystyrene (PS), polypropylene (PP), and polyvinyl chloride (PVC). Fig. 1.2 shows the different types of plastics available in market as per BIS codification.

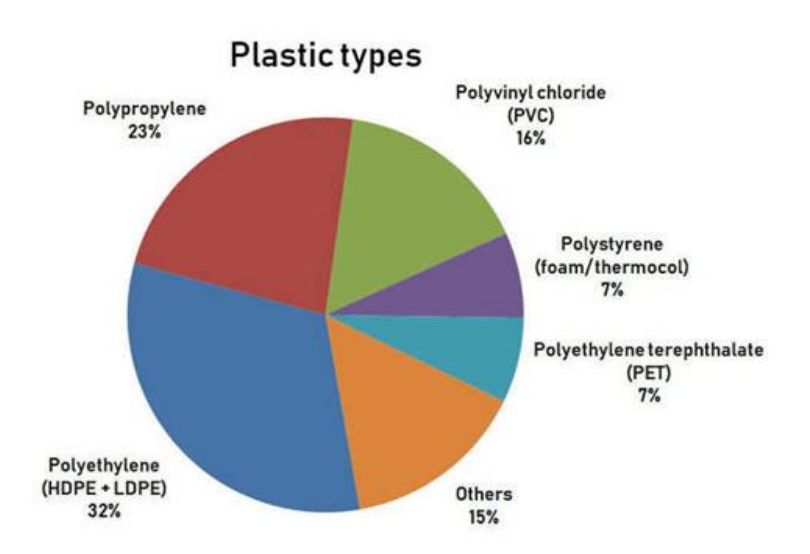


Figure 1.2 Different types of plastic

These plastics are given certain codes for the ease of identification and sorting. Fig. 1.3 shows the various plastic types with their codification and applications.

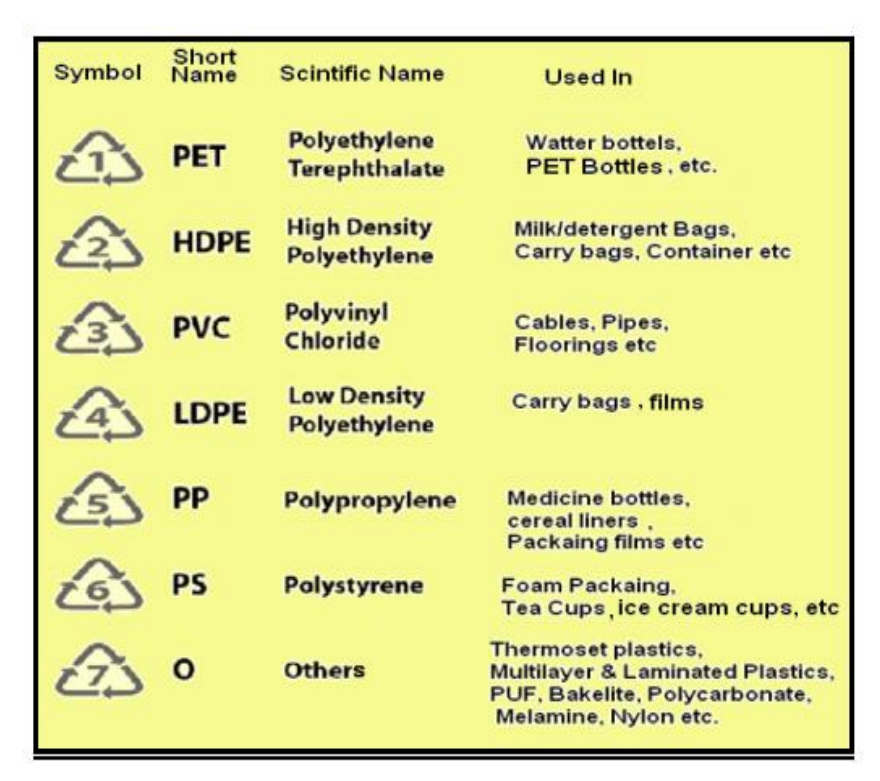


Figure 1.3 Various plastic types with their codification and application

1.2.2. Plastic and plastic waste generation

Since 1907, the June 2018 issue of National Geographic magazine had reported that until 2017, 9.2 billion tons of plastic was produced and of these 6.9 billion tons became waste. Out of 6.9 billion tons, 6.3 billion tons of plastic kept staggering and have never been to the recycling bin. An UNEP report, "Drowning in Plastics – Marine Litter and Plastic Waste Vital Graphics" had reported that, in the year 2020 solely 400 million tons of plastic were produced. If this trend continues then it is estimated that the annual global plastic production will reach above 1.1 billion tons by the year 2050.

About 8% to 10% of the world's total crude oil production goes for plastic production. For example, the United States uses 12 million barrels of oil per year for making plastic bags. UNEP report published

in 2018 estimated that by 2050, world-wide plastic industries would account for 20% of oil consumption. Fig. 1.4 shows the trend of world-wide production of plastic and plastic waste.

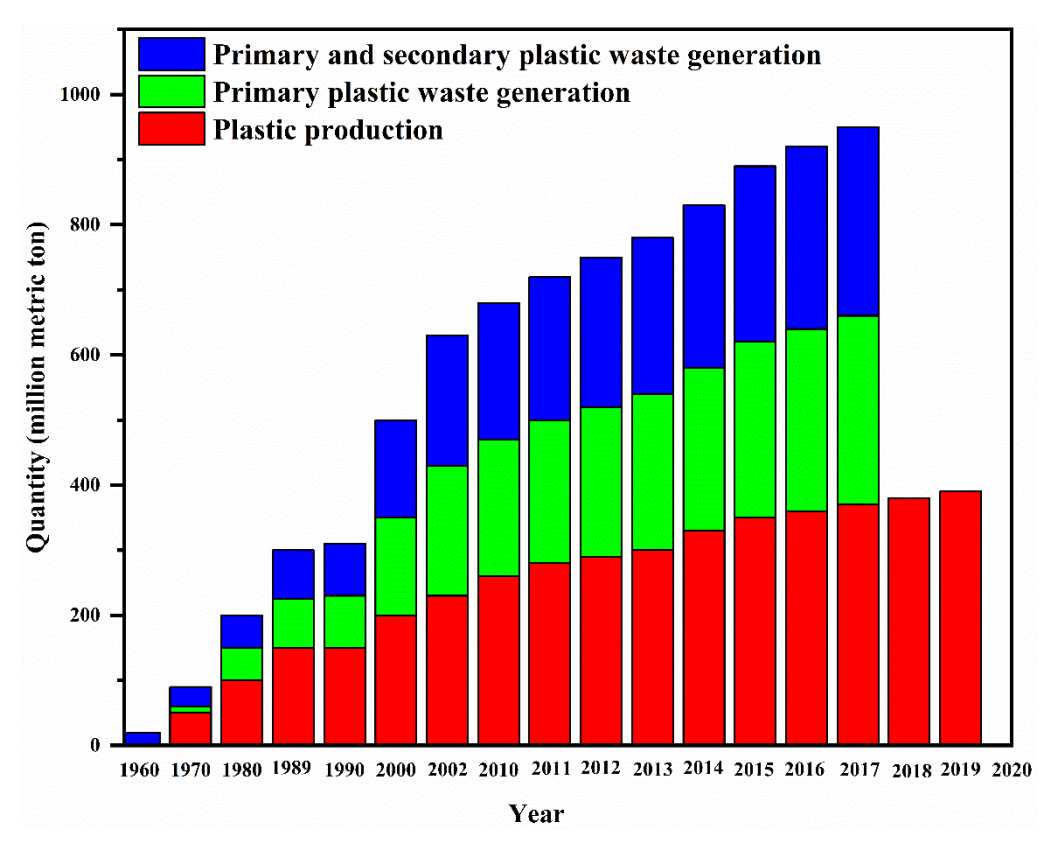


Figure 1.4 World-wide production of plastic and plastic waste since 1950 (Geyer, R., Jambeck, J.R., Law, K.L., 2017. Production, use, and fate of all plastics ever made. Sci. Adv. 3, 25–29.)

Plastics dominates the present market in various sectors. To account the plastics usage in different sectors, it is estimated that approximately 50% of total plastics are used for single-use disposable applications, such as disposable consumer items, packaging, and agricultural films. Around 20 - 25% of plastics are employed in long-term infrastructure such as cable coatings, pipes, and structural materials. And rest is used in durable consumer applications, such as in electronic goods, furniture, vehicles, etc. it is evident that packaging uses the highest % of the plastic production. However, other applications are also becoming significant sources of generating plastic wastes (Hopewell et al., 2009).

1.2.3. Plastic waste management techniques:

The conventional technique used for managing the huge heaps of plastic wastes are disposal, landfilling and incineration. These conventional techniques not only have become a threat to the societies because of adding to the emission of greenhouse gases in the environment but also are contributing in the exploitation of great amount of crude oil reserves for their production. Therefore, using the waste plastic for the production of alternative fuel source will provide an economic route to meet the energy demand and also assist in carbon dioxide emission reduction (Hopewell et al., 2009).

1.2.3.1 Pyrolysis process

Pyrolysis of plastic waste is the most desirable thermochemical waste management technique for the conversion of the waste into energy resource. Plastics originating from fossil fuels have higher calorific value associated that favours the process of their conversion into valuable energy products (Anuar Sharuddin et al., 2016). The end products of pyrolysis process are liquid hydrocarbon fuel and value-added chemicals. Therefore, it is a valuable hydrocarbon reenergizing process (Thahir et al., 2021b). Pyrolysis process of plastic waste

Pyrolysis is a decomposition process in which on providing thermal energy in the absence of oxygen the long-chain (heavier) hydrocarbon molecules are cracked into a smaller size (lighter) molecules and produces volatile hydrocarbons and carbon as residues that can be condensed to liquid fuel (Anuar Sharuddin et al., 2016; Arena and Mastellone, 2006; Lee, 2006; Thahir et al., 2021b). It can be classified into two distinct types: (i) thermal pyrolysis and (ii) catalytic pyrolysis. Each of these types of pyrolysis process can further be sub divided into three categories depending upon the operating heating rate condition: (i) slow, (ii) fast, and (iii) flash pyrolysis. Pyrolysis is a very complex multistep process. And the variations in operating parameters greatly affects the product distribution of the process. Slow pyrolysis entails a decomposition process that occurs at low temperatures, with a gradual heating rate and extended residence time. This process primarily yields char as a significant byproduct. On the other hand, fast pyrolysis is characterized by the production of bio-oil, achieved through controlled temperature conditions at approximately 500 °C, short residence times of less than 2 sec, and high heating rates exceeding 200 °C/sec. Flash pyrolysis, in contrast, is distinguished by its

extremely short reaction time and even higher heating rates compared to fast pyrolysis (Cozier, 2014). Table 1.1 is showing the various operating parameters of three different types of pyrolysis process.

Table 1.1 Various operating parameters of different type of pyrolysis process

| Parameters | Slow pyrolysis | Fast pyrolysis | Flash pyrolysis |
|-----------------------|----------------|----------------|-----------------|
| Operating | 550–950 | 850–1250 | 1050–1300 |
| Temperature (°C) | | | |
| Heating rate (°C/sec) | 0.1–10 | 10–200 | >1000 |
| Particle size (mm) | 5–50 | < 1 | < 0.2 |
| Residence time | 450–550 | 0.5–10 | <0.5 |
| (sec) | | | |

1.2.3.2 Catalytic pyrolysis

Catalytic pyrolysis process outdoes the thermal pyrolysis because it employs catalyst for carrying out the cracking of the plastic waste. Generally, catalyst reduces the activation energy requirement of the reaction and thereby providing lower energy pathway. Hence, catalytic pyrolysis process cracks down the long chain plastic wastes into smaller and lighter compounds at comparatively lower temperatures as compared with that of the thermal pyrolysis process.

1.2.3.3 Various factors affecting pyrolysis process

Apart from the reaction temperature, there are various other significant factors that affects the pyrolysis process as shown in the fig. 1.5 below.

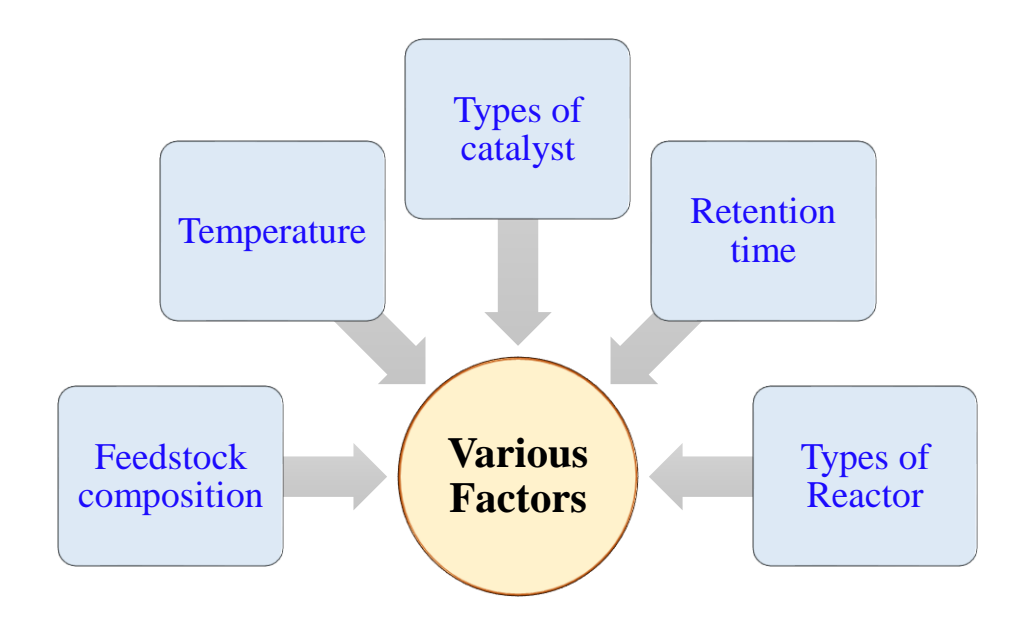


Figure 1.5 Various factors affecting the pyrolysis process of plastic waste

i. Types of reactors; there are batch and semi batch reactors, fixed -bed reactors, and fluidized bed reactors vastly used for conducting pyrolysis process of plastic waste. Recently, conical spouted bed reactor and microwave assisted technology are also being used for carrying out the pyrolysis process of plastic waste. The type of reactors plays an important role in the mixing of the plastics and catalysts, residence time, heat transfer and efficiency of the reaction towards achieving the final desired product. Most plastic pyrolysis in the lab scale were performed in batch, semi-batch, or continuous-flow reactors such as fluidized bed, fixed-bed reactor, and conical spouted bed reactor (CSBR). Among these, the fluidized bed reactor provides the best heat and mass transfer during the process. Also, there is better availability of the catalyst during the process, since the catalyst is well-mixed with the fluid and offers larger surface area of the catalyst for the reaction to occur (Kaminsky and Kim, 1999). However, the fixed-bed reactor

holds the advantage in case of designing, operating, and handling. Mostly, the fixed-bed reactors are used in two-stage process, and fixed-bed reactor being the second reactor (Onu et al., 1999; Vasile et al., 2002).

- ii. Feedstock composition; Fundamentally, proximate analysis provides the basic knowledge about the different composition of different plastics in terms of volatile matter, ash content, moisture content and fixed carbon content. For obtaining higher liquid yield, higher volatile matter is the significant parameter. Whereas the higher ash content decreases the amount of liquid oil, consequently increased the gaseous yield and char formation. Usually, the volatile matter is higher and the ash content is very low in the plastics, hence these results confirms that plastics have great potential for producing higher quality liquid oil.
- *Retention time;* the average amount of time spent by a particle inside the reactor is known as the retention time and it may influence product distribution (Mastral et al., 2001). Longer residence time increases the conversion of primary product, thus more thermal stable product is yielded such as light molecular weight hydrocarbons and non-condensable gas (Ludlow-Palafox and Chase, 2001). However it was observed that the effect of retention time on product distribution was at lower temperatures only (Anuar Sharuddin et al., 2016).
- *Type of catalyst;* Catalyst speeds up chemical reaction but remains unchanged towards the end of the process. Catalysts are widely used in industries and researches to optimize product distribution and increase the product selectivity. There are three main categories of the catalysts used in the pyrolysis of plastic waste as shown in the fig. 1.6 below.

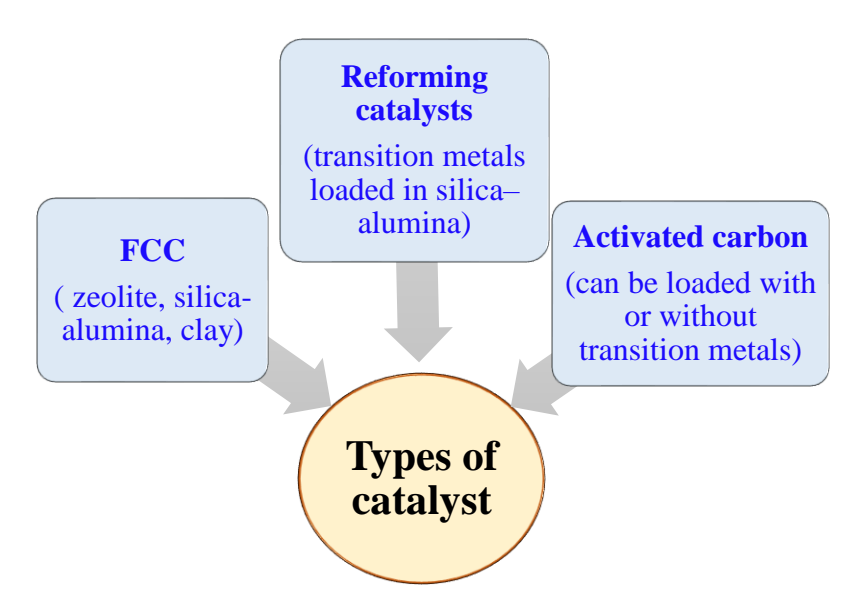


Figure 1.6 Types of catalysts used in the catalytic pyrolysis of plastic waste

v. Reaction temperature; Reaction temperature is the most important parameter in the pyrolysis of plastic waste because it influences the reaction rate and hence affects the product distribution. The operating temperature required relies strongly on the product preference. Higher temperature more than 500 °C favoured gaseous or char product whereas the liquid is obtained at comparatively lower temperature in the range of 300 – 500 °C and this condition is applicable for all plastics.

1.2.3.4 Kinetic modelling of pyrolysis process

Pyrolysis kinetics and the product yields from various pure forms of plastic sources have been reported in the literature. However, these findings display huge deviation in case of waste forms of plastic due to the inherent variations in physio-chemical properties. Therefore, conducting a new series of experiments by using real-world plastic waste becomes imperative to comprehensively understand the kinetic behaviors and product distribution. Consequently, model- based studies are widely used and preferred to gain insight and investigate the plastic pyrolysis process. Due to the intrinsic complex behavior of the pyrolysis process, it is extremely challenging to develop a general mathematical

model. Nonetheless, the application of computational methods based on machinelearning offers a promising solution to overcome this complexity.

In this thesis, we aim to address the existing gaps in understanding plastic pyrolysis by developing a comprehensive computational model. This model will incorporate a range of experimental data obtained from pure plastic samples, allowing for more accurate predictions and deeper insights into the pyrolysis process. By combining fundamental scientific principles with advanced machine learning techniques, we can unlock a deeper understanding of plastic pyrolysis, contributing to the development of efficient and sustainable energy conversion technologies.

1.3. Motivation and thesis content

The motivation behind this work was to find a cost-effective plastic waste management technique which can convert the plastic waste back into a valuable source of energy that can be used as an alternative to fossil fuels via a sustainable route. In this regard the principal objective is to convert the real-world plastic waste into fuel grade hydrocarbon via thermal and catalytic pyrolysis process.

1.3.1. Objectives of the research work

The thesis work focuses on concerned with addressing the following specific interrelated problems:

- i. Selection of raw materials favoring higher liquid oil production.
- ii. Design a suitable reactor to carry out the pyrolysis process.
- iii. Optimization of reaction parameters and performing thermal pyrolysis.
- iv. To study the kinetics and reaction mechanism through thermogravimetric analysis.
- v. Application of the thermal pyrolysis process in the treatment of industrial waste.
- vi. Preparation and characterization of hierarchical zeolite catalyst.
- vii. To investigate and optimize the reaction condition using catalytic pyrolysis.

1.3.2. Thesis outline

This thesis aims to explore the aspects of obtaining aromatic rich fuel grade hydrocarbons from the thermal and catalytic pyrolysis process of real-world plastic waste, specifically, high-density polyethylene (HDPE), low-density polyethylene (LDPE), polypropylene (PP), and polystyrene (PS) wastes in a tubular fixed bed reactor. To enhance the aromatic content in the liquid oil obtained from the thermal pyrolysis process, hierarchical ZSM-5 catalyst was synthesized and tested. The characteristics and fuel properties of the obtained liquid oil have been studied extensively and compared with that of the commercial fuels like diesel and kerosene. The thesis is organized as follows.

Chapter 1 – Introduction: The introductory chapter gives an overview of the motivation, discusses the significance of various aspects of plastic pyrolysis reported in the literature, such as feed characterization, kinetics, parametric influence, product distribution, objectives, and contributions of this thesis work in detail. It introduces the characteristics of plastics and their pervasive nature encountered in day-to-day life.

Chapter 2 - Literature review: The chapter reviews existing study published for predicting different aspects of thermal and catalytic pyrolysis of plastic waste conversion, kinetics, pyrolysis behavior, and product yields and selectivity. Additionally, the chapter highlights the findings and limitations in the field of waste plastic pyrolysis, specifically product distribution and selectivity in thermal as well as catalytic pyrolysis process.

Chapter 3 - Materials and Method: outlines the specific problems considered in this work. This is followed by the demonstration of the feedstock collection, raw material preparation, catalyst preparation method and the schematic of the experimental set-up. Specific issues associated with the raw material preparation have also been discussed and alternatives to overcome the inherently insulating nature of the plastics are introduced here. Finally, this is followed by the detailed discussion about various analytical techniques employed for characterization of the raw materials, catalyst, and the products (liquid oil) obtained from the pyrolysis process have been outlined.

Chapter 4 - Thermal Pyrolysis: This chapter deals with the detailed overview about the various factors affecting the thermal pyrolysis process of plastic wastes. It includes a detailed study about the

optimization of the important parameters like reaction temperature, heating rate, inert gas flowrate, and cooling temperature. Subsequently, the effect of these parameters on the product distribution is discussed. Finally, the liquid oil produced from the thermal pyrolysis process is being characterized and the results are discussed in detail and corroborated with the fuel properties of the commercial fuel like diesel and kerosene.

Chapter 5 - Kinetic study of thermal pyrolysis process: This chapter is dedicated to study and understand the behaviour of the complex multistep thermal pyrolysis process by kinetic modelling in detail. It presents the extensive results on study of kinetic modelling using different model – free isoconversional methods (Kissinger-Akahira-Sunose (KAS), Ozawa Flynn Wall (OFW), Starink, Boswell and Tang) and two model fitting methods namely; Coats-Redfern and Criado method to determine the kinetic triplets i.e., activation energy, frequency factor and reaction mechanism.

Chapter 6 - Catalytic Pyrolysis: The catalytic pyrolysis process of real-world plastic wastes is investigated in detail in this chapter. This includes the operating parameters optimization, effect of using hierarchical zeolite catalyst on product yield, product distribution and characterization of the liquid oil obtained. It also compares the fuel properties of the oil obtained from the thermal pyrolysis with that of the oil obtained from catalytic pyrolysis.

Finally, a summary of the major findings of this work is presented in *Chapter 7*. This is followed by identifying the areas meriting further investigation.

1.4. References

- [1] Al-Salem, S.M., Lettieri, P., Baeyens, J., 2009. Recycling and recovery routes of plastic solid waste (PSW): A review. Waste Manag. 29, 2625–2643. https://doi.org/10.1016/j.wasman.2009.06.004
- [2] Anuar Sharuddin, S.D., Abnisa, F., Wan Daud, W.M.A., Aroua, M.K., 2016. A review on pyrolysis of plastic wastes. Energy Convers. Manag. 115, 308–326. https://doi.org/10.1016/j.enconman.2016.02.037
- [3] Arena, U., Mastellone, M.L., 2006. Fluidized Bed Pyrolysis of Plastic Wastes, Feedstock Recycling and Pyrolysis of Waste Plastics: Converting Waste Plastics into Diesel and Other Fuels. https://doi.org/10.1002/0470021543.ch16
- [4] Cozier, M., 2014. Business highlights: Collaboration: Bigger and beta. Biofuels, Bioprod. Biorefining 8, 743. https://doi.org/10.1002/BBB
- [5] Geyer, R., Jambeck, J.R., Law, K.L., 2017. Production, use, and fate of all plastics ever made. Sci. Adv. 3, 25–29. https://doi.org/10.1126/sciadv.1700782
- [6] Holechek, J.L., Geli, H.M.E., Sawalhah, M.N., Valdez, R., 2022. A Global Assessment: Can Renewable Energy Replace Fossil Fuels by 2050? Sustain. 14. https://doi.org/10.3390/su14084792
- [7] Hopewell, J., Dvorak, R., Kosior, E., 2009. Plastics recycling: Challenges and opportunities. Philos. Trans. R. Soc. B Biol. Sci. 364, 2115–2126. https://doi.org/10.1098/rstb.2008.0311
- [8] Kaminsky, W., Kim, J.S., 1999. Pyrolysis of mixed plastics into aromatics. J. Anal. Appl. Pyrolysis 51, 127–134. https://doi.org/10.1016/S0165-2370(99)00012-1
- [9] Lee, K.H., 2006. Thermal and catalytic degradation of waste HDPE, Feedstock Recycling and Pyrolysis of Waste Plastics: Converting Waste Plastics into Diesel and Other Fuels. https://doi.org/10.1002/0470021543.ch5
- [10] Ludlow-Palafox, C., Chase, H.A., 2001. Microwave-induced pyrolysis of plastic wastes. Ind. Eng. Chem. Res. 40, 4749–4756. https://doi.org/10.1021/ie010202j
- [11] Mastral, A.M., García, T., Callén, M.S., Navarro, M. V., Galbán, J., 2001. Assessement of phenanthrene removal from hot gas by porous carbons. Energy and Fuels 15, 1–7. https://doi.org/10.1021/ef000116g
- [12] Mohseni-Roodbari, S., Seyed Mousavi, S.A.H., Sadrameli, S.M., Pahlavanzadeh, H., 2022. Thermal pyrolysis of linseed waste to produce a renewable biofuel using response surface methodology in a fixed bed reactor. J. Anal. Appl. Pyrolysis 168, 105701. https://doi.org/10.1016/j.jaap.2022.105701
- [13] N., S., 2021. Plastic waste management: A road map to achieve circular economy and recent innovations in pyrolysis. Sci. Total Environ. 151160. https://doi.org/10.1016/j.scitotenv.2021.151160

- [14] Onu, P., Vasile, C., Ciocîlteu, S., Iojoiu, E., Darie, H., 1999. Thermal and catalytic decomposition of polyethylene and polypropylene. J. Anal. Appl. Pyrolysis 49, 145–153. https://doi.org/10.1016/S0165-2370(98)00109-0
- [15] Sakthipriya, N. (2022). Plastic waste management: A road map to achieve circular economy and recent innovations in pyrolysis. *Science of The Total Environment*, 809, 151160.
- [16] Subhashini, Mondal, T., 2023. Experimental investigation on slow thermal pyrolysis of real-world plastic wastes in a fixed bed reactor to obtain aromatic rich fuel grade liquid oil. J. Environ. Manage. 344, 118680. https://doi.org/10.1016/j.jenvman.2023.118680
- [17] Thahir, R., Irwan, M., Alwathan, A., Ramli, R., 2021a. Effect of temperature on the pyrolysis of plastic waste using zeolite ZSM-5 using a refinery distillation bubble cap plate column. Results Eng. 11, 100231. https://doi.org/10.1016/j.rineng.2021.100231
- [18] Thahir, R., Irwan, M., Alwathan, A., Ramli, R., 2021b. Effect of temperature on the pyrolysis of plastic waste using zeolite ZSM-5 using a refinery distillation bubble cap plate column. Results Eng. 11, 100231. https://doi.org/10.1016/j.rineng.2021.100231
- [19] Vasile, C., Brebu, M., Darie, R., Darie, H., Uddin, M.A., Sakata, Y., 2002. Thermal and catalytic decomposition of mixed plastics. III1 PVC-containing mixed plastics. Rev. Roum. Chim. 47, 1185–1191.
- [20] Xu, F., Wang, B., Yang, D., Hao, J., Qiao, Y., Tian, Y., 2018. Thermal degradation of typical plastics under high heating rate conditions by TG-FTIR: Pyrolysis behaviors and kinetic analysis. Energy Convers. Manag. 171, 1106–1115. https://doi.org/10.1016/j.enconman.2018.06.047

2.1. Introduction

Pyrolysis reaction involves the molecular breakdown of heavier and larger molecules into lighter and smaller molecules under the effect of heat in the absence of oxygen. There are several terms used for pyrolysis such as cracking, thermal cracking, depolymerization, thermolysis, etc. Pyrolysis of waste plastic appears to be a promising technique for waste conversion into fuel. Pyrolysis helps in preserving the resource of virgin fuel by strengthening recycling industries and decreasing of plastic landfilling (Al-Salem et al., 2009). High calorific value associated with plastics due to their origin from fossil fuels makes them most suitable for producing valuable energy(Anuar Sharuddin et al., 2016). The plastic pyrolysis process produces chemical industry materials and liquid hydrocarbon fuel (Thahir et al., 2021b). Pyrolysis can be performed in two ways i.e., thermally, and catalytically under different experimental conditions and parameters. Temperature, type of reactor, catalyst, pressure and residence time, type and rate of fluidizing gas are significant parameters in plastic pyrolysis reaction(Kaminsky and Kim, 1999; Li et al., 2021; López et al., 2011).

2.2. Thermal pyrolysis of plastic waste

Pyrolysis is a decomposition process in which on providing thermal energy in the absence of oxygen the long-chain (heavier) hydrocarbon molecules are cracked into a smaller size (lighter) molecules and produces volatile hydrocarbons and carbon as residues that can be condensed to liquid fuel (Anuar Sharuddin et al., 2016; Arena and Mastellone, 2006; Lee, 2006; Thahir et al., 2021a). Pyrolysis outdoes traditional plastic waste management techniques as it does not require any pre-maintenance and presorting of heterogenic plastic polymers(Devi et al., 2021; Ignatyev et al., 2014), also there are not much environmental harmful emissions. Pyrolysis can be performed in two ways i.e., thermally, and catalytically under different experimental conditions or parameters and yields solid char, liquid oil, and non-condensable gases as their end products (Miandad et al., 2017; Rehan et al., 2017). Parameters such as temperature, type of reactor, catalyst, pressure and residence time, type and rate of fluidizing gas plays an important role in carrying out the pyrolysis reaction of the plastic waste (Anuar Sharuddin et al., 2016; Hussein et al., 2021; Kaminsky, 2021; López et al., 2011; Panda, 2018; Unnikrishnan and

Srinivas, 2016) Various research groups have already studied and reported the effect of these parameters in the thermal pyrolysis degradation of various types of plastics. Different feedstocks have different effect on the pyrolytic fuel composition. The condensation of evolved volatiles from the degradation of the feedstocks results in the production of the oil in plastic pyrolysis process (Al-Salem, 2019). Several studies have reported that various organic compounds such as aromatic, alicyclic, and aliphatic hydrocarbons constitute the pyrolytic oil obtained from plastic pyrolysis (Rathsack et al., 2015); Whereas, Kumar et al., 2011, had studied in detail the pyrolysis of high-density polyethylene (HDPE) and found significance of feedstock pre-treatment. With the minimal pre-treatment, they were able to produce pyrolytic oils from HDPE within fuel grade hydrocarbon range (Kumar et al., 2011). As it is already known that the source origin of plastic waste and type of pretreatment method also affects the products composition, several research groups reported the trace amounts of oxygen, sulphuric compounds and nitrogen-based chemicals found in the pyrolytic liquid oil Al-Salem et al., 2017; Ignatyev et al., 2014; Kunwar et al., 2016; Quek and Balasubramanian, 2013, had also investigated about the high higher heating values (HHV) of pyrolytic oil obtained from plastic and found them comparable with conventional fuels ranging between 42.1 and 49.4 MJ kg⁻¹. Al-Salem (2019), further studied the effect of fixed bed (batch) reactor on thermal pyrolysis of HDPE. Another prime product obtained from plastic pyrolysis is solid char. However, due to limited availability of the literature and work done, recently researchers have begun to explore the dynamic applications of plastic char with great enthusiasm. Plastic char serves as the chief component in the applications such as; precursors to produce activated carbon, CO2 adsorbents, and adsorbent materials (Álvarez-Gutiérrez et al., 2018; Jamradloedluk and Lertsatitthanakorn, 2014; Mulu et al., 2021). The next most important parameter that greatly influences the thermal degradation of plastics and its product distribution is the heating rate of the process (Li et al., 2015). To study the thermal degradation behaviours of plastic waste during the pyrolysis processes, Thermogravimetry-Fourier Transform Infrared Spectroscopy (TG-FTIR) is one of the most widely used methods (Xu et al., 2018). In this coupled study the effect of various heating rates on thermal pyrolysis process can be determined. Many researches have been done and reported on determining the pyrolysis characteristics of plastics by TG-FTIR (Wu et al., 2014; Zhu et al., 2008). Subsequently it was observed that the oil generated in PE degradation has a wider range of compounds than PP and PS. PP pyrolysis lead to the production of lighter compounds as compared with those obtained from PE pyrolysis, due to the easier breakage of tertiary carbons in PP. Whereas PS pyrolysis produced aromatic rich liquid oil and lead the production of styrene (Calero et al., 2023).

2.3. Kinetic study of thermal pyrolysis of plastic

Apart from the operating conditions, the pertinent reactor design can also affect the product yields. Hence, for designing of the reactor with well-defined reactor's configuration, size and internals, the most important requirements are a set of known reliable kinetic parameters (also known as kinetic triplets), including apparent activation energy (E_{α}) , reaction mechanism $(f(\alpha))$, and pre-exponential factor or frequency factor (A₀). To study the plastic thermal degradation process, Thermogravimetry-Fourier Transform Infrared Spectroscopy (TG-FTIR) is the most widely used technique (Xu et al., 2018). In this coupled study the effect of various heating rates on thermal pyrolysis process can be determined. These TG-FTIR studies of plastics pyrolysis have been reported by many researchers (Wu et al., 2014; Xu et al., 2018; Zhu et al., 2008). For analysing solid-state kinetic data from TGA the various methods can be grouped into two sub categories; model free and model-fitting methods ("Application of solid-state kinetics to desolvation reactions," 2007; Republic, 2004; Sbirrazzuoli et al., 2009; Senneca et al., 2002). Model free or isoconversional method employs kinetic curves obtained from TGA for analysis. Thereafter, from the plots of these isoconversional methods the kinetic parameters are calculated. The independent nature of isoconversional methods from prerequisite information about $f(\alpha)$ for E_{α} calculation is their biggest advantage (Vyazovkin and Wight, 1999). However, Isoconversional methods are unable in predicting A_0 and $f(\alpha)$ values, which leads to the need for development of methods such as master plot (evaluation of $f(\alpha)$) and compensation effect (evaluation of A₀) (Luiz et al., 2019). Whereas, various models are tried for fitting the data in modelfitting methods (Nisar et al., 2019). The best fitted model is selected for studying and evaluation of kinetic parameters. Therefore, in solid-state reactions to calculate E_{α} , A_0 and $f(\alpha)$ from a single TGA data, model-fitting techniques are used.

The external stresses during thermal cracking of plastics brings changes in their physical properties and chemical structure (Das and Tiwari, 2017), resulting in a complex mechanism in nature. Furthermore, the heterogeneity of plastic solid waste (PSW) composition causes imprecise evaluation of kinetic parameters. Several researchers have studied kinetics of different plastic wastes in different forms of composition such as; single component, simple binary mixture, tertiary mixture or varying

one of the component in mixtures (Aboulkas et al., 2010; Das and Tiwari, 2017; Dubdub and Al-Yaari, n.d.; Kremer et al., 2021; Özsin and Eren, 2019; Qin et al., 2018). However, the results obtained from these kinetic analysis studies are inconsistent and scattered. For example, the values of activation energy obtained for PS, PP, LDPE, and HDPE in the work of Sùrum et al., 2001, were 311.5 kJ/mol, 336.7 kJ/mol, 340.8 kJ/mol and 445.1 kJ/mol respectively. Whereas Wu et al., 1993 had obtained 172 kJ/mol for PS, 184-265 kJ/mol for PP, 194-206 kJ/mol for LDPE and 233-326 kJ/mol for HDPE. Peterson et al., 2001 were able to calculate 200 kJ/mol activation energy for PS in an inert environment whereas it was observed to be 125 kJ/mol in the presence of air.

2.4. Catalytic pyrolysis of plastic waste

Recently, waste plastics are considered as an ideal carbon and hydrogen resource, which can be transformed into H₂-enriched syngas, chemicals, and high-value carbon materials (Cai et al., 2023; Genuino et al., 2023). Thermochemical conversion processes like pyrolysis (thermal and catalytic) and gasification have been gaining the major attention of researchers and technologists worldwide to manage the huge plastic wastes by converting them into desirable energy resources. Lately, one of these thermochemical processes i.e. catalytic pyrolysis has been the most fascinating process among scientific society due to its various advantages such as; lower reaction temperatures and activation energy, shorter reaction time, accelerate reaction rate, efficient and extensive production of multiple products from plastic waste pyrolysis (Anuar Sharuddin et al., 2016; Budsaereechai et al., 2019; Cai et al., 2021a, 2021b; Miandad et al., 2017). Various key process parameters that significantly influence the performance of the catalytic pyrolysis are: reaction temperature, heating rate, residence time, type of reactor, type and size of feedstock and type of catalyst. The selection of the catalyst is the most important step in determining the efficiency of the catalytic pyrolysis (Bhandari et al., 2021). Although the liquid oil obtained from both, thermal and catalytic pyrolysis of plastic waste cannot be used directly as a transportation fuel but the use of catalyst enhances the production of lighter hydrocarbon compounds and reduces the oxygenated hydrocarbons (Ding, K. et al., 2018). Heterogeneous catalysts like ZnO, MgO, CaCO₃, CaC₂, SiO₂, Al₂O₃, SiO₂-Al₂O₃, ZSM-5 zeolite, red mud, and FCC are more widely used for plastic pyrolysis (Budsaereechai et al., 2019; Ratnasari et al., 2017). Recently, various modifications in heterogeneous catalyst like doping with transition metals (Fe, Ni, Co) and different support materials (Al₂O₃ and carbon) have been studied extensively (Acomb et al., 2016; Cai et al.,

2021b; Jiang et al., 2022; Zhang et al., 2022). More importantly, the compositions of plastics played a critical role in the distribution and quality of the targeted products. In view of achieving higher liquid yield and fine hydrocarbon composition, zeolite catalysts (HZSM-5/HY) have been further modified by adding transition metals which strongly affect the catalytic properties having tuned textural and acidic characteristics(Miskolczi et al., 2019; Ren et al., 2012).

Zeolites have been the most suitable and preferred industrial catalyst used in the conversion of the plastic waste. The intrinsic properties of zeolite such as thermal stability at higher temperatures, flexible frameworks, uniform and small pore size, providing higher active surface area and ease in framework modification makes them outperforming among other catalysts used in plastic waste pyrolysis (Srivastava, R, 2018). G. Elordi et. al. (Elordi, G. et al., 2009) had explored the HZSM-5, HY and H-β catalyst in the cracking of HDPE plastic in a conical spouted bed reactor and obtained only 14% of the aromatic content in the liquid oil 500 °C. However, they observed that HZSM-5 catalyst had aided in more specific shape selective cracking and provided higher number of lighter compounds in the liquid oil. Uemichi, et al. (Uemichi, Y. et al., 1998) studied the performance of HZSM-5 catalyst to convert polyethylene in a fixed-bed reactor. At a reaction temperature of 526 °C and catalyst temperature of 450 °C, they obtained aromatic and iso alkane comprised gasoline range hydrocarbons. More importantly, the compositions of plastics played a critical role in the distribution and quality of the targeted products. In view of achieving higher liquid yield and fine hydrocarbon composition, zeolite catalysts (HZSM-5/HY) have been further modified by adding transition metals which strongly affect the catalytic properties having tuned textural and acidic characteristics (Z. Tang et al., 2015; N. Miskolczi, et al., 2019). In most of the studies, it was observed that reaction temperatures used for carrying out the catalytic pyrolysis process were ranging 450- 550 °C. Also, even after using ZSM-5 and HZSM-5 catalyst, the production of lighter hydrocarbon compounds was only 20-30%.

A vast literature and several industrial reports have reported that the zeolites have been the most successful acid catalysts for converting plastic waste into source of energy. But still there are certain research scopes that may lead to new directions in exploring these versatile zeolite catalysts. One of the major limitations of using ZSM-5 zeolites in plastic pyrolysis is their smaller pore size, because it causes diffusion limitation to branched hydrocarbons containing more than ten carbon, semi- heavy and light aromatic compounds from their pores (Vollmer, I., 2020). Since, these high carbon aromatic

and branched hydrocarbons could not diffuse from the cavities of the ZSM-5, and end up decomposing and coking the active sites. Therefore, incorporating the mesopores in the framework can be a possibility to enhance the catalyst performance.

2.5. References

- [1] Aboulkas, A., El harfi, K., El Bouadili, A., 2010. Thermal degradation behaviors of polyethylene and polypropylene. Part I: Pyrolysis kinetics and mechanisms. Energy Convers. Manag. 51, 1363–1369. https://doi.org/10.1016/j.enconman.2009.12.017
- [2] Acomb, J.C., Wu, C., Williams, P.T., 2016. The use of different metal catalysts for the simultaneous production of carbon nanotubes and hydrogen from pyrolysis of plastic feedstocks. Appl. Catal. B Environ. 180, 497–510. https://doi.org/10.1016/j.apcatb.2015.06.054
- [3] Al-Salem, S.M., 2019. Thermal pyrolysis of high density polyethylene (HDPE) in a novel fixed bed reactor system for the production of high value gasoline range hydrocarbons (HC). Process Saf. Environ. Prot. 127, 171–179. https://doi.org/10.1016/j.psep.2019.05.008
- [4] Al-Salem, S.M., Antelava, A., Constantinou, A., Manos, G., Dutta, A., 2017. A review on thermal and catalytic pyrolysis of plastic solid waste (PSW). J. Environ. Manage. 197, 177–198. https://doi.org/10.1016/j.jenvman.2017.03.084
- [5] Al-Salem, S.M., Lettieri, P., Baeyens, J., 2009. Recycling and recovery routes of plastic solid waste (PSW): A review. Waste Manag. 29, 2625–2643. https://doi.org/10.1016/j.wasman.2009.06.004
- [6] Álvarez-Gutiérrez, N., Gil, M. V., Rubiera, F., Pevida, C., 2018. Simplistic approach for preliminary screening of potential carbon adsorbents for CO2 separation from biogas. J. CO2 Util. 28, 207–215. https://doi.org/10.1016/j.jcou.2018.10.001
- [7] Anuar Sharuddin, S.D., Abnisa, F., Wan Daud, W.M.A., Aroua, M.K., 2016. A review on pyrolysis of plastic wastes. Energy Convers. Manag. 115, 308–326. https://doi.org/10.1016/j.enconman.2016.02.037
- [8] Khawam, A. (2007). Application of solid-state kinetics to desolvation reactions. The University of Iowa.
- [9] Arena, U., Mastellone, M.L., 2006. Fluidized Bed Pyrolysis of Plastic Wastes, Feedstock Recycling and Pyrolysis of Waste Plastics: Converting Waste Plastics into Diesel and Other Fuels. https://doi.org/10.1002/0470021543.ch16
- [10] Budsaereechai, S., Hunt, A.J., Ngernyen, Y., 2019. Catalytic pyrolysis of plastic waste for the production of liquid fuels for engines. RSC Adv. 9, 5844–5857.

- https://doi.org/10.1039/c8ra10058f
- [11] Cai, N., Li, X., Xia, S., Sun, L., Hu, J., Bartocci, P., Fantozzi, F., Williams, P.T., Yang, H., Chen, H., 2021a. Pyrolysis-catalysis of different waste plastics over Fe/Al2O3 catalyst: High-value hydrogen, liquid fuels, carbon nanotubes and possible reaction mechanisms. Energy Convers. Manag. 229, 113794. https://doi.org/10.1016/j.enconman.2020.113794
- [12] Cai, N., Xia, S., Li, X., Sun, L., Bartocci, P., Fantozzi, F., Zhang, H., Chen, H., Williams, P.T., Yang, H., 2021b. Influence of the ratio of Fe/Al2O3 on waste polypropylene pyrolysis for high value-added products. J. Clean. Prod. 315, 128240. https://doi.org/10.1016/j.jclepro.2021.128240
- [13] Cai, N., Xia, S., Xiao, H., Chen, Y., Chen, W., Yang, H., Wu, C., Chen, H., 2023. Distinguishing the impact of temperature on iron catalyst during the catalytic-pyrolysis of waste polypropylene. Proc. Combust. Inst. 39, 835–845. https://doi.org/10.1016/j.proci.2022.06.008
- [14] Calero, M., Solís, R.R., Muñoz-Batista, M.J., Pérez, A., Blázquez, G., Ángeles Martín-Lara, M., 2023. Oil and gas production from the pyrolytic transformation of recycled plastic waste: An integral study by polymer families. Chem. Eng. Sci. 271, 118569. https://doi.org/10.1016/j.ces.2023.118569
- [15] Das, P., Tiwari, P., 2017. Thermal degradation kinetics of plastics and model selection. Thermochim. Acta 654, 191–202. https://doi.org/10.1016/j.tca.2017.06.001
- [16] Devi, M., Rawat, S., & Sharma, S. (2021). A comprehensive review of the pyrolysis process: From carbon nanomaterial synthesis to waste treatment. *Oxford Open Materials Science*, *I*(1), itab014.
- [17] Dubdub, I., & Al-Yaari, M. (2020). Pyrolysis of mixed plastic waste: I. kinetic study. *Materials*, *13*(21), 4912.
- [18] Genuino, H.C., Pilar Ruiz, M., Heeres, H.J., Kersten, S.R.A., 2023. Pyrolysis of mixed plastic waste: Predicting the product yields. Waste Manag. 156, 208–215. https://doi.org/10.1016/j.wasman.2022.11.040
- [19] Hussein, Z.A., Shakor, Z.M., Alzuhairi, M., Al-Sheikh, F., 2021. Thermal and catalytic cracking of plastic waste: a review. Int. J. Environ. Anal. Chem. 00, 1–18. https://doi.org/10.1080/03067319.2021.1946527

- [20] Ignatyev, I.A., Thielemans, W., Vander Beke, B., 2014. Recycling of polymers: A review. ChemSusChem 7, 1579–1593. https://doi.org/10.1002/cssc.201300898
- [21] Jamradloedluk, J., Lertsatitthanakorn, C., 2014. Characterization and utilization of char derived from fast pyrolysis of plastic wastes. Procedia Eng. 69, 1437–1442. https://doi.org/10.1016/j.proeng.2014.03.139
- [22] Jiang, J., Shi, K., Zhang, X., Yu, K., Zhang, H., He, J., Ju, Y., Liu, J., 2022. From plastic waste to wealth using chemical recycling: A review. J. Environ. Chem. Eng. 10, 106867. https://doi.org/10.1016/j.jece.2021.106867
- [23] Kaminsky, W., 2021. Chemical recycling of plastics by fluidized bed pyrolysis. Fuel Commun. 8, 100023. https://doi.org/10.1016/j.jfueco.2021.100023
- [24] Kaminsky, W., Kim, J.S., 1999. Pyrolysis of mixed plastics into aromatics. J. Anal. Appl. Pyrolysis 51, 127–134. https://doi.org/10.1016/S0165-2370(99)00012-1
- [25] Kremer, I., Tomić, T., Katančić, Z., Hrnjak-Murgić, Z., Erceg, M., Schneider, D.R., 2021. Catalytic decomposition and kinetic study of mixed plastic waste. Clean Technol. Environ. Policy 23, 811–827. https://doi.org/10.1007/s10098-020-01930-y
- [26] Kumar, S., Panda, A.K., Singh, R.K., 2011. A review on tertiary recycling of high-density polyethylene to fuel. Resour. Conserv. Recycl. 55, 893–910. https://doi.org/10.1016/j.resconrec.2011.05.005
- [27] Kunwar, B., Cheng, H.N., Chandrashekaran, S.R., Sharma, B.K., 2016. Plastics to fuel: a review. Renew. Sustain. Energy Rev. 54, 421–428. https://doi.org/10.1016/j.rser.2015.10.015
- [28] Lee, K.H., 2006. Thermal and catalytic degradation of waste HDPE, Feedstock Recycling and Pyrolysis of Waste Plastics: Converting Waste Plastics into Diesel and Other Fuels. https://doi.org/10.1002/0470021543.ch5
- [29] Li, C., Hayashi, J. ichiro, Sun, Y., Zhang, L., Zhang, S., Wang, S., Hu, X., 2021. Impact of heating rates on the evolution of function groups of the biochar from lignin pyrolysis. J. Anal. Appl. Pyrolysis 155, 105031. https://doi.org/10.1016/j.jaap.2021.105031
- [30] López, A., de Marco, I., Caballero, B.M., Laresgoiti, M.F., Adrados, A., 2011. Influence of time and temperature on pyrolysis of plastic wastes in a semi-batch reactor. Chem. Eng. J. 173, 62–71. https://doi.org/10.1016/j.cej.2011.07.037
- [31] Luiz, J., Alves, F., Constantino, J., Francisco, V., Francisco, R., Venicio, W., Galdino,

- D.A., Felix, R., Sena, D., 2019. Biomass and Bioenergy Kinetics and thermodynamics parameters evaluation of pyrolysis of invasive aquatic macrophytes to determine their bioenergy potentials. Biomass and Bioenergy 121, 28–40. https://doi.org/10.1016/j.biombioe.2018.12.015
- [32] Miandad, R., Barakat, M.A., Rehan, M., Aburiazaiza, A.S., Ismail, I.M.I., Nizami, A.S., 2017. Plastic waste to liquid oil through catalytic pyrolysis using natural and synthetic zeolite catalysts. Waste Manag. 69, 66–78. https://doi.org/10.1016/j.wasman.2017.08.032
- [33] Miskolczi, N., Juzsakova, T., Sója, J., 2019. Preparation and application of metal loaded ZSM-5 and y-zeolite catalysts for thermo-catalytic pyrolysis of real end of life vehicle plastics waste. J. Energy Inst. 92, 118–127. https://doi.org/10.1016/j.joei.2017.10.017
- [34] Mulu, E., M'Arimi, M.M., Ramkat, R.C., 2021. A review of recent developments in application of low cost natural materials in purification and upgrade of biogas. Renew. Sustain. Energy Rev. 145, 111081. https://doi.org/10.1016/j.rser.2021.111081
- [35] Nisar, J., Ali, G., Shah, A., Iqbal, M., Ali, R., Anwar, F., Ullah, R., Salim, M., 2019. Fuel production from waste polystyrene via pyrolysis: Kinetics and products distribution. Waste Manag. 88, 236–247. https://doi.org/10.1016/j.wasman.2019.03.035
- [36] Özsin, G., Eren, A., 2019. TGA / MS / FT-IR study for kinetic evaluation and evolved gas analysis of a biomass / PVC co-pyrolysis process. Energy Convers. Manag. 182, 143–153. https://doi.org/10.1016/j.enconman.2018.12.060
- [37] Panda, A.K., 2018. Thermo-catalytic degradation of different plastics to drop in liquid fuel using calcium bentonite catalyst. Int. J. Ind. Chem. 9, 167–176. https://doi.org/10.1007/s40090-018-0147-2
- [38] Qin, L., Han, J., Zhao, B., Wang, Y., Chen, W., Xing, F., 2018. Thermal degradation of medical plastic waste by in-situ FTIR, TG-MS and TG-GC/MS coupled analyses. J. Anal. Appl. Pyrolysis. https://doi.org/10.1016/j.jaap.2018.10.012
- [39] Quek, A., Balasubramanian, R., 2013. Liquefaction of waste tires by pyrolysis for oil and chemicals A review. J. Anal. Appl. Pyrolysis 101, 1–16. https://doi.org/10.1016/j.jaap.2013.02.016
- [40] Rathsack, P., Riedewald, F., Sousa-Gallagher, M., 2015. Analysis of pyrolysis liquid obtained from whole tyre pyrolysis with molten zinc as the heat transfer media using

- comprehensive gas chromatography mass spectrometry. J. Anal. Appl. Pyrolysis 116, 49–57. https://doi.org/10.1016/j.jaap.2015.10.007
- [41] Ratnasari, D.K., Nahil, M.A., Williams, P.T., 2017. Catalytic pyrolysis of waste plastics using staged catalysis for production of gasoline range hydrocarbon oils. J. Anal. Appl. Pyrolysis 124, 631–637. https://doi.org/10.1016/j.jaap.2016.12.027
- [42] Rehan, M., Miandad, R., Barakat, M.A., Ismail, I.M.I., Almeelbi, T., Gardy, J., Hassanpour, A., Khan, M.Z., Demirbas, A., Nizami, A.S., 2017. Effect of zeolite catalysts on pyrolysis liquid oil. Int. Biodeterior. Biodegrad. 119, 162–175. https://doi.org/10.1016/j.ibiod.2016.11.015
- [43] Ren, N., Bronić, J., Subotić, B., Song, Y.M., Lv, X.C., Tang, Y., 2012. Controllable and SDA-free synthesis of sub-micrometer sized zeolite ZSM-5. Part 2: Influence of sodium ions and ageing of the reaction mixture on the chemical composition, crystallinity and particulate properties of the products. Microporous Mesoporous Mater. 147, 229–241. https://doi.org/10.1016/j.micromeso.2011.06.022
- [44] Republic, S., 2004. ISOCONVERSIONAL METHODS Fundamentals, meaning and application 76, 123–132.
- [45] Sbirrazzuoli, N., Vincent, L., Mija, A., Guigo, N., 2009. Chemometrics and Intelligent Laboratory Systems Integral, differential and advanced isoconversional methods Complex mechanisms and isothermal predicted conversion time curves. Chemom. Intell. Lab. Syst. 96, 219–226. https://doi.org/10.1016/j.chemolab.2009.02.002
- [46] Senneca, O., Chirone, R., Masi, S., Salatino, P., 2002. A Thermogravimetric Study of Nonfossil Solid Fuels . 1 . Inert Pyrolysis 653–660.
- [47] Thahir, R., Irwan, M., Alwathan, A., Ramli, R., 2021a. Effect of temperature on the pyrolysis of plastic waste using zeolite ZSM-5 using a refinery distillation bubble cap plate column. Results Eng. 11, 100231. https://doi.org/10.1016/j.rineng.2021.100231
- [48] Thahir, R., Irwan, M., Alwathan, A., Ramli, R., 2021b. Effect of temperature on the pyrolysis of plastic waste using zeolite ZSM-5 using a refinery distillation bubble cap plate column. Results Eng. 11, 100231. https://doi.org/10.1016/j.rineng.2021.100231
- [49] Unnikrishnan, P., Srinivas, D., 2016. Heterogeneous Catalysis, Industrial Catalytic Processes for Fine and Specialty Chemicals. Elsevier Inc. https://doi.org/10.1016/B978-0-12-

801457-8.00003-3

- [50] Vyazovkin, S., Wight, C.A., 1999. Model-free and model-® tting approaches to kinetic analysis of isothermal and nonisothermal data 341, 53–68.
- [51] Wu, Jingli, Chen, T., Luo, X., Han, D., Wang, Z., Wu, Jinhu, 2014. TG/FTIR analysis on co-pyrolysis behavior of PE, PVC and PS. Waste Manag. 34, 676–682. https://doi.org/10.1016/j.wasman.2013.12.005
- [52] Xu, F., Wang, B., Yang, D., Hao, J., Qiao, Y., Tian, Y., 2018. Thermal degradation of typical plastics under high heating rate conditions by TG-FTIR: Pyrolysis behaviors and kinetic analysis. Energy Convers. Manag. 171, 1106–1115. https://doi.org/10.1016/j.enconman.2018.06.047
- [53] Zhang, J., Ren, S., Xu, W., Liang, C., Li, J., Zhang, H., Li, Y., Liu, X., Jones, D.L., Chadwick, D.R., Zhang, F., Wang, K., 2022. Effects of plastic residues and microplastics on soil ecosystems: A global meta-analysis. J. Hazard. Mater. 435, 129065. https://doi.org/10.1016/j.jhazmat.2022.129065
- [54] Zhu, H.M., Jiang, X.G., Yan, J.H., Chi, Y., Cen, K.F., 2008. TG-FTIR analysis of PVC thermal degradation and HCl removal. J. Anal. Appl. Pyrolysis 82, 1–9. https://doi.org/10.1016/j.jaap.2007.11.011
- [55] Ganesh, B., Barmavatu, P., Pohořelý, M., Jeremias, M., & Sikarwar, V. S. Optimization of Value-Added Products Using Response Surface Methodology from the Hdpe Waste Plastic by Thermal Cracking. *Available at SSRN 4581039*.
- [56] Ding, K., Zhong, Z., Wang, J., Zhang, B., Fan, L., Liu, S., ... & Ruan, R. (2018). Improving hydrocarbon yield from catalytic fast co-pyrolysis of hemicellulose and plastic in the dual-catalyst bed of CaO and HZSM-5. *Bioresource technology*, 261, 86-92.
- [57] Srivastava, R. (2018). Synthesis and applications of ordered and disordered mesoporous zeolites: Present and future prospective. *Catalysis Today*, *309*, 172-188.
- [58] Elordi, G., Olazar, M., Lopez, G., Amutio, M., Artetxe, M., Aguado, R., Bilbao, J., 2009. Catalytic pyrolysis of HDPE in continuous mode over zeolite catalysts in a conical

- spouted bed reactor. J. Anal. Appl. Pyrolysis 85, 345–351. doi.org/10.1016/j.jaap.2008.10.015
- [59] Uemichi, Y., Hattori, M., Itoh, T., Nakamura, J., & Sugioka, M. (1998). Deactivation behaviors of zeolite and silica—alumina catalysts in the degradation of polyethylene. *Industrial & engineering chemistry research*, *37*(3), 867-872.
- [60] Z. Tang *et al.*, "Contamination and risk of heavy metals in soils and sediments from a typical plastic waste recycling area in North China," *Ecotoxicol. Environ. Saf.*, vol. 122, pp. 343–351, 2015, doi: 10.1016/j.ecoenv.2015.08.006.
- [61] Vollmer, I., Jenks, M. J., Roelands, M. C., White, R. J., Van Harmelen, T., De Wild, P., ... & Weckhuysen, B. M. (2020). Beyond mechanical recycling: giving new life to plastic waste. *Angewandte Chemie International Edition*, 59(36), 15402-15423.

3.1. Introduction

This chapter presents a detailed description of the research methodology adapted to achieve the defined objectives in the thesis. Subsequently, elaborating the process of feedstock collection, raw material preparation and synthesis of catalyst. Various characterization techniques used for analyzing raw material, catalyst, as well as the obtained products are thoroughly elucidated. Additionally, a detailed experimental methodology and several methods applied to evaluate the kinetic parameters of the pyrolysis process are described.

3.2. Preparation of raw material

3.2.1 Feedstock used

The real - world plastic wastes like bottles, single-use plastic cutlery and straws, ice-cream cups, polythene cover, thermocol packaging materials etc., were collected from neighbouring surroundings and Institute's laboratories. The household waste bottles are the major source of HDPE, LDPE, PP, and PET, whereas the waste plastic obtained from cafeteria complex and laboratories are the major source of HDPE, PP, and PS.

3.2.2 Procedure of raw material preparation

To prepare the samples for the pyrolizer, the raw materials were washed and then kept in sun for drying and then oven dried at a temperature of 70-80 °C to remove any trace amount of moisture left behind. These oven dried raw materials were crushed into smaller pieces of size 0.5-1 mm using a mechanical crusher as shown in fig 3.1. These crushed forms were used to prepare pellets of size 13 and 25 mm with the help of a mechanically pressurized pelletizer. The bulk density of the waste polymers is in the range of 930 - 950 kgm⁻³.



Figure 3.1 Depicting the procedure of raw material preparation for pyrolysis process

3.3 Synthesis of catalyst

3.3.1 Materials used

Tetraethyl orthosilicate (TEOS, Si $(OC_2H_5)_4$, 28% SiO₂), tetra propylammonium hydroxide, 10% in water (TPAOH 10 wt.%, $C_{12}H_{29}NO$), and sodium aluminate (NaAlO₂, 52–54% Al₂O₃), were procured from Sigma-Aldrich Co. Ltd. Punjab, India.

3.3.2 Preparation of catalyst

Hierarchical mesoporous ZSM-5 catalyst was prepared by hydrothermal method as depicted in fig 3.2. The synthesis method was adapted from Wang et. al. and Krisnandi et. al. (Rohayati et al., 2017; Wang et al., 2010) with little modifications. Initially, NaAlO₂ (0.164 g), TPAOH 10 wt.% (2.1 mL), TEOS (14.3 mL) and 64.3 mL of double distilled H₂O were mixed under continuous stirring at 70 °C for 3 h until a homogeneous gel was obtained. The gel was having a molar ratio of 1Al₂O₃: 64.35SiO₂: 10.08 TPAOH: 3571.66 H₂O (Wang et al., 2010). Unless otherwise specified, the homogeneous gel was aged for 6 h at 1500 rpm and 90 °C on a hot plate stirrer. After aging, for crystallization, the gel was shifted into a 500 mL Teflon lined stainless steel (ss) autoclave and kept in an oven for 100 h at 180 °C. The crystallized powder was separated by filtration, dried in oven at 70 °C for 2 h, and calcined in muffle furnace at 550 °C for 8 h to remove the mesoporous template. Thus, obtained white powder was named hierarchical ZSM-5 and characterized by different scientific characterizations.

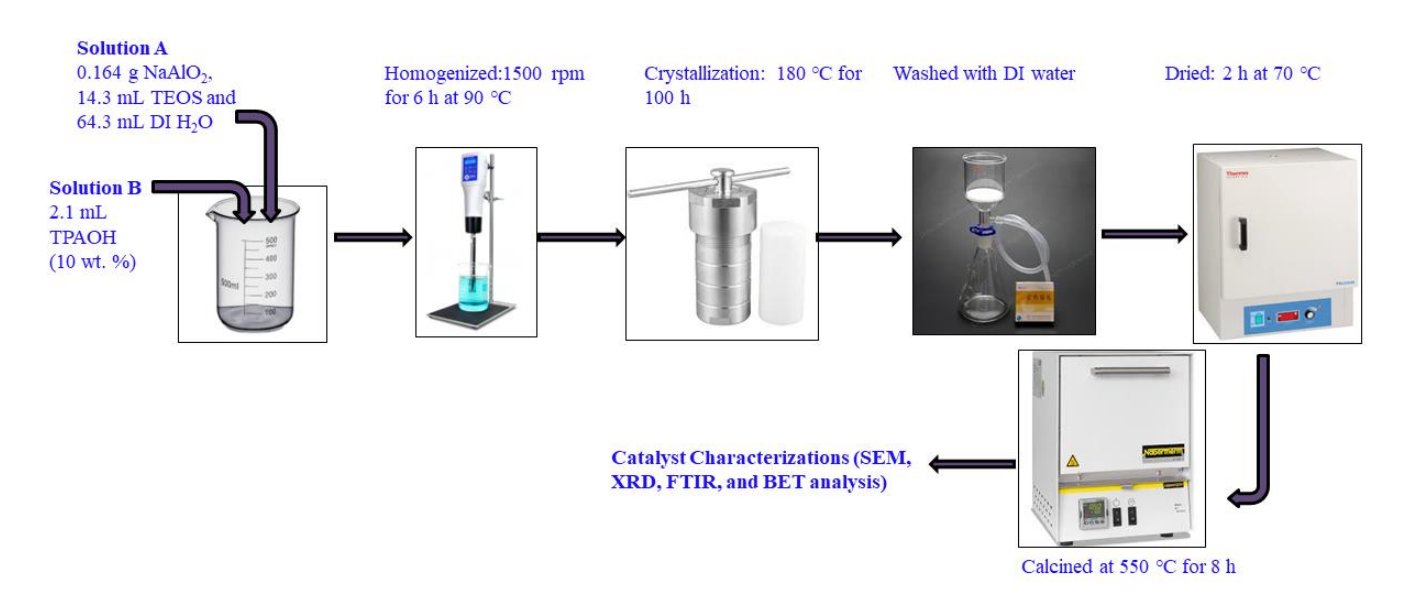


Figure 3.2 Catalyst preparation method for catalytic pyrolysis process

3.4 Various analytical characterization techniques used

The various analytical characterization techniques used for characterizing the raw material,

synthesized catalyst and obtained products are listed below:

- 1. Fourier transform infrared spectroscopy (FTIR)
- 2. BET-surface area
- 3. Thermo gravimetric analysis (TGA)
- 4. X-ray diffraction (XRD)
- 5. Scanning electron microscopy (SEM)
- 6. RAMAN Spectroscopy
- 7. Nuclear magnetic resonance spectroscopy (NMR)
- 8. Gas chromatography mass spectroscopy (GC-MS)

3.4.1 Fourier transform infrared spectroscopy (FTIR)

FT-IR is a simple, non-destructive, and efficient chemical technique used for identifying different types of plastic polymers. The Attenuated Total Reflectance-Fourier Transform Infrared (ATR-FTIR) spectroscopy is a common technique that can be used to investigate the molecular composition and structure through the determination of the various functional groups. It is a well-known and powerful analysis tool which produces characteristic spectrum called "inferogram" on transmission or absorbance of the IR radiation. On interaction of an infrared light with oil, chemical bond will stretch, contract, and absorb infrared radiation in a specific wavelength range regardless of the structure of the rest of the molecules. These inferograms represent different chemical functionalities present in materials, thereby helping in identification of various types of plastic polymers (Chércoles Asensio et al., 2009; Guidelli et al., 2011; I Noda et al., 2007; Smith, 2018; Tennakoon et al., 2020). These inferograms were acquired with a resolution of 4 cm⁻¹ averaging 64 scans with a total acquisition time of around 45 seconds for each spectrum in an ATR assembly of NICOLET iS50 FT-IR spectrometer. All the samples of raw material, catalyst and obtained liquid oil were analyzed in the wavenumber range of 4000 to 400.

3.4.2 BET- surface area

The textural properties of the catalyst, such as average pore size, pore volume and BET surface area, were determined using a Belsorp mini-X instrument. Prior to analysis, the catalysts were subjected to degassing at 300 °C for 3 h in a degassing chamber to remove any adsorbed moisture and impurities. Specific surface area and pore size distribution were determined through the application of the Brunauer-Emmett-Teller (BET) equation and the Barrett-Joyner-Halenda (BJH) method, respectively, in a relative pressure range of 0.01 to 0.9. Adsorption-desorption isotherms were also generated for the catalyst samples.

3.4.3 Thermogravimetric analysis (TGA)

During the non-isothermal TG analysis of different types of plastic, initially a certain amount of each of the samples was taken in an alumina (90 µl) crucible. The TG temperature was increased from 50 °C to 600 °C at different heating rates of 10, 15, 20, and 25 °C/min in each of the experiments. The nitrogen gas at a flowrate of 100 mL/min was selected to be the inert gas to maintain the inert environment like that of the actual pyrolysis experiment performed in the fixed bed reactor. Similarly, the TG analysis was performed for both the modal as well as the waste plastic samples. Also, the catalyst sample's thermal stability was checked by conducting TG analysis.

3.4.4 X-ray diffraction (XRD)

The crystal structure of calcined perovskite catalysts was investigated using X-ray diffraction (XRD) by utilizing a Rigaku Miniflex 600 diffractometer. The instrument was set at 30 kV and 10 mA and utilized Cu K α radiation (λ =1.5406 Å) within a 2 θ range of 5° to 90°, with a scanning speed of 4°/min. The identification of crystalline phases was carried out by utilizing the technique of X-ray diffraction, specifically by comparing the 2 θ values or d-spacing of the characteristic Bragg reflections of the investigated samples to those of reference samples as listed in the Inorganic crystal structure database (ICSD) database. The average crystallite size (D) of catalyst samples was obtained through the application of the Scherrer equation to the full width at half maximum (FWHM) of the X-ray diffraction peaks, after correcting for the instrumental broadening effect.

$$d = \frac{K * \lambda}{\beta * \cos\theta}$$

Where d is the crystallite size, K is dimensionless shape factor (taken as 0.9, by assuming spherical crystal), λ is wavelength of X-ray, and β represents instrumental broadening of the diffraction line, which corresponds to the Bragg angle (θ), quantitatively represented by the full width at half maximum (FWHM) of the corresponding diffraction peaks.

3.4.5 Scanning electron microscopy (SEM)

The scanning electron microscope (SEM) characterization technique utilizes a high-energy, focused electron beam to obtain a variety of signals from the specimen through interactions. The region within the specimen where the primary electron beam interacts with the sampleis referred to as the interaction volume. As the electron beam interacts with the sample surface, it produces various signals such as Auger electrons, secondary electrons, backscattered electrons, and X-rays. These signals provide information about the sample'smorphology, texture, and chemical composition. A typical SEM signal used to generate a 2D image of the sample's morphology is the secondary electrons. The SEM can achieve magnification levels between 20X and 105X with a spatial resolution of 20 nm. The electron gun, consisting of a filament and shield, generates a highly focused and energetic electronbeam through thermionic emission in an ultra-high vacuum. JEOL 6610LV scanning electron microscope (SEM) at 10 kV was used to study the surface morphology of the catalyst. Since the sample was highly conductive in nature, hence it was coated with a thin layer of platinum (Pt) before the examination.

3.4.6 RAMAN spectroscopy

Raman spectroscopy is a non-invasive technique used to analyze chemical compounds and determine their structural characteristics, phases, and polymorphs. This method is based on how light interacts with the chemical structure of a material, leading to most photons being scattered at the same wavelength as the incident light, known as Rayleigh scattering. A small fraction of photons is scattered at different wavelengths, known as Raman scattering, and the energy difference between the incident and scattered photons is called the Raman shift. Scattered photons with less energy than the incident photons are

known as Stokes scattering, while those with more energy are known as Anti-Stokes scattering. In the current study, Raman scattering measurements were conducted using a Renishaw via Raman microscope and a LabRam Horiba scientific instrument with 532 nm excitation laser.

3.4.7 Nuclear magnetic resonance spectroscopy (NMR)

NMR spectra are unique, well-resolved, analytically tractable, and often highly predictable for small molecules. NMR is used to identify the molecular structure of any compound at their atomic level. NMR technique uses specific magnetic properties of atomic nuclei and produces the different signals in the form of chromatogram when exposed to external magnetic field. This technique is very helpful in distinguishing identical functional groups having differing neighboring substituents. A JEOL JNM ECS400 type spectrometer performing at 400 MHz was used for measuring ¹H nuclear magnetic resonance spectra of pyrolytic oil. ¹H NMR spectra were recorded in Chloroform-d (CDCl3) (99.8%, Sigma- Aldrich). Tetramethyl silane (TMS) was used as an internal standard and reference for chemical shifts. The measuring conditions were 32 scans, 2 s recycle delay, 7.6 μs /2 pulse length and 16 K time-domain data.

3.4.8 Gas chromatography mass spectroscopy (GC-MS)

GC–MS technique which is a strong tool to identify the hydrocarbon composition of liquid fuels. It provides critical information about unsaturated and saturated carbon species by estimating the carbon number distribution quantitatively and qualitatively in higher hydrocarbons. GC-MS mounted with AGILENT DB-5 column (length 30 m, diameter 0.25mm. thickness 0.25 µm and temperature 60-325 °C) was used to identify the compounds present in the liquid product obtained from thermal and catalytic cracking of the plastic wastes. To detect the compounds, the following temperature program was used in GC-MS: the injector temperature was set at 280 °C, and high-purity helium gas was used as carrier gas with the split ratio of 1:20. Initially, the oven was heated to 50 °C and held at this temperature for 5 min; afterwards, the oven temperature was increased from 50 to 280 °C at a ramping rate of 5 °C/min and held for 5 min. For the MS measurements, an ionization energy of 70 eV from the electron ionization (EI) was used with a scan per second over the m/z range of 30–500 amu, and

3.5 Experimental set-up for thermal pyrolysis process

A schematic diagram of experimental set up used for thermal cracking of the plastic waste is shown in fig. 3.3. The thermal cracking experimental set up consisted of an electrical furnace, fixed-bed pyrolizer, condenser, chiller, liquid product collector and a nitrogen gas cylinder. The pyrolizer is the heart of the experimental set up. The pyrolizer was designed with the following dimensions; diameter = 50 mm and height = 1000 mm with stainless steel 316 grade material to enhance the resistance to chemical corrosion and to withstand the inside pressure up to 15 bar. It was heated by an external vertical two-zone electric furnace and was able to attain higher temperatures up to 800 °C at different heating rates. Thermocouples were mounted in each of the two zones of the electric furnace to monitor the temperature at the wall of the reactor at different positions along the length of the pyrolizer. These thermocouples provided in both zones were made moveable only in the horizontal direction to provide the freedom of using reactors of different diameters in the same electric furnace. The bottom flange of the pyrolizer is connected with the Nitrogen gas flow stream and the top flange is connected with a condenser and a thermocouple to monitor the inside temperature of the pyrolizer during the thermal cracking reaction. An inert environment is maintained inside the pyrolizer by using a continuous flow of the nitrogen gas in an upward direction. The condenser is used for condensing the organic vapors into liquid formed during the thermal cracking of the plastic. The condensing fluid (water) is pumped inside the condenser with the help of a chilling unit to maximize the condensation of the organic vapors into liquid. A 2-neck round bottom flask is connected at the bottom of the condenser for collecting the liquid product. The uncondensed vapors (gases) formed during the thermal cracking is vent out from the round bottom flask through an exhaust stream. After the reactor got cooled down the residue (char) and wax of the pyrolysis process was collected in a Petri dish and measured for material balance.

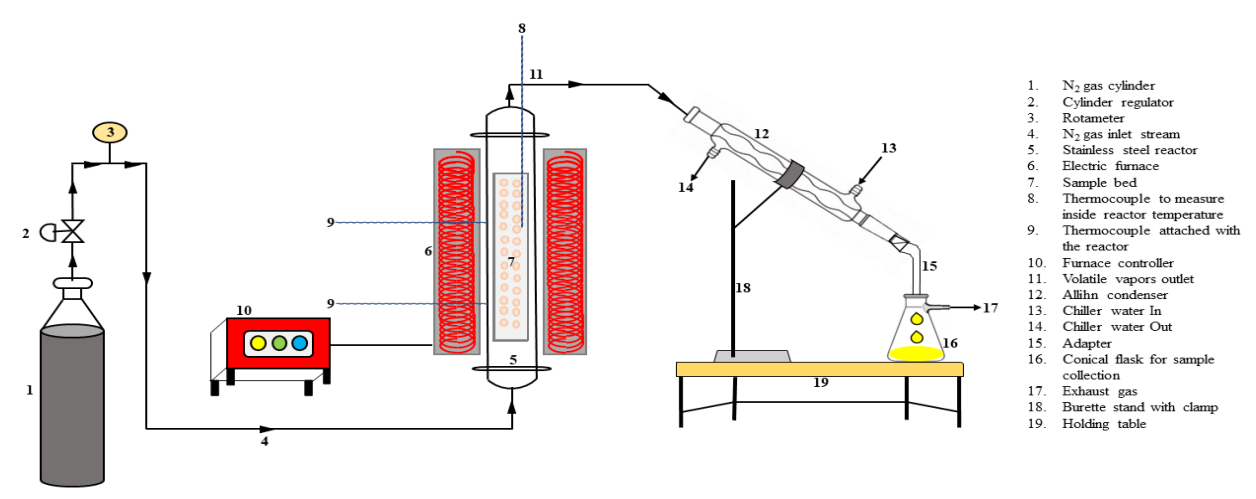


Figure 3.3 Fixed -bed reactor set-up for thermal pyrolysis of different plastic waste

Thermal cracking of the plastic wastes LDPE, HDPE, PP, PS and PET were carried in the fixed-bed pyrolizer maintained at a desired temperature range of 450 - 480 °C from room temperature with a heating rate of 15 °C/min for 60 min. The fixed-bed pyrolizer was loaded with 20 g of plastic waste (pellets = 25 mm) supported on a bed of super fine glass wool (high temperature insulating material). The pyrolizer was purged continuously with nitrogen gas at a flowrate of 60 mL/min to maintain an inert environment for the thermal pyrolysis reaction. The range of desired heating rate and the optimum cracking temperature for the different types of real-world plastic wastes were determined by TGA analysis performed in TA SDT 650 thermal analyzer.

The yields of liquid, wax(solid), residue and gas products were calculated using following equations (1), (2), (3) and (4) respectively.

$$Liquidyield(\%) = \left(\frac{Weight \ of \ the \ liquid \ product}{Weight \ of \ plastics \ feed}\right) 100 \tag{3.1}$$

Wax (solid) yield (%) =
$$\left(\frac{Weight\ of\ wax\ product}{weight\ of\ plastic\ feed}\right)$$
100 (3.2)

Residue yield (%) =
$$\left(\frac{Weight\ of\ residue\ product}{Weight\ of\ the\ plastic\ feed}\right)$$
100 (3.3)

Gas yield (%) =
$$100 - wt$$
. % (liquid yield + wax yield + residue yield) (3.4)

3.6.1

Fig. 3.4 depicts the schematic diagram of the fixed-bed reactor set-up used for carrying out the catalytic pyrolysis process of the real-world plastic wastes. The catalytic pyrolysis process of the plastic wastes HDPE, LDPE, PP, and PS was accomplished in the fixed-bed pyrolizer. After running a few sets of test runs, the optimized process conditions were achieved and accordingly, the pyrolizer was heated with a heating rate of 15 °C/min to maintain a temperature range of 400 – 430 °C for 45 min.

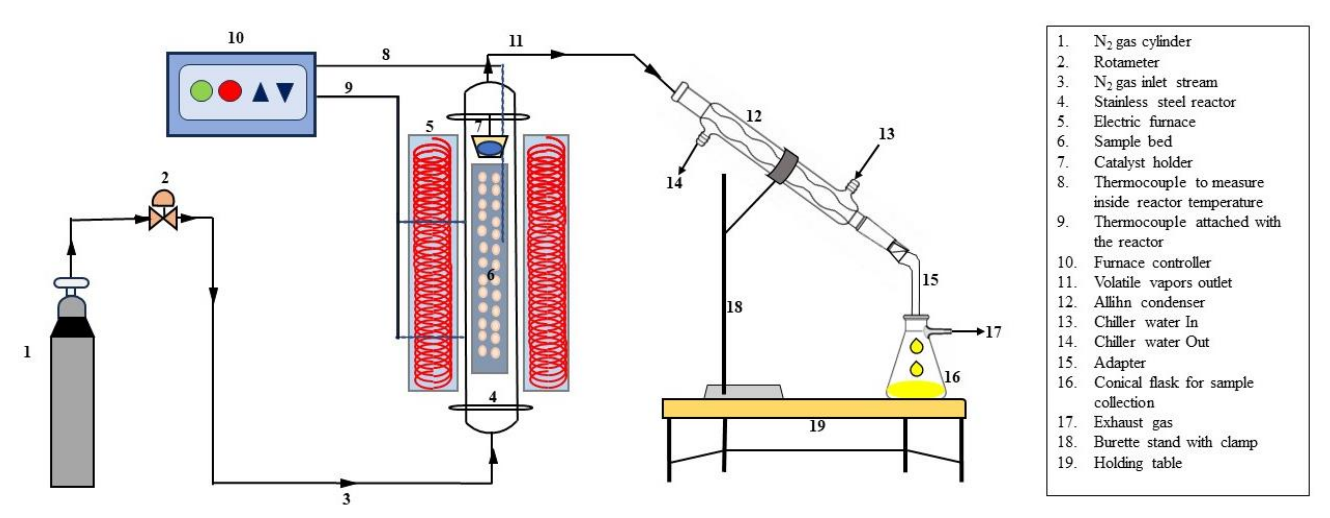


Figure 3.4 Schematic diagram of catalytic pyrolysis process of different plastic wastes in a fixedbed reactor set-up

The pyrolizer was loaded with 20 g of plastic waste (pellets = 25 mm) supported on a bed of super fine glass wool (high temperature insulating material). 2g of catalyst (pellets = 13mm, were broken into pieces) was taken in the catalyst holder to maintain the ratio of 10:1 of plastic to catalyst. A continuous flowrate of 60 mL/min of N_2 gas was employed to purge the pyrolizer and to maintain an inert environment within during the process.

The liquid oils obtained from thermal and catalytic pyrolysis of plastic wastes were characterized by various analytical techniques as mentioned earlier. Also, fuel properties like HHV and viscosity of the obtained liquid oils were analyzed by using bomb calorimeter and rheometer respectively. The manual calculation procedure used to calculate the HHV of the obtained liquid oils is as follows;

Step 1: Calculate water equivalent

$$W = \frac{6318 \times wt. of \ sample + (Gross \ calorific \ value \ _{Nichrome \ wire} + Gross \ calorific \ value \ _{Cotton \ thread})}{\Delta T}$$

Here, weight of cotton thread of 10 cm length = 0.015g weight of nichrome wire of 8 cm length = 0.022g

Step 2: Gross calorific value (HHV)

$$HHV = \frac{W \times \Delta T - (Gross\ calorific\ value\ _{Nichrome\ wire} + Gross\ calorific\ value\ _{Cotton\ thread})}{wt.\ of\ sample}$$

3.7 Theoretical considerations for kinetic study of thermal pyrolysis

Pyrolysis of the real-world plastic waste is an example of solid-state reaction. During thermal pyrolysis the conversion (a) of solid reactant into gas phase product by heat manifests the extent of the degradation reaction. Hence the calculation of α becomes dependent on the temperature (T) employed to the reaction. The amount of heat required by the reactants to convert into products i.e., E_{α} plays a significant role in determining the extent of the reaction. Since pyrolysis of real-world plastic waste is a multistep process and has a complex reaction mechanism, the determination of E_{α} at each step is highly complicated. The thermal degradation of real-world plastic waste during pyrolysis causes the cracking of large molecular weight waste polymers into smaller molecular weight polymers via several physicochemical phenomena such as; melting, sublimation, polymorphic transformation, degradation, occurring simultaneously etc (Bujak, 2015). Therefore, to get an understanding about the multistep reaction mechanism of thermal cracking reaction, a comprehensive study of reaction kinetics and mechanism is necessary. Kinetic analysis of the solid-state reaction lays the foundation for the designing and implementation of the thermal cracking reaction (thermal pyrolysis) for plastic materials. Meticulous calculation of the kinetic triplet, E_{α} , A_0 and $f(\alpha)$ manifests the accuracy of the thermal cracking reaction (Das and Tiwari, 2017). The non-isothermal TGA, is a promising and only route to determine the macroscopic kinetics of the complex thermal cracking process (Das and Tiwari, 2017). This helps in building the backbone of understanding any complex process like pyrolysis. However, several computational methods are required to analyze the datasets obtained from TGA experiment. International Confederation for Thermal Analysis Calorimetry (ICTAC) has recommended various Isoconversional methods for evaluation of the kinetic parameters (Kremer et al., 2021). The activation energy distribution is calculated by using the thermal degradation data obtained from TGA analysis by these isoconversional methods (Vyazovkin and Wight, 2010). This

variance in the E_{α} accounts for the complexity of the thermal degradation process at different steps by quantifying the energy barrier of individual steps (Das and Tiwari, 2017; Friedman, 2007).

Generally, the conversion of solid plastic waste into gaseous products by thermal cracking is shown as follow:

$$\alpha = \frac{m0 - mt}{m0 - mf} \tag{3.5}$$

Here, α = the reaction conversion

 m_0 = the initial mass of sample at t = 0

 $m_t = mass of sample at time t and$

 m_f = the final mass of sample at t = f, respectively. The rate of conversion in this solid-gas reaction usually follows the following fundamental rate equation:

$$\frac{d\alpha}{dt} = kf(\alpha) \tag{3.6}$$

where $f(\alpha)$ = reaction model and

k = the rate constant. The rate constant k, is expressed as shown in equation (7) according to Arrhenius equation:

$$k = Aexp\left(-\frac{E}{RT}\right) \tag{3.7}$$

Here, A = pre-exponential factor or frequency factor, (min^{-1})

 $E = activation energy, (kJ.mol^{-1})$

 $R = universal gas constant (8.314 J·mol^{-1}·K^{-1})$

T =the reaction temperature, (K)

On combining the equations. (6) and (7), the rate of reaction is expressed as shown in equation (8):

$$\frac{d\alpha}{dt} = A \exp\left(-\frac{E}{RT}\right) f(\alpha) \tag{3.8}$$

It is assumed that β is the heating rate and expressed as, $\beta = dT/dt$. On combining the β with the equation (8), it results in a new equation as follow:

$$\frac{\beta d\alpha}{dT} = A \exp\left(-\frac{E}{RT}\right) f(\alpha) \tag{3.9}$$

On rearranging equation (9), we obtain equation (10) as follows:

$$\frac{d\alpha}{df}(\alpha) = \left(\frac{A}{\beta}\right) exp\left(-\frac{E}{RT}\right) \tag{3.10}$$

It is assumed that $\alpha = \int_0^\alpha \frac{d\alpha}{df(\alpha)}$, the equation is expressed as shown below:

$$g(\alpha) = \int_0^\alpha \frac{d\alpha}{df(\alpha)} = \left(\frac{A}{B}\right) \int_{T_0}^T exp\left(-\frac{E}{RT}\right) dT = \left(\frac{AE}{BR}\right) p\left(\frac{E}{RT}\right)$$
(3.11)

As discussed already several model free or isoconversional methods and model fitting methods are used to calculate the kinetic triplets. These kinetic models basically help in predicting the rate of reaction by determining the three kinetic parameters i.e., A_0 , E_α , and $f(\alpha)$.

3.7.1 Evaluation of kinetic parameters by isoconversional or model-free methods

Model-free methods or the isoconversional methods are one type of mathematical kinetic models extensively used for evaluating the kinetic parameters of the pyrolysis process. Iso-conversional methods works in a model-independent way to estimate the E_{α} required for achieving different conversion (Özsin and Pütün, 2017). These basically employ the principle that with change in heating rate (β), the rate of reaction (d α /dt) changes at a constant conversion (α). In this study, five model-free methods such as Ozawa-Flynn-Wall (OFW) (Flynn and Wall, 1966; Ozawa T., 1965), Kissinger-Akahira- Sunose (KAS) (Kissinger HE. 1957; Akahira T and Sunose T., 1971), Starink (Friedman HL. 1964), Tang and Boswell method were used for carrying out kinetic study of thermal degradation of real-world plastic waste.

3.7.1.1 Ozawa-Flynn-Wall (OFW) method

The OFW method is an iso-conversational and integral model free method that includes measurement of the temperature at given values of conversion at various heating rates [17]. In this method, Equation (9) is integrated utilizing Doyle's approximation to evaluate the kinetic constants.

$$ln(\beta) = \ln\left(\frac{A E_{\alpha}}{Rg(x)}\right) - 4.9575 - 1.052 \frac{E_{\alpha}}{RT}$$
 (3.12)

The E α can be obtained from the slope by plotting term ln(b) against 1/T, where the term ln $\left(\frac{A E_{\alpha}}{Rg(x)}\right)$ – 4.9575 is the integration constant that can be determined from the y-intercept.

The following relationship can be used to determine A for known values of x and Eα:

$$A = \frac{-\beta R}{E_{\alpha}} (\ln[1 - x]) 10^{\alpha}$$
 (3.13)

where a is a numerical integration constant based on the Doyle approximation.

3.7.1.2 Kissinger-Akahira- Sunose (KAS) method

KAS is an alternative model free method that considers in the derivation the peak temperature (T_m) at the maximum reaction rate value. Therefore, this method adopts the following equation to estimate the E_{α} for different values of T_m and β .

$$\ln \frac{\beta}{T_m^2} = \ln \left(\frac{RA}{g(x) E_\alpha} \right) - \frac{E_\alpha}{RT}$$
 (3.14)

For a progressive value of conversion degree, the term $\ln \frac{\beta}{T_m^2}$ is plotted against 1/T to give a straight-line slope of E_{α}/R ; hence, the apparent E_{α} can be determined, while the value of A can be calculated from Equation (11).

$$A(\beta) = \frac{\beta E_{\alpha}}{RT_{m}^{2}} e^{-\frac{E_{\alpha}}{RT_{p}}}$$
(3.15)

3.7.1.3 Starink method

Starink (1996) examined the above two iso-conversional techniques i.e., KAS (Kissinger-Akhira-Sunose) and OFW (Ozawa- Flynn-Wall) and further optimised the values of constants to much more accurate order of magnitude and can be expressed as shown in the equation 3.16.

$$\ln\left(\frac{\beta_i}{T_{\alpha i}^{1.92}}\right) = const - 1.0008 \left(\frac{E_{\alpha}}{RT_{\alpha}}\right) \tag{3.16}$$

The slope of the graph obtained from $\ln (\beta / T^{1.92})$ vs 1/T provides the value of kinetic parameters at each conversion.

3.7.1.4 Tang method

Similarly, Tang offered another kinetic equation for evaluation of the kinetic parameters.

$$\ln\left(\frac{\beta}{T^{1.894661}}\right) = -1.00145033 \left(\frac{E}{RT}\right) + C \tag{3.17}$$

The slope of the graph obtained from ln (β /T^{1.894661}) vs 1/T provides the value of kinetic parameters at each conversion.

3.7.1.5 Boswell method

$$\ln\left(\frac{\beta}{T}\right) = \left(\frac{E}{RT}\right) + C \tag{3.18}$$

The slope of the graph obtained from $\ln (\beta / T)$ vs 1/T provides the value of kinetic parameters at each conversion.

3.7.2 Prediction of decomposition model

By using model-free methods only the E_{α} can be calculated out of the three kinetic parameters. Whereas model-fitting methods uses the principle of fitting data in different models. For following this procedure, the model fitting methods first consider the reaction mechanism function $g(\alpha)$, and check the best fitting mechanism into the kinetic data. And then evaluates other kinetic parameters. In the present work, the kinetic analysis was studied by Criado method (Criado, 1978) and Coats-Redfern (CR) method (Coats AW and Redfern JP., 1964). The most commonly used reaction mechanisms for solid-state thermal degradation (Vyazovkin et al., 2011) are listed in Table 3.1.

Table 3.0.1 Most commonly used reaction mechanism for the solid-state thermal degradation

| Models | Reaction mechanisms | Code | f(a) | g(a) |
|------------------|----------------------|------|--|--------------------------------------|
| Diffusion models | 1D diffusion | D1 | $1/2\alpha^{-1}$ | α^2 |
| | 2D diffusion | D2 | $[-\ln{(1-\alpha)}]^{-1}$ | $(1-\alpha) \ln (1-\alpha) + \alpha$ |
| | 3D diffusion | D3 | $(3/2) (1-\alpha)^{2/3}/[(1-(1-\alpha)1/3)]^{-1}$ | $[1 - (1 - \alpha)^{1/3}]^2$ |
| Geometrical | 1D phase boundary | R1 | 1 | α |
| contraction | Contracting Sphere | R2 | $2(1-\alpha)^{1/2}$ | $[1 - (1 - \alpha)^{1/2}]$ |
| models | Contracting Cylinder | R3 | $3(1-\alpha)^{2/3}$ | $[1 - (1 - \alpha)^{1/3}]$ |
| Nucleation | 2D nucleation | A2 | $2(1 - \alpha) [-\ln (1 - \alpha)]^{1/2}$ | $[-\ln{(1-\alpha)}]^{1/2}$ |
| models | (Avarami-Erofe've) | | | |
| | 3D nucleation | A3 | $3(1 - \alpha) \left[-\ln (1 - \alpha) \right]^{2/3}$ | $[-\ln{(1-\alpha)}]^{1/3}$ |
| | (Avarami-Erofe've) | | | |
| | Avarami-Erofe've | A4 | $4(1 - \alpha) \left[-\ln (1 - \alpha)\right]^{3/4}$ | $[-\ln{(1-\alpha)}]^{1/4}$ |
| | Power law | P2 | $2 \alpha^{1/2}$ | $lpha^{1/2}$ |
| | Power law | P3 | $3 \alpha^{2/3}$ | $lpha^{1/3}$ |
| | Power law | P4 | $4 \alpha^{3/4}$ | $lpha^{1/4}$ |
| Reaction order | First order | F1 | 1- α | -ln (1- α) |
| models | Second order | F2 | $(1 - \alpha)^2$ | $(1-\alpha)^{-1}-1$ |
| | Third order | F3 | $(1 - \alpha)^3$ | $(1/2)[(1-\alpha)^{-2}-1]$ |

The Coats-Redfern method can be derived from equations (11) and (9) by using an asymptotic approximate, and expressed as follow:

$$g(\alpha) = \left(\frac{ART2}{\beta E}\right) \left(1 - \frac{2RT}{E}\right) \exp\left(-\frac{E}{RT}\right)$$
(3.19)

Here, $g(\alpha)$ = reaction mechanism function. By taking logs on both sides of the equation (3.19), a new equation correlating $\ln(g(\alpha)/T^2)$ with (1/T) is obtained. Also, the second term in equation (3.19) can be neglected as (2RT/E >> 1):

$$\ln\left[\frac{g\left(\alpha\right)}{T^{2}}\right] = \ln\left(\frac{AR}{\beta T}\right) - \frac{E}{RT} \tag{3.20}$$

The second model fitting method used was Criado method. The experimental data obtained from the TGA experiment were compared with the theoretical data obtained from $g(\alpha)$, to identify the best suitable $f(\alpha)$ of the thermal degradation for each of the real-world plastic waste. Equation 3.20, expresses the Criado method.

$$\frac{Z(\alpha)}{Z(0.5)} = \frac{f(\alpha).g(\alpha)}{f(0.5).g(0.5)} = \left(\frac{T_{\alpha}}{T_{0.5}}\right)^2 = \frac{\left(\frac{d\alpha}{dt}\right)_{\alpha}}{\left(\frac{d\alpha}{dt}\right)_{0.5}}$$
(3.20)

Here, $T_{0.5}$ = temperature at $\alpha = 0.5$

 $(d\alpha/dt)_{0.5}$ = conversion rate at $\alpha = 0.5$

 $\frac{f(\alpha).g(\alpha)}{f(0.5).g(0.5)}$ = theoretical curve, and are expressed in table 2.

 $\frac{\left(\frac{d\alpha}{dt}\right)_{\alpha}}{\left(\frac{d\alpha}{dt}\right)_{0.5}}$ = the reduced rate curve, obtained from TG experimental data.

3.8 References

- [1] Bujak, J.W., 2015. Thermal utilization (treatment) of plastic waste. Energy 90, 1468–1477. https://doi.org/10.1016/j.energy.2015.06.106
- [2] Chércoles Asensio, R., San Andrés Moya, M., De La Roja, J.M., Gómez, M., 2009. Analytical characterization of polymers used in conservation and restoration by ATR-FTIR spectroscopy. Anal. Bioanal. Chem. 395, 2081–2096. https://doi.org/10.1007/s00216-009-3201-2
- [3] Criado, J.M., 1978. Kinetic analysis of DTG data from master curves. Thermochim. Acta 24, 186–189. https://doi.org/10.1016/0040-6031(78)85151-X
- [4] Das, P., Tiwari, P., 2017. Thermal degradation kinetics of plastics and model selection. Thermochim. Acta 654, 191–202. https://doi.org/10.1016/j.tca.2017.06.001
- [5] Guidelli, E.J., Ramos, A.P., Zaniquelli, M.E.D., Baffa, O., 2011. Green synthesis of colloidal silver nanoparticles using natural rubber latex extracted from Hevea brasiliensis. Spectrochim. Acta Part A Mol. Biomol. Spectrosc. 82, 140–145. https://doi.org/10.1016/j.saa.2011.07.024
- [6] Kremer, I., Tomić, T., Katančić, Z., Hrnjak-Murgić, Z., Erceg, M., Schneider, D.R., 2021. Catalytic decomposition and kinetic study of mixed plastic waste. Clean Technol. Environ. Policy 23, 811–827. https://doi.org/10.1007/s10098-020-01930-y
- [7] Noda, I., Dowrey, A. E., Haynes, J. L., & Marcott, C. (2007). Group frequency assignments for major infrared bands observed in common synthetic polymers. In Physical properties of polymers handbook (pp. 395-406). New York, NY: Springer New York.
- [8] Özsin, G., Pütün, E., 2017. Kinetics and evolved gas analysis for pyrolysis of food processing wastes using TGA / MS / FT-IR. https://doi.org/10.1016/j.wasman.2017.03.020
- [9] Rohayati, Krisnandi, Y.K., Sihombing, R., 2017. Synthesis of ZSM-5 zeolite using Bayat natural zeolite as silica and alumina source. AIP Conf. Proc. 1862, 5–10. https://doi.org/10.1063/1.4991198
- [10] Smith, B. C. (2018). Infrared spectral interpretation: a systematic approach. CRC press. https://doi.org/10.1201/9780203750841
- [11] Tennakoon, A., Wu, X., Paterson, A.L., Patnaik, S., Pei, Y., LaPointe, A.M., Ammal, S.C., Hackler, R.A., Heyden, A., Slowing, I.I., Coates, G.W., Delferro, M., Peters, B., Huang, W., Sadow, A.D., Perras, F.A., 2020. Catalytic upcycling of high-density polyethylene via a processive mechanism. Nat. Catal. 3, 893–901. https://doi.org/10.1038/s41929-020-00519-4

- [12] Vyazovkin, S., Burnham, A.K., Criado, J.M., Pérez-Maqueda, L.A., Popescu, C., Sbirrazzuoli, N., 2011. ICTAC Kinetics Committee recommendations for performing kinetic computations on thermal analysis data. Thermochim. Acta 520, 1–19. https://doi.org/10.1016/j.tca.2011.03.034
- [13] Vyazovkin, S., Wight, C.A., 2010. International Reviews in Physical Chemistry Isothermal and non-isothermal kinetics of thermally stimulated reactions of solids. https://doi.org/10.1080/014423598230108
- [14] Wang, L., Zhang, Z., Yin, C., Shan, Z., Xiao, F.S., 2010. Hierarchical mesoporous zeolites with controllable mesoporosity templated from cationic polymers. Microporous Mesoporous Mater. 131, 58–67. https://doi.org/10.1016/j.micromeso.2009.12.001

4.1 Introduction

Thermal pyrolysis process is a thermochemical reaction used for thermally degrading polymeric heavy molecular weight compounds into lighter and smaller molecular weight compounds in the absence of oxygen. In plastic pyrolysis process, larger plastic molecules are treated at higher temperatures to initiate the molecular breakdown resulting into smaller molecules such as liquid oil, gas and carbon residue or char molecules.

This chapter presents a comprehensive study about the thermal pyrolysis of the real - world plastic waste in a tubular fixed- bed reactor to convert heavy plastic molecules into lighter fuel grade aromatic rich liquid oil. It includes a detailed perusal of various parameters affecting the thermal pyrolysis process of real-world plastic waste for effective conversion and highest yield of the desired product. These significant parameters include reaction temperature, heating rate, reaction time and inert gas flowrate. In the present work, the different plastic wastes were exposed to controlled heat treatment in a fixed-bed reactor under inert environment condition to undergo thermal cracking and producing volatile vapors. These volatile vapors are then condensed into lighter molecular weight i.e., $C_6 - C_{22}$ hydrocarbon liquid oil. The non-condensable gases are then passed through hydro traps and then vent out. The obtained liquid oils were characterized by different techniques such as, FTIR, GC-MS, 1H-NMR, rheometer, bomb calorimeter.

4.2 Results and discussion

4.2.1 Raw material characterizations

This section contains the detailed discussion about the physicochemical composition by proximate and ultimate analysis, functional groups determining the polymeric nature of the raw materials by FTIR and to investigate the thermal decomposition of the raw materials under inert environment as a function of time and temperature by TGA.

4.2.1.1 Proximate and Ultimate analysis of the raw material

The proximate analysis is used to determine the volatile content, moisture content, ash content and fixed carbon content present in the different types of plastic waste taken in the present work, i.e., LDPE, HDPE, PP, and PS. Whereas the ultimate analysis helps in quantifying the presence of the elements such as carbon, hydrogen, nitrogen, sulphur, and oxygen in the given plastic wastes.

The proximate analysis was done in accord with the standards ASTM E790, E897 and E830. The standard ASTM E790 is used to determine the residual moisture content in the materials, usually the fuel materials. In the present study, for determining the moisture content in each of the raw material, 1 g of each of the plastic waste was taken into a silica crucible and placed inside the oven at a temperature of the 105 °C for 1 hour duration. Volatile matter was determined by using standard ASTM E897. For this, 1 g of each of the plastic waste was taken in a crucible and kept in a muffle furnace at 950 °C for 7 min and then left to cool down. Similarly, the standard ASTM E830 was used for determining the ash content. And for this, 1 g of each of the plastic was taken in a crucible and kept in the muffle furnace for 1 hour at 550 °C. The fixed carbon content is obtained from the difference between the total mass taken of the plastic waste sample and the sum of volatile matter and ash content. For determining the elemental composition of carbon, hydrogen, nitrogen, and sulphur, FLASH 2000 CHNS/O Analyzer (Thermo Scientific) was employed. The analysis was performed with the oven maintained at 65 °C and the furnace maintained at 950 °C. The difference between the elemental analyzer report provides the oxygen percentage. To have a comparison between the physicochemical properties of the waste and virgin plastics, the virgin forms of plastics were procured commercially and processed through the same three standards for determining the volatile matter, moisture content and ash content respectively. These virgin forms of plastics were referred as "modal" in this work.

Table 4.1 shows the results of volatile matter, moisture and ash contents obtained in waste plastics and their modal forms. Higher quantities of volatile matter with lower values of ash content and fixed carbon content were observed. This result is designated with the production of liquid oil from plastic wastes when treated thermally under controlled heating and inert environment (Anuar Sharuddin et al., 2016). It was observed that the oxygen content in the waste forms were higher as compared with that of the modal forms. These higher oxygen contents are responsible for the presence of the oxygen

derivative compounds in the liquid oil. The presence of oxygen derivative compounds contributes to the impurities in the liquid oil and results in lowering of the calorific value. To remove these oxygen derivative compounds from the liquid oil, further oil upgradation techniques are required and these in turn causes the increase in the cost of processing.

Table 4.1 Proximate and ultimate analysis of modal plastic and real-world plastic waste

| Plastic | Source | Proximate analysis (wt.% dry basis) | | | Ultimate analysis (wt.% dry basis) | | | | | |
|--------------|--------|-------------------------------------|------|---------|------------------------------------|------|------|------|-------|--|
| | | | | | | | | | | |
| | | Volatile matter | Ash | Fixed | C | Н | N | S | O_p | |
| | | | | carbona | | | | | | |
| HDPE | Modal | 99.95 | - | 0.05 | 84.8 | 14.3 | - | - | 0.9 | |
| $(C_2H_4)_n$ | Waste | 96.08 | - | 3.92 | 68.7 | 5.1 | 4.1 | 3.2 | 18.9 | |
| LDPE | Modal | 99.94 | - | 0.06 | 84.1 | 14.1 | - | - | 1.8 | |
| $(C_2H_4)_n$ | Waste | 93.00 | - | 7.00 | 64 | 6.5 | 1.4 | 4.7 | 23.4 | |
| PP | Modal | 99.95 | - | 0.05 | 84 | 14 | - | - | 2.0 | |
| $(C_3H_6)_n$ | Waste | 95.57 | - | 4.43 | 69.1 | 7.1 | 4.7 | 4 | 15.1 | |
| PS | Modal* | 99.30 | 0.50 | 0.20 | 90.40 | 8.56 | 0.18 | 0.07 | 0.08 | |
| $(C_8H_8)_n$ | Waste | 99.96 | - | 0.04 | 62.3 | 4.1 | 4.2 | 3.7 | 25.7 | |

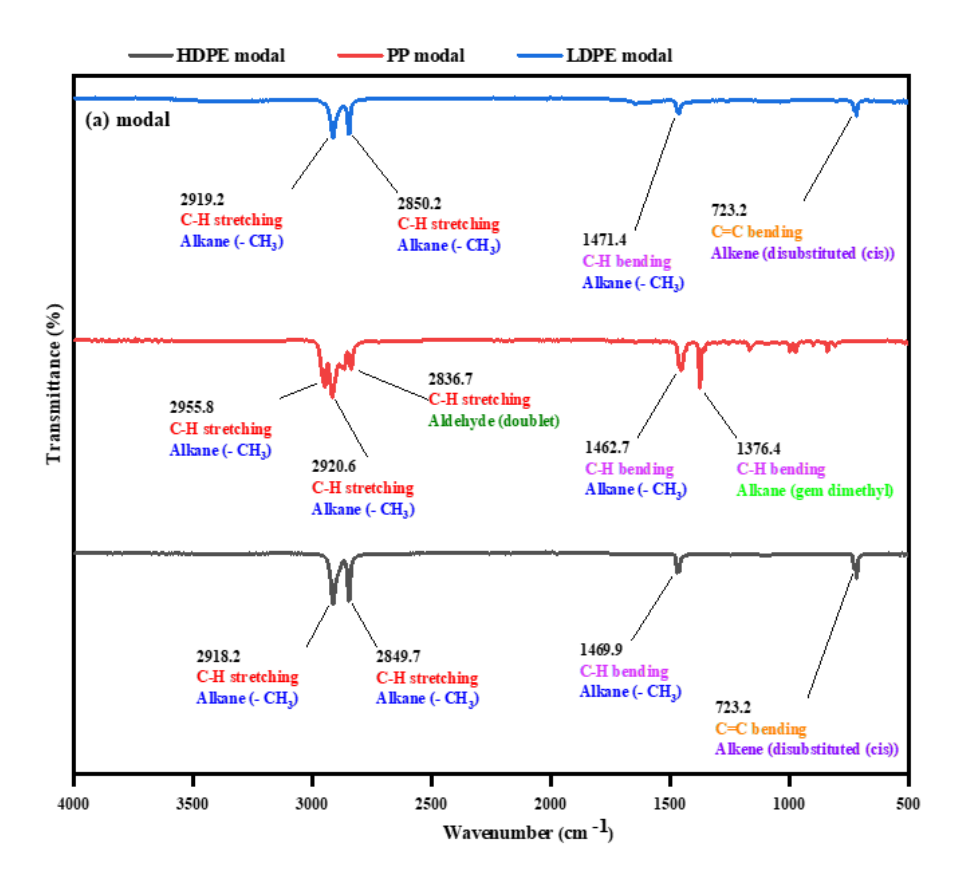
a,b By difference

4.2.1.2 FT-IR

The FT-IR of raw plastic wastes and modal compounds was performed using ATR assembly of IS50 NICOLET FT-IR instrument. Fig. 4.1(a) and (b) shows the various spectrums of the different plastic modal and waste compounds respectively. The modal compounds spectrum corresponds to their fingerprint spectrum. In Fig. 4.1(a), bands observed at 2919, 2955, 2918, 2849, 2850, 2920 and 2849 cm⁻¹, correspond to characteristics peaks of alkanes showing medium to strong C–H stretching vibration of aliphatic –CH₂ and –CH₃ groups (Das and Tiwari, 2018a; Yu, 2021). The bands observed at 2836, 1471, 1462, and 1469 cm⁻¹ confirms the presence of aldehyde and alkane (–CH₃) functional groups respectively. The peaks at wavenumber position of 1376, 723 and 720 shows the presence C–

^{*} The data were taken from the literature(Yao et al., 2018)

H bending of alkane (gem dimethyl) groups and C=C bending of alkene (disubstituted (cis)) group respectively. The presence of these cis isomers of alkenes confirms that the modal plastics also contain some unsaturated hydrocarbon compounds in it. The FT-IR spectra of different real-world plastic wastes are shown in Fig. 4.1(b). These are analogous to that of their corresponding modal materials. This manifests the presence of similar molecular composition and structure (Almohamadi et al., 2021; Sharma et al., 2014). The peak at 2836 cm⁻¹ in the spectra of modal PP is missing in the spectra of PP waste compound, this indicates the absence of the aliphatic aldehyde (CHO) group in the waste compound. Also, from the FTIR of both i.e., the waste and modal forms of the plastic it can be inferred that the plastic remains unaltered and non-degradable when dumped in open environment even for a long period of time. Hence, plastics are called non-biodegradable.



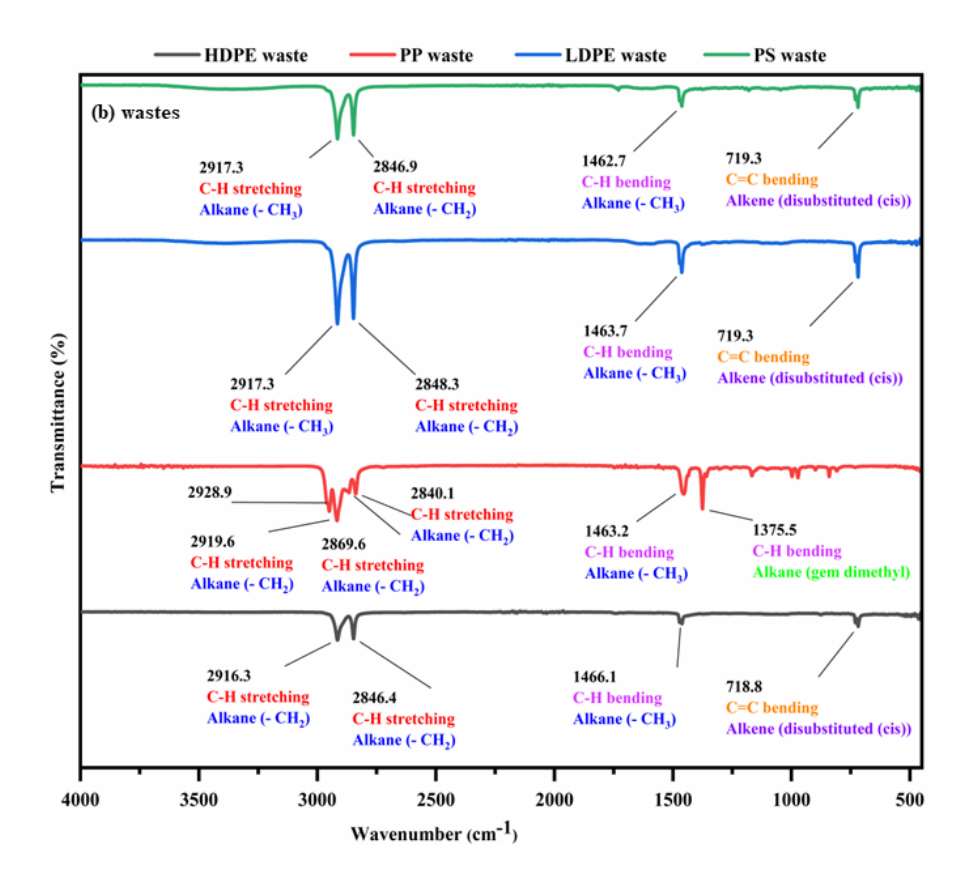


Figure 4.1 FT-IR spectra of (a) modal plastic and (b) real-world plastic waste compounds

4.2.1.3 Thermogravimetric analysis

Fig. 4.2 (a) and (b) represents TG and DTG curves of HDPE, LDPE, and PP (modal plastic) at the heating rate of 15 °C/min. A single stage weight loss was seen in the thermogravimetric curve of all the polymers. Similarly, the DTG curves of all the polymers, also contain single dominant peak occurring in the temperature range 350–500 °C. Thus, both TG/DTG curves had shown the same trend in the depolymerisation process of all polymers which concluded that all the three types of polymers followed the same pyrolysis behaviour due to similar chemical bonds in their molecular structures (Aboulkas et al., 2010). The thermal stability increases in the following order: PP < LDPE < HDPE. The peak decomposition temperatures are 458, 473 and 477 °C, respectively. Also, Fig. 4.3 shows a mass loss (TG curves) and derivative mass loss (DTG curves) of modal plastic compounds HDPE,

LDPE, and PP at four different heating rates (10, 15, 20 and 25 °C/min) respectively. This study was conducted to investigate the effect of heating rates on the pyrolysis process. In compliance with the degradation at 15 °C/min, the mass loss of all the polymers occurred in a single stage but with a delay in the maximum weight loss temperature on increasing the heating rates. Subsequently, showing that on increasing the heating rate there was a delay in the thermal degradation reaction.

Fig. 4.2 (c), (d), (e), and (f). depicts the TG and DTG curves of LDPE, HDPE, PP and PS wastes at four different heating rates; 10, 15, 20 and 25 °C/min respectively. The TG curves for all the wastes showed similar pattern of thermal degradation as shown by that of the modal compounds. Although the TG curve showed the similar trend but the maximum weight loss temperature (T_{max}), the maximum weight loss and the temperature interval of thermal degradation process of each of the real-world plastic waste and their modal compounds varied at four heating rates and are tabulated in Table 4.2 below.

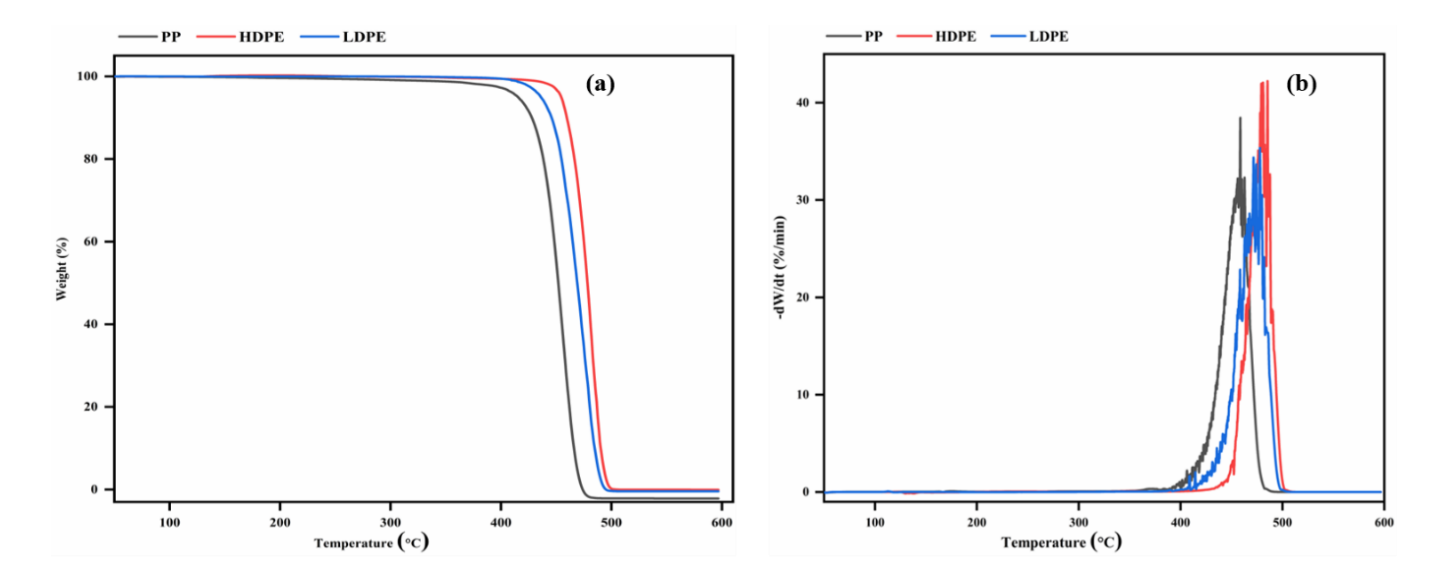
Table 4.2 Providing the temperature interval of thermal degradation process, the maximum wt. loss temperature (T_{max}), and the maximum wt. loss of real-world waste and modal compounds of HDPE, PP, LDPE, and PS at different heating rates

| Plastic type | β | Thermal | degradation | T | max | Weight | Loss |
|--------------|-------------------------|--------------|-------------|-------|-------|---------|-------|
| | (°C.min ⁻¹) | interval (°C | C) | (°C) | | (wt. %) | |
| | | Waste | Modal | Waste | Modal | Waste | Modal |
| HDPE | 10 | 388 – 509 | 317-507 | 475 | 478 | 95.2 | 99.2 |
| | 15 | 397 - 512 | 336-515 | 479 | 484 | 99.2 | 99.5 |
| | 20 | 404 - 528 | 369-524 | 485 | 486 | 94.5 | 99.4 |
| | 25 | 425 - 534 | 406-524 | 497 | 487 | 95.6 | 97.9 |
| PP | 10 | 365 - 477 | 341-493 | 456 | 455 | 95.0 | 99.6 |
| | 15 | 387 - 484 | 351-503 | 461 | 461 | 99.4 | 99.7 |
| | 20 | 349 - 492 | 341-510 | 466 | 468 | 98.9 | 99.7 |
| | 25 | 352 - 487 | 379-510 | 471 | 475 | 93.0 | 98.1 |
| LDPE | 10 | 378 - 498 | 391-496 | 477 | 471 | 99.0 | 99.3 |
| | 15 | 392 - 505 | 398-513 | 484 | 477 | 99.7 | 99.5 |
| | 20 | 425 - 509 | 400-515 | 488 | 481 | 98.9 | 99.5 |
| | 25 | 435 - 513 | 411-528 | 491 | 489 | 98.8 | 99.1 |

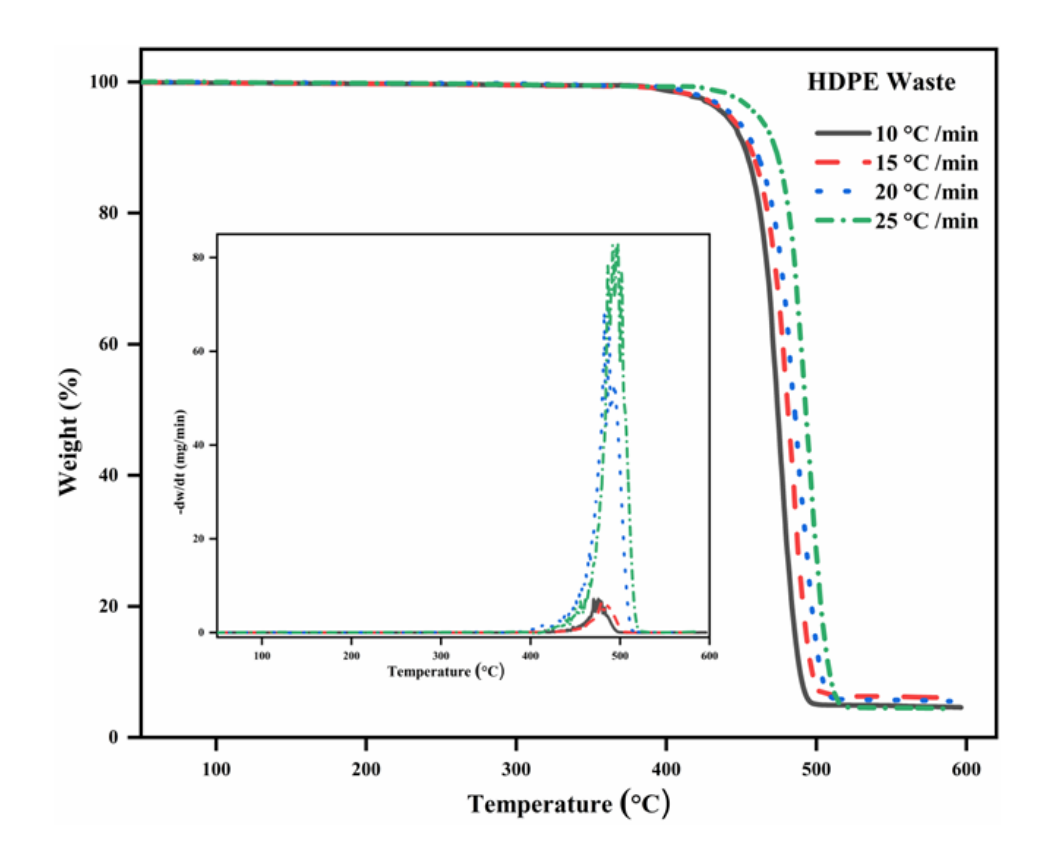
| PS | 10 | 255 - 425 | NA | 409 | NA | 99.4 | NA |
|----|----|-----------|----|-----|----|------|----|
| | 15 | 246 - 458 | | 417 | | 98.9 | |
| | 20 | 279 - 463 | | 423 | | 96.6 | |
| | 25 | 250 - 450 | | 430 | | 99.1 | |

^{*}NA – Not applicable, due to unavailability of PS modal compounds.

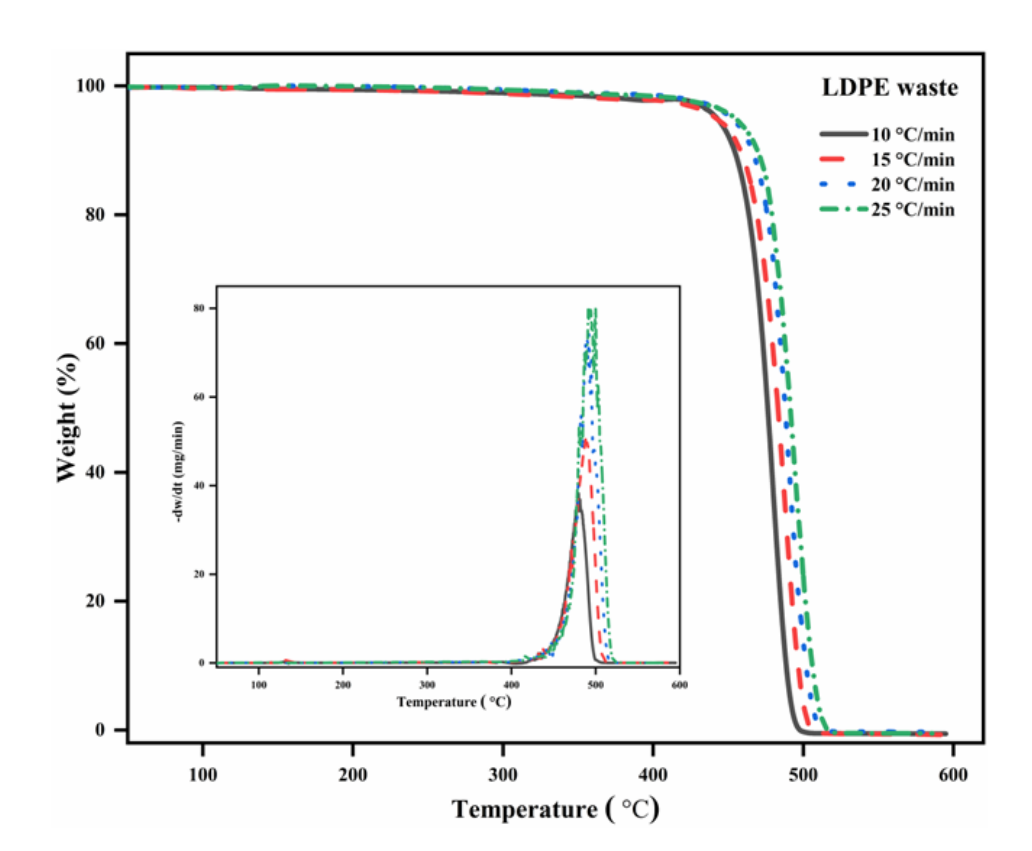
From Figs. 4.3 and 4.2 (c), (d), (e), and (f), it is evident that thermal degradation of the polymers is not much affected by the variation in their elemental composition. However, a slight delay in the initial degradation temperature of the plastic waste forms was observed which can be due to the presence of different types of additives added into the plastics to make them more effective (Gao et al., 2020; Nel et al., 2021). Strong similar pattern in TG and DTG curves of PS, PP, LDPE, and HDPE plastics in both forms i.e., waste and modal, and having similar molecular composition and structure (confirmed in Fig. 4.1), manifests that thermal degradation of polymers follows chain or random chain scission at weaker bonds (Gałko and Sajdak, 2022; Singh et al., 2019). It was observed that the heating rate of 15 °C/min favoured the maximum weight loss in all the plastic types in both of their forms. Hence, all the thermal pyrolysis experiments were conducted at this heating rate. Additionally, in all the DTG curves of different plastics either in Fig. 4.3 or Fig. 4.2 (c), (d), (e), and (f), it was observed that, thermal degradation interval was expanding on increasing the heating rates hence resulting in broader peaks, and further higher temperatures were required to attain the same degree of conversion (Dwivedi et al., 2021). This phenomenon of peak broadening and peak offsetting had gathered attention of various research groups, and obtained scattered set of arguments from them. Most of the researchers observed that the thermal lag during the thermogravimetric experiment and heat transfer limiting property of plastic polymer are the two significant reasons for this phenomenon (Al-Salem et al., 2017). At higher heating rates, it was observed that the furnace temperature and sample temperature in the thermogravimetric holder differs largely, and this in turn causes the existing thermal lag (Khedri and Elyasi, 2016; Kunwar et al., 2016). Also, the heat transfer into the reacting solid surface becomes more difficult at higher heating rates. Whereas a few researchers had reported that the change in the reaction mechanism during the thermal degradation at varying heating rate can be a suitable reason for the phenomenon (V et al., 1985; Wu et al., 1993).



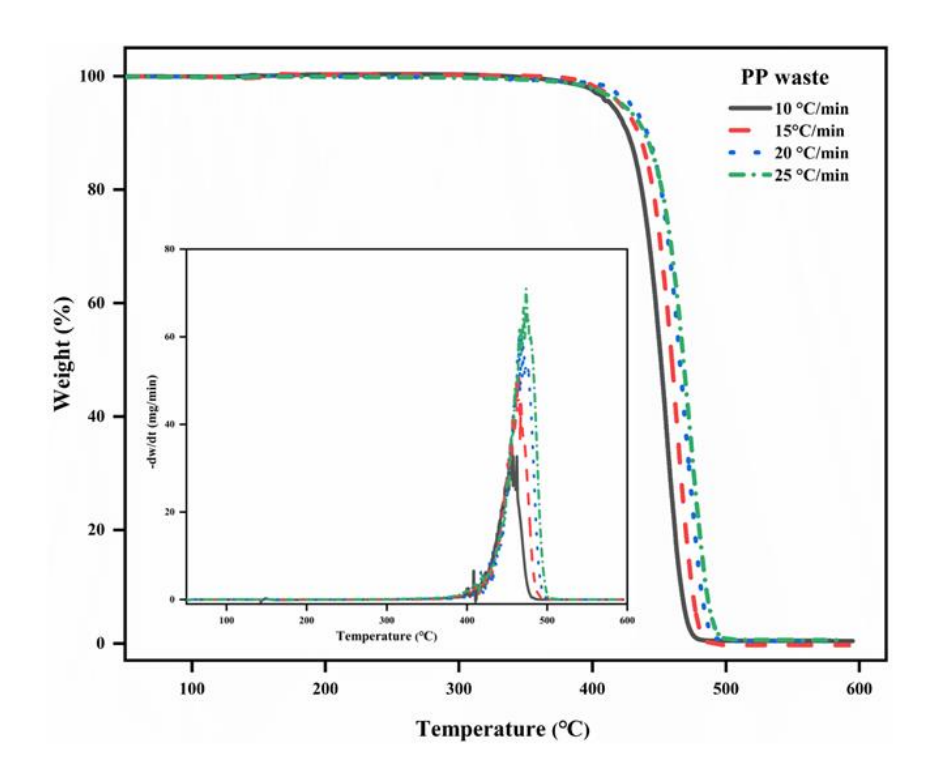








(e)



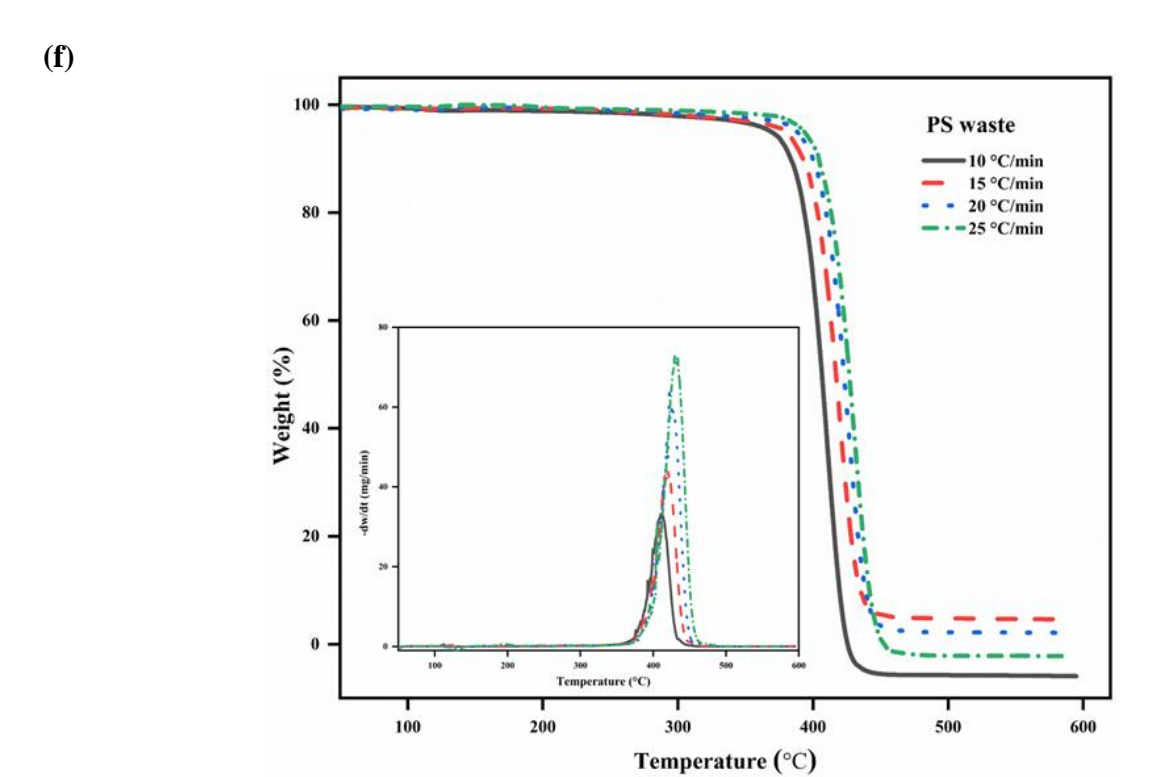


Figure 4.2 (a) TG plot and (b) DTG plot for PP, HDPE, and LDPE modal compounds at 15°C/min; (c), (d), (e), and (f) are showing the TG plots with inset DTG plots at four different heating rates for HDPE, LDPE, PP and PS waste compounds respectively.

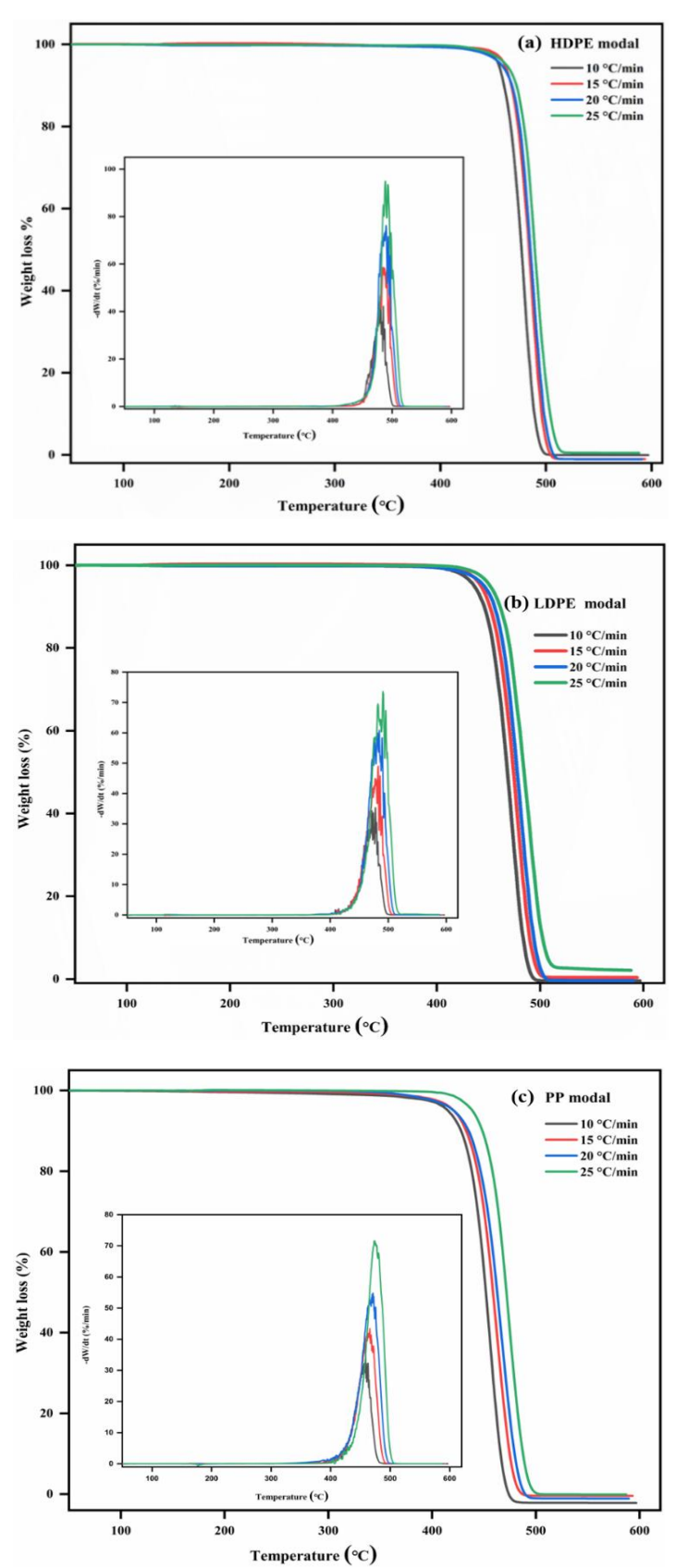


Figure 4.3 (a), (b), and (c) depicts TG and DTG (inset) plots for HDPE, LDPE, and PP modal 57

compounds at four different heating rates respectively

4.2.2 Distribution of pyrolysis products

4.2.2.1 Product yield

The products obtained during the thermal pyrolysis of PS, PP, LDPE, and HDPE are liquid oil, wax, gas, and residue (char). Fig. 4.4 shows the various percentage yield of the obtained products. Since the feedstock elemental composition affects the products distribution significantly, this was evident from the varying yield percentages of products. The maximum liquid oil yield percentage of 53.4% was obtained from the thermal pyrolysis of PS with the minimum production of residue of 0.07%. The PP, LDPE, and HDPE wastes produced almost half of the amount of the liquid oil in the same temperature range of the thermal pyrolysis process. 21%, 15.1%, and 16% were the liquid oil yield percentage obtained from PP, LDPE, and HDPE wastes respectively. The liquid oils obtained from the PS were pale yellow in colour, whereas light brownish to dark brownish coloured liquid oils were obtained from PP, LDPE, and HDPE wastes as shown in Fig. 4.5. It was observed that the slow thermal pyrolysis at a heating rate of 15 °C/min had favoured the wax formation from all the four types of plastic wastes (Pérez-Huertas et al., 2023). The yield percentages of wax from PS, PP, LDPE, and HDPE wastes obtained were 40.9%, 61%, 60.8%, and 62.3% respectively. The colour of the wax products varied from whitish yellow to dark brown. Mostly, the wax obtained from PS and PP were whitish yellow in colour and those wax from LDPE and HDPE were found to have different shades of brown colour. Also, the gas yield percentages were in small amounts as compared with that of the liquid oil and wax. 5.6%, 7%, 10.2%, and 8.7% were the gas yield percentage obtained from PS, PP, LDPE, and HDPE respectively. Similarly, residue yield percentage ranging in between 11-14% was obtained from PP, LDPE, and HDPE wastes. These residue yield percentages can be corelated with the fixed carbon content present in the different plastic wastes shown in Table 4.3. The smaller amounts of gas and huge amounts of wax and liquid oil are following the lower pyrolysis temperature range (Al-Salem et al., 2017; Calero et al., 2023; Maqsood et al., 2021; Pérez-Huertas et al., 2023). The obtained results showed comparable values with the already reported work done (Dwivedi et al., 2021; Jaafar et al., 2022; Pyra et al., 2021). It is noteworthy to mention that all these product distribution percentages

were obtained from real-world plastic wastes, collected from the surroundings. One of the most significant parameters is temperature in thermal pyrolysis (Al-Salem et al., 2009; López et al., 2011). And attaining the proper temperature distribution inside the reactor chamber is the most critical factor in achieving the maximum degree of polymer cracking process due to the natural insulating nature of plastics.

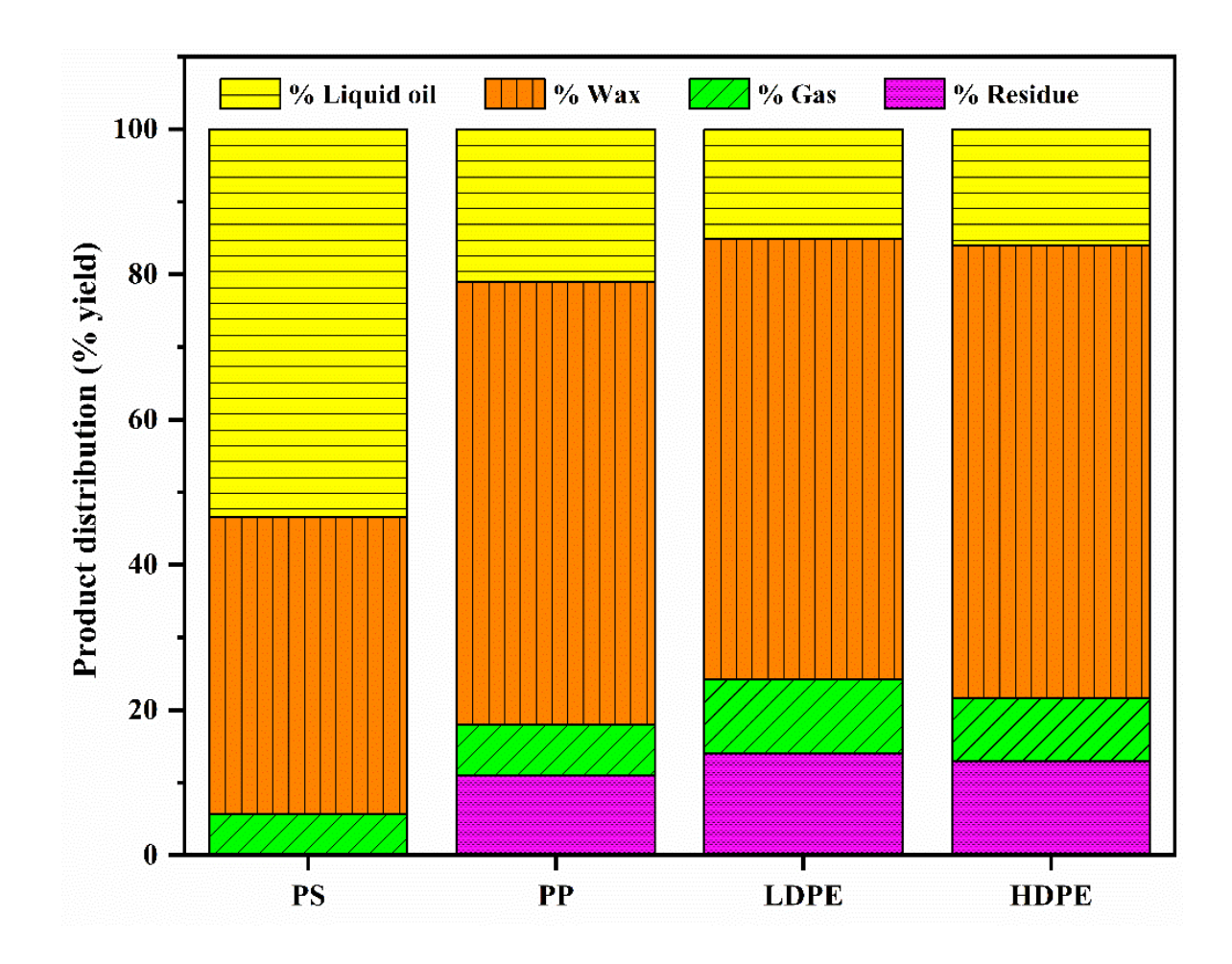


Figure 4.4 Percentage yield (by wt.) of the liquid oil, wax, gas, and residue (char) during the thermal pyrolysis experiment of PS, PP, LDPE, and HDPE

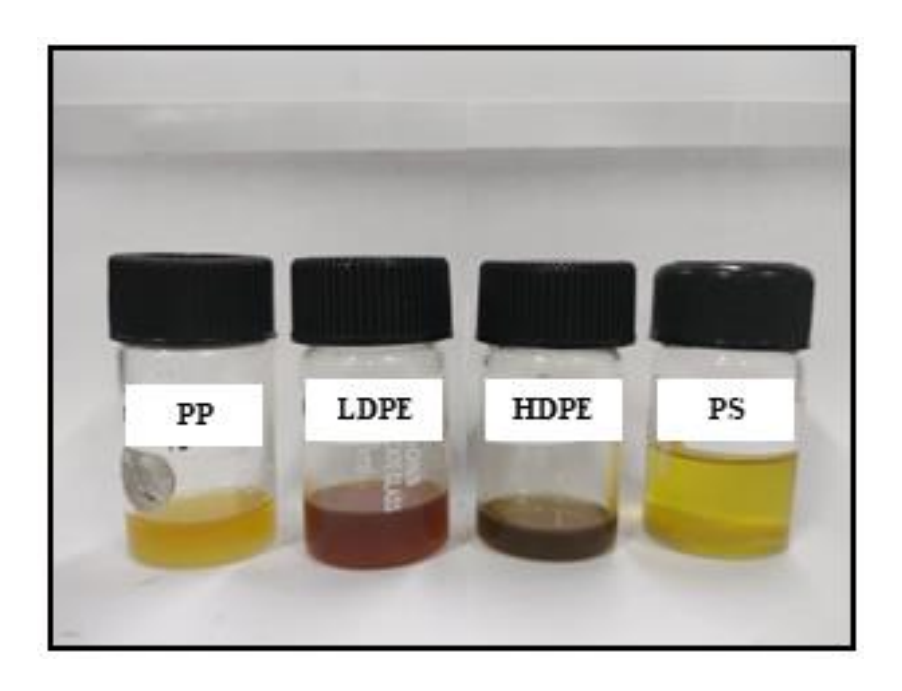


Figure 4.5 Liquid oil product obtained from thermal pyrolysis of different plastic wastes

Therefore, the reactor dimensions used in the present study had helped in achieving the desired temperature distribution within and hence the desired liquid oil was obtained.

4.2.3 Liquid oil characterizations

4.2.3.1 Viscosity and HHV

Viscosity and HHV of liquid oils obtained from thermal pyrolysis of different plastic wastes are shown in the below Table 4.3. It was observed that the viscosity of the obtained liquid oil was in good relevance with that of the commercial grade diesel and kerosene oil. Also, the HHV values of the obtained liquid oils were as good as that of the petro fuels (Budsaereechai et al., 2019; Dwivedi et al., 2021).

Table 4.0.3 Viscosity and HHV of pyrolytic oils obtained from different plastic wastes

| Properties | Pyrolysis oil obtained from different plastic waste | | | | | | |
|-------------------|---|-------|-------|-------|--|--|--|
| | HDPE | LDPE | PP | PS | | | |
| Viscosity (mPa.s) | 8.23 | 3.08 | 2.37 | 1.09 | | | |
| HHV (MJ/Kg) | 48.61 | 42.48 | 38.26 | 33.15 | | | |

4.2.3.2 FT-IR

Fig. 4.6 shows the FTIR of the liquid oil obtained after the thermal pyrolysis of the different plastic wastes. FTIR technique detects various characteristic functional groups present in oil. On interaction of an infrared light with oil, chemical bond will stretch, contract, and absorb infrared radiation in a specific wavelength range regardless of the structure of the rest of the molecules. The C–H stretching vibrations at frequency 3019.015 cm⁻¹ indicate the presence of alkenes in oil obtained from PP. The presence of alkanes with C-H stretching vibrations is detected at 2922.59 cm⁻¹, 2853.16 cm⁻¹, 2921.62 cm⁻¹, 2854.13 cm⁻¹, in the liquid oil obtained from thermal pyrolysis of HDPE and LDPE (Das and Tiwari, 2018b; Singh et al., 2019). The C=O stretching vibrations at frequency 1585.2 present in the pyrolysis oil obtained from PS confirms the presence of amides in it. The CH2 bending vibrations at frequency 1467.56 cm⁻¹, and 1469.49 cm⁻¹, in the oil obtained from HDPE and LDPE, respectively indicate the presence of alkenes. The presence of alkanes was detected by C-H scissoring and bending vibrations at 1418.38 cm⁻¹. The presence of alcohols, ethers, carboxylic acids, and esters is detected by C-O stretching vibrations at 907.34 cm⁻¹, 910.23 cm⁻¹ in the oil obtained from HDPE and LDPE, and the C=C bending vibrations at 991.23 cm⁻¹ confirms the presence of monosubstituted alkenes in the oil obtained from PS, and the C=C bending vibrations at frequency 662.42 cm⁻¹ indicates the presence of disubstituted (cis) alkanes in the oil obtained from PP. The results were found consistent when compared with the results of GC-MS.

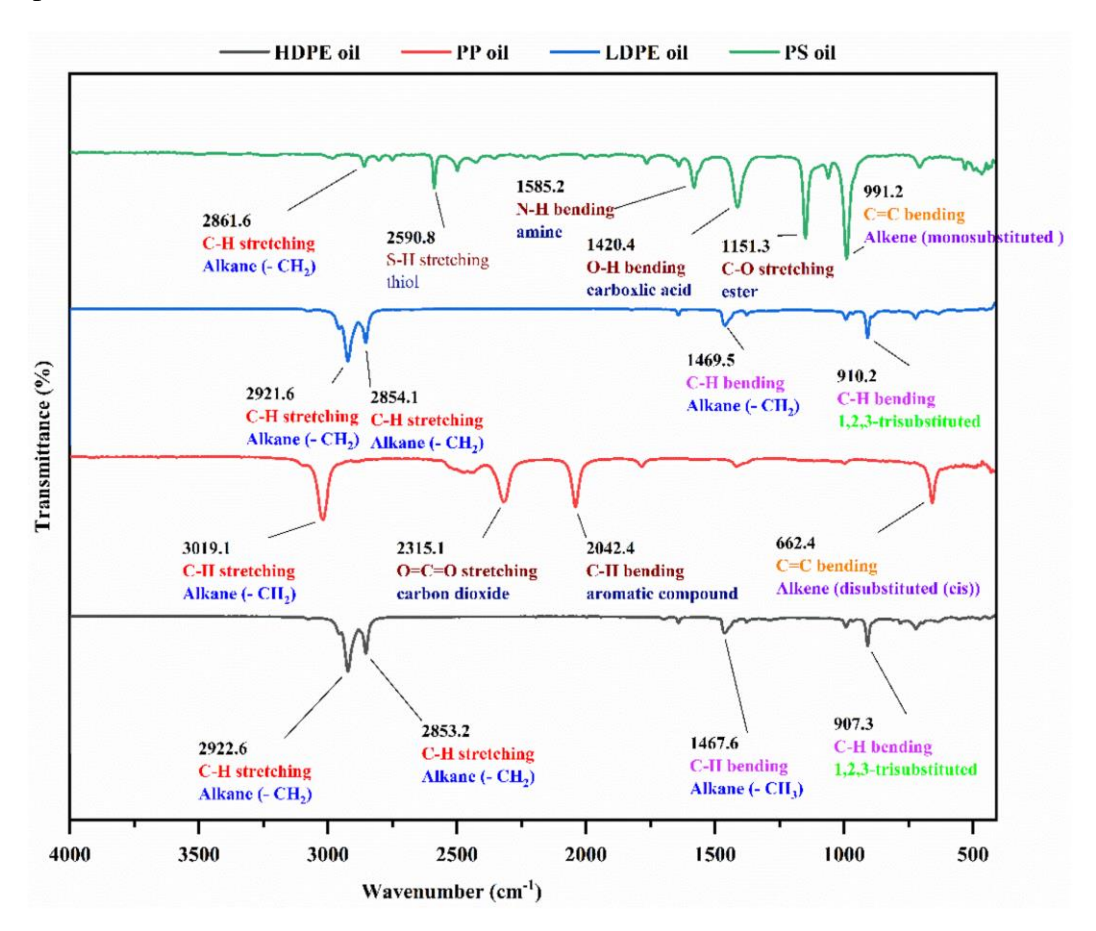


Figure 4.6 FT-IR of liquid oils obtained from different plastic wastes

4.2.3.3 GC-MS

GC-MS technique which is a strong tool to identify the hydrocarbon composition of liquid fuels (Yan et al., 2015). Hydrocarbon components observed in mass-spectrums of the liquid products obtained from the thermal pyrolysis of different plastic wastes are shown in Fig. 4.7. GC-MS technique provide critical information about unsaturated and saturated carbon species by estimating the carbon number distribution quantitatively and qualitatively in higher hydrocarbons (Budsaereechai et al., 2019; Sharma et al., 2014). From Fig. 4.7, it is observed that liquid products contain major fraction of paraffinic, olefinic and aromatic hydrocarbons indicating fuel characteristics of liquid products and is comparable with the hydrocarbon components of commercial diesel fuel.

Fig. 4.8, shows the further distribution of the different hydrocarbon compounds present in the liquid oil products obtained from GC-MS results. The liquid oil obtained from HDPE waste majorly contained aromatics around 35%, followed by alkenes and alkanes accounting for 23% and 16% respectively. The aldehydes and alcohols contributed 4% and 2% respectively. And the rest around 20% were marked by the presence of other groups such as ketones, amines, carboxylic acids etc. in trace amounts (Das and Tiwari, 2018b). Similarly, the LDPE oil and PP oil contained alkanes, alkenes, aldehydes, alcohols, aromatics, and others as follows: 17% and 11%, 33% and 7%, 9% and 1%, 16% and 12%, 10% and 40%, and 15% and 28% respectively (Yu, 2021; Yu et al., 2021). However, it was observed that the PS oil contained the maximum percentage of aromatics i.e., 90%. And the rest were alkanes 3% and alkenes 7% (Calero et al., 2023).

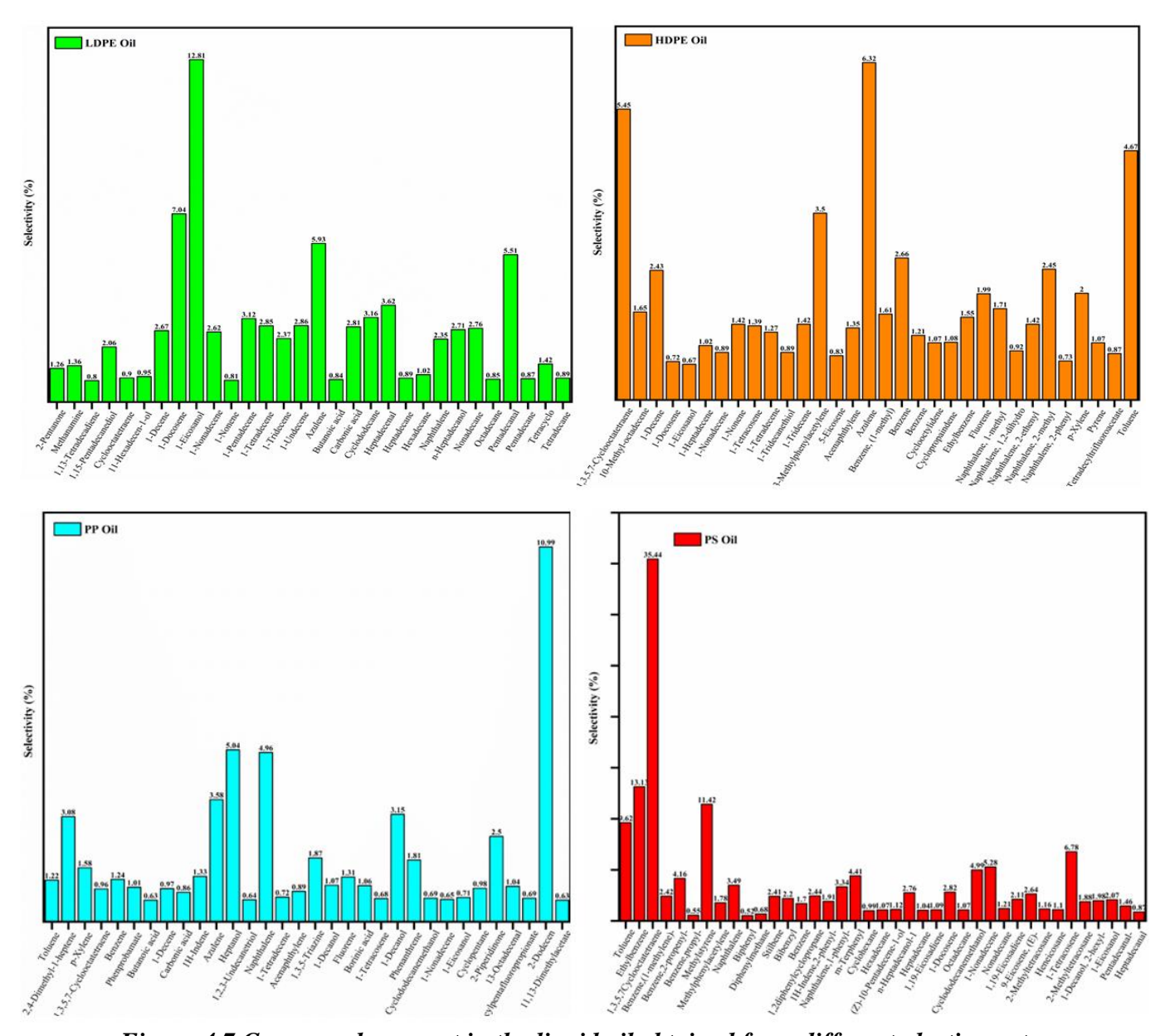


Figure 4.7 Compounds present in the liquid oil obtained from different plastic wastes

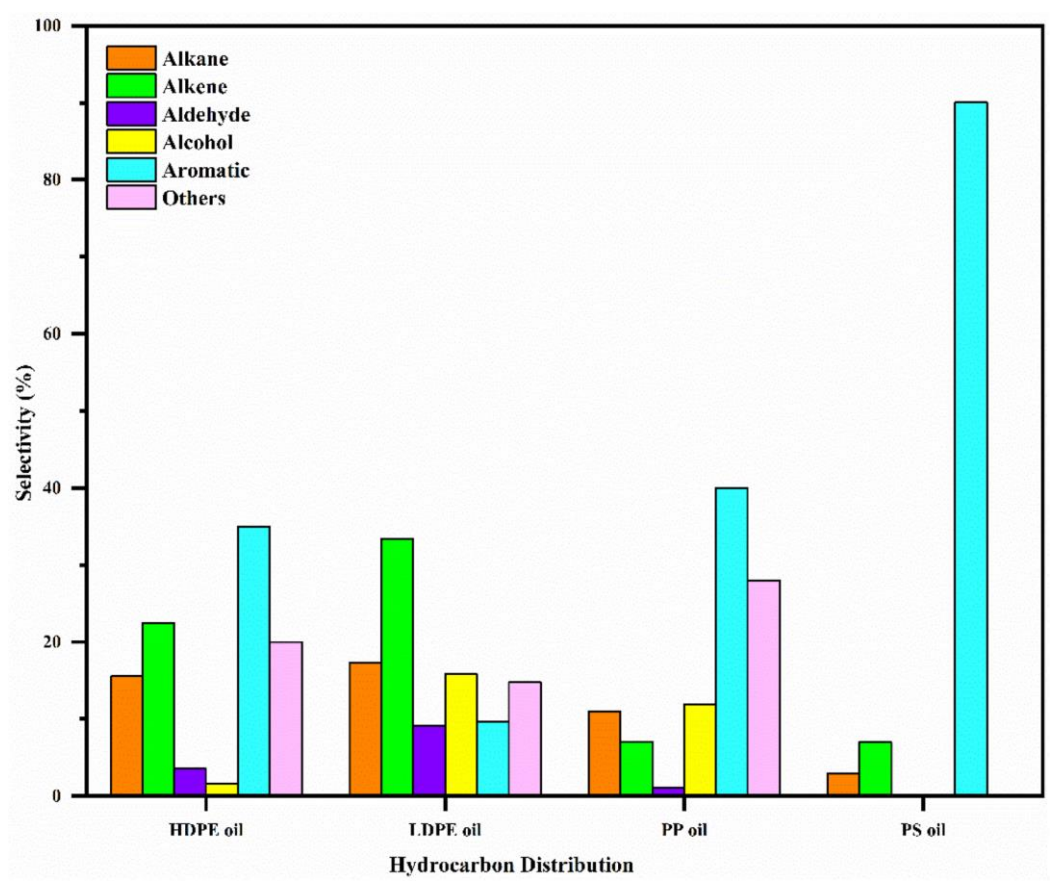


Figure 4.8 Hydrocarbon distribution in liquid oils obtained from different plastic wastes

4.2.3.4 ¹H NMR

In addition to FT-IR and GC-MS analysis, NMR spectroscopic study is also performed to investigate the hydrocarbon characteristics of liquid products. Basically, ¹H NMR spectroscopy is used to analyze the nature of hydrocarbons (Sharma et al., 2014). All ¹H NMR spectra of liquid samples of plastic wastes are shown in Fig. 4.9. ¹H NMR spectra of liquid products confirm the presence of methyl (CH3), methylene (CH2), methane and quaternary hydrocarbon protons as demonstrated in Fig. 5. In ¹H NMR spectra of liquid product, large number of over-lapped proton signals are observed due to presence of wide range of hydrocarbons (Sharma et al., 2014; Yan et al., 2015). It is observed that hydrocarbon composition of liquid products contains 94% and 96% selectivity towards paraffinic (CH3-CH2) protons respectively (Kumar and Singh, 2013). This shows resemblance with the fuel

range hydrocarbons.

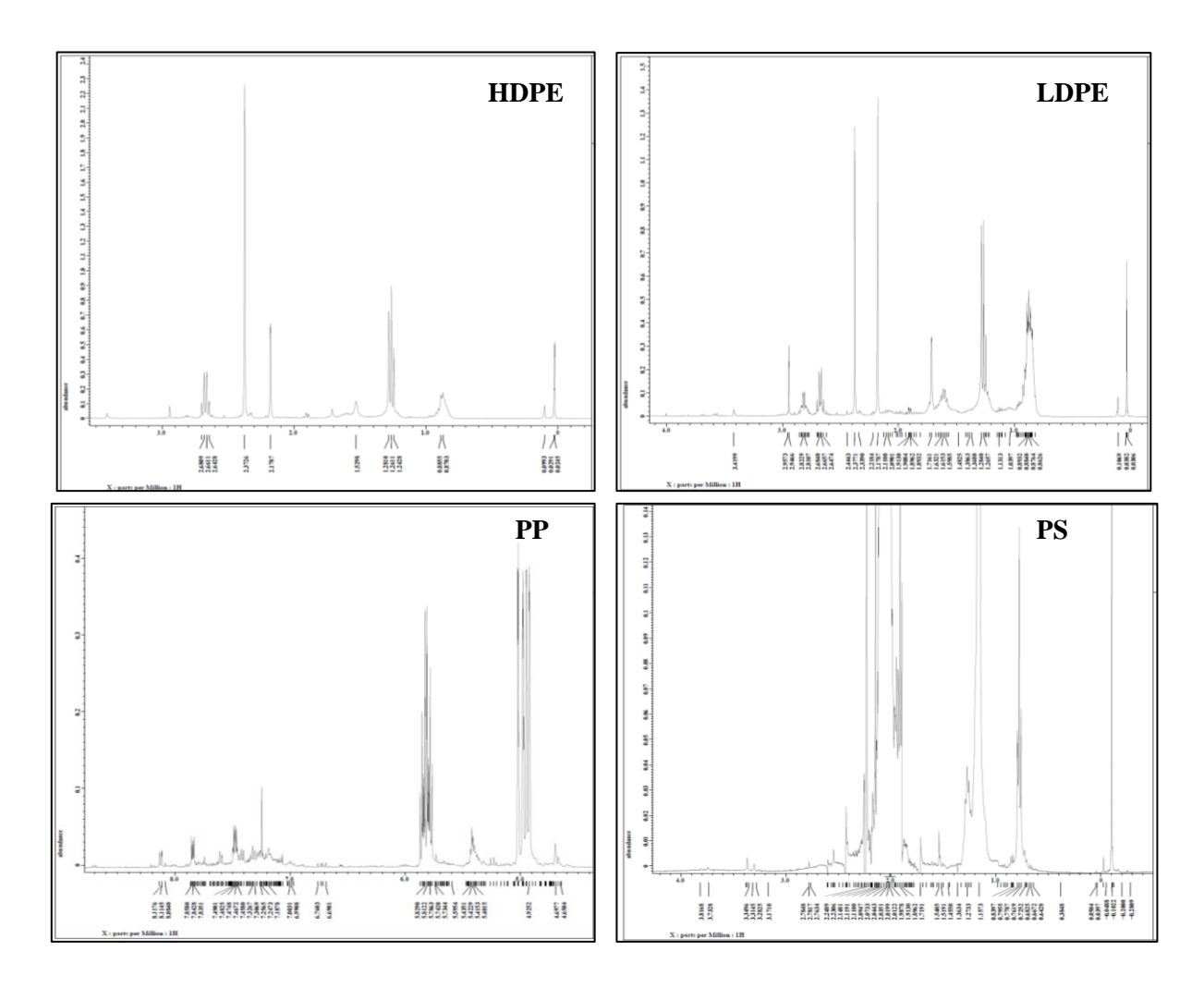


Figure 4.9 1H NMR of liquid oil obtained from different real-world plastic wastes

4.3 Conclusion:

In this work, the effect of elemental composition of modal plastic and waste plastic on their thermal degradation process was studied. The results obtained from TG, DTG curves and FT-IR studies of the modal plastic and waste plastic confirmed the presence of similar molecular composition and structure, and following similar degradation mechanism. Subsequently, the slow thermal pyrolysis of real-world plastic waste was performed in the temperature range of 450 - 480 °C at a heating rate of 15 °C. min⁻¹

in a tubular fixed bed reactor and their product distribution, liquid oil composition and its various characteristics were investigated. It was observed that parameters such as reactor dimensions, slower heating rate, pelletized form of feedstock had significantly altered the lumped product yield as well as the composition of the products. Considerable amount of aromatic rich liquid oil and wax were obtained from all the wastes without catalyst assistance. The obtained liquid oil from different plastic wastes were composed of alkanes (C8–C25), alkenes (C9–C24) along with aromatics, alcohols, aldehydes and trace amounts of ketones and acids etc. The tubular fixed bed reactor provided better thermal distribution and enhancing the thermal cracking reaction mechanism. The viscosity of the obtained liquid oil was comparable with that of the commercial grade diesel and kerosene oil. Also, the HHV values of the obtained liquid oils were as good as that of the petro fuels. It can be concluded that a controlled slow thermal pyrolysis of the real-world plastic waste produces liquid oil with fuel properties that are suitable to be used as an alternative for fossil fuels.

4.4 Reference

- [1] Aboulkas, A., El harfi, K., El Bouadili, A., 2010. Thermal degradation behaviors of polyethylene and polypropylene. Part I: Pyrolysis kinetics and mechanisms. Energy Convers. Manag. 51, 1363–1369. https://doi.org/10.1016/j.enconman.2009.12.017
- [2] Al-Salem, S.M., Antelava, A., Constantinou, A., Manos, G., Dutta, A., 2017. A review on thermal and catalytic pyrolysis of plastic solid waste (PSW). J. Environ. Manage. 197, 177–198. https://doi.org/10.1016/j.jenvman.2017.03.084
- [3] Al-Salem, S.M., Lettieri, P., Baeyens, J., 2009. Recycling and recovery routes of plastic solid waste (PSW): A review. Waste Manag. 29, 2625–2643. https://doi.org/10.1016/j.wasman.2009.06.004
- [4] Almohamadi, H., Aljabri, A., Mahmoud, E.R.I., Khan, S.Z., Aljohani, M.S., Shamsuddin, R., 2021. Catalytic pyrolysis of municipal solid waste: Effects of pyrolysis parameters. Bull. Chem. React. Eng. Catal. 16, 342–352. https://doi.org/10.9767/bcrec.16.2.10499.342-352
- [5] Anuar Sharuddin, S.D., Abnisa, F., Wan Daud, W.M.A., Aroua, M.K., 2016. A review on pyrolysis of plastic wastes. Energy Convers. Manag. 115, 308–326. https://doi.org/10.1016/j.enconman.2016.02.037
- [6] Calero, M., Solís, R.R., Muñoz-Batista, M.J., Pérez, A., Blázquez, G., Ángeles Martín-Lara, M., 2023. Oil and gas production from the pyrolytic transformation of recycled plastic waste: An integral study by polymer families. Chem. Eng. Sci. 271, 118569. https://doi.org/10.1016/j.ces.2023.118569
- [7] Das, P., Tiwari, P., 2018. The effect of slow pyrolysis on the conversion of packaging waste plastics (PE and PP) into fuel. Waste Manag. 79, 615–624. https://doi.org/10.1016/j.wasman.2018.08.021
- [8] Dwivedi, U., Naik, S.N., Pant, K.K., 2021. High quality liquid fuel production from waste plastics via two-step cracking route in a bottom-up approach using bi-functional Fe/HZSM-5 catalyst. Waste Manag. 132, 151–161. https://doi.org/10.1016/j.wasman.2021.07.024
- [9] Gałko, G., Sajdak, M., 2022. Trends for the Thermal Degradation of Polymeric Materials: Analysis of Available Techniques, Issues, and Opportunities. Appl. Sci. 12. https://doi.org/10.3390/app12189138
- [10] Gao, N., Sipra, A.T., Quan, C., 2020. Thermogravimetric analysis and pyrolysis

- product characterization of municipal solid waste using sludge fly ash as additive. Fuel 281. https://doi.org/10.1016/j.fuel.2020.118572
- [11] Jaafar, Y., Abdelouahed, L., Hage, R. El, Samrani, A. El, Taouk, B., 2022. Pyrolysis of common plastics and their mixtures to produce valuable petroleum-like products. Polym. Degrad. Stab. 195, 109770. https://doi.org/10.1016/j.polymdegradstab.2021.109770
- [12] Khedri, S., Elyasi, S., 2016. Kinetic analysis for thermal cracking of HDPE: A new isoconversional approach. Polym. Degrad. Stab. 129, 306–318. https://doi.org/10.1016/j.polymdegradstab.2016.05.011
- [13] Kunwar, B., Cheng, H.N., Chandrashekaran, S.R., Sharma, B.K., 2016. Plastics to fuel: a review. Renew. Sustain. Energy Rev. 54, 421–428. https://doi.org/10.1016/j.rser.2015.10.015
- [14] López, A., de Marco, I., Caballero, B.M., Laresgoiti, M.F., Adrados, A., 2011.
 Influence of time and temperature on pyrolysis of plastic wastes in a semi-batch reactor. Chem.
 Eng. J. 173, 62–71. https://doi.org/10.1016/j.cej.2011.07.037
- [15] Maqsood, T., Dai, J., Zhang, Y., Guang, M., Li, B., 2021. Pyrolysis of plastic species: A review of resources and products. J. Anal. Appl. Pyrolysis 159, 105295. https://doi.org/10.1016/j.jaap.2021.105295
- [16] Nel, H.A., Chetwynd, A.J., Kelly, C.A., Stark, C., Valsami-Jones, E., Krause, S., Lynch, I., 2021. An Untargeted Thermogravimetric Analysis-Fourier Transform Infrared-Gas Chromatography-Mass Spectrometry Approach for Plastic Polymer Identification. Environ. Sci. Technol. 55, 8721–8729. https://doi.org/10.1021/acs.est.1c01085
- [17] Pérez-Huertas, S., Calero, M., Ligero, A., Pérez, A., Terpiłowski, K., Martín-Lara, M.A., 2023. On the use of plastic precursors for preparation of activated carbons and their evaluation in CO2 capture for biogas upgrading: a review. Waste Manag. 161, 116–141. https://doi.org/10.1016/j.wasman.2023.02.022
- [18] Pyra, K., Tarach, K.A., Góra-Marek, K., 2021. Towards a greater olefin share in polypropylene cracking Amorphous mesoporous aluminosilicate competes with zeolites. Appl. Catal. B Environ. 297. https://doi.org/10.1016/j.apcatb.2021.120408
- [19] Sharma, B.K., Moser, B.R., Vermillion, K.E., Doll, K.M., Rajagopalan, N., 2014. Production, characterization and fuel properties of alternative diesel fuel from pyrolysis of waste plastic grocery bags. Fuel Process. Technol. 122, 79–90.

- https://doi.org/10.1016/j.fuproc.2014.01.019
- [20] Singh, R.K., Ruj, B., Sadhukhan, A.K., Gupta, P., 2019. Thermal degradation of waste plastics under non-sweeping atmosphere: Part 1: Effect of temperature, product optimization, and degradation mechanism. J. Environ. Manage. 239, 395–406. https://doi.org/10.1016/j.jenvman.2019.03.067
- [21] Mookherjee, S., Ray, H. S., & Mukherjee, A. (1985). Thermogravimetric studies on the reduction of hematite ore fines by a surrounding layer of coal or char fines: Part 2. Non-isothermal kinetic studies. *Thermochimica acta*, 95(1), 247-256.
- [22] Wu, C. H., Chang, C. Y., Hor, J. L., Shih, S. M., Chen, L. W., & Chang, F. W. (1993). On the thermal treatment of plastic mixtures of MSW: pyrolysis kinetics. *Waste Management*, *13*(3), 221-235.
- [23] Yao, D., Yang, H., Chen, H., Williams, P.T., 2018. Co-precipitation, impregnation and so-gel preparation of Ni catalysts for pyrolysis-catalytic steam reforming of waste plastics. Appl. Catal. B Environ. 239, 565–577. https://doi.org/10.1016/j.apcatb.2018.07.075
- [24] Yu, D., 2021. Composite Pyrolysis of Biomass and Plastic for High-quality Fuel Oil over HZSM-5. Am. J. Chem. Eng. 9, 39. https://doi.org/10.11648/j.ajche.20210902.12

CHAPTER 5: KINETIC STUDY OF THERMAL PYROLYSIS OF REAL-WORLD PLASTIC WASTE

5.1 Introduction

This study aims to depict the complexity of slow thermal pyrolysis of real-world plastic waste. Non-isothermal thermogravimetric analysis (TGA) of polypropylene (PP), polystyrene (PS), high-density polyethylene (HDPE) and low-density polyethylene (LDPE) was performed at 10, 15, 20 and 25 °C/min heating rates from 50 °C to 600 °C, under inert environment condition. A combined strategy of employing model-free (OFW, KAS, Starink, Tang and Boswell) isoconversional methods and model-fitting (Criado and Coats–Redfern) methods was used to study kinetics of thermal degradation process. From TGA, the ease of performing thermal degradation of the real-world plastic wastes follows the order PS < PP < LDPE < HDPE. The activation energies were calculated by using different model-free isoconversional methods and compared with that obtained from the Coats–Redfern model for all of the different waste polymers, and were found to be ranging from 149.59 to 227.38 kJ/mol. Criado model was used to determine the most suitable reaction mechanism $f(\alpha)$. It was found that thermal degradation of PS, PP, LDPE, and HDPE followed A2 (2D nucleation: Avarami-Erofe've), A3 (3D nucleation: Avarami-Erofe've), R2 (contracting sphere), and R3 (contracting cylinder) reaction mechanisms respectively.

5.2 Results and discussions

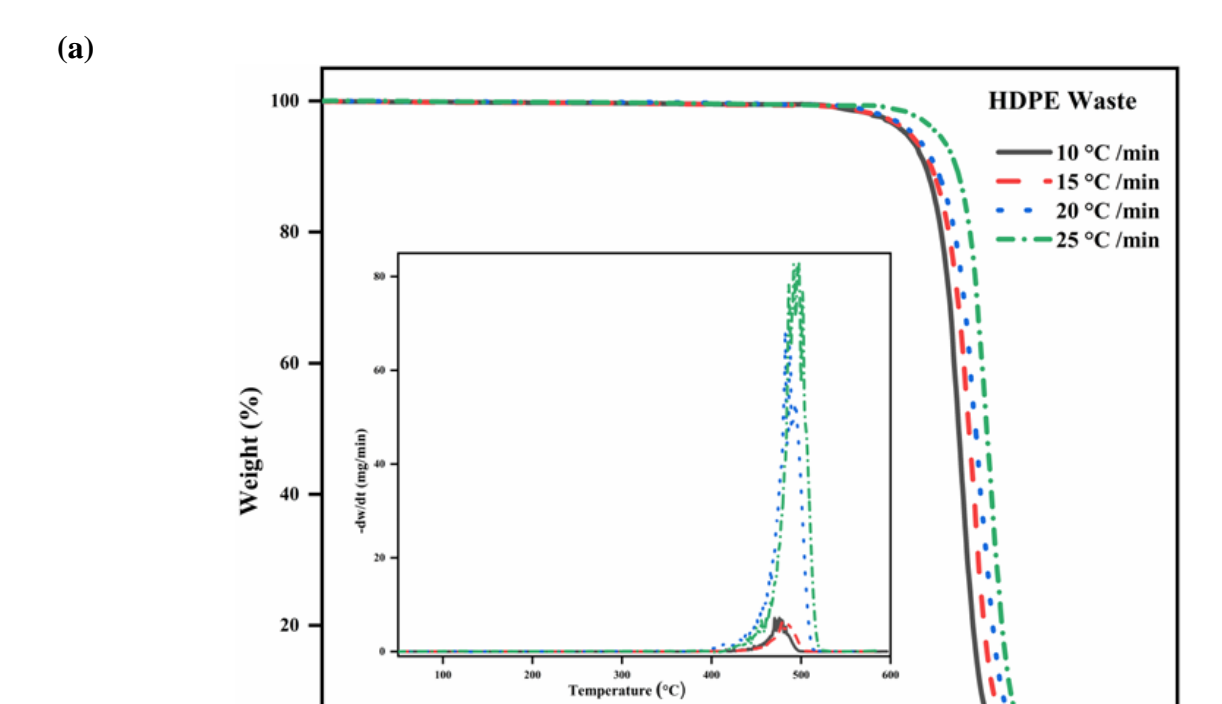
5.2.1 Feedstock characteristics

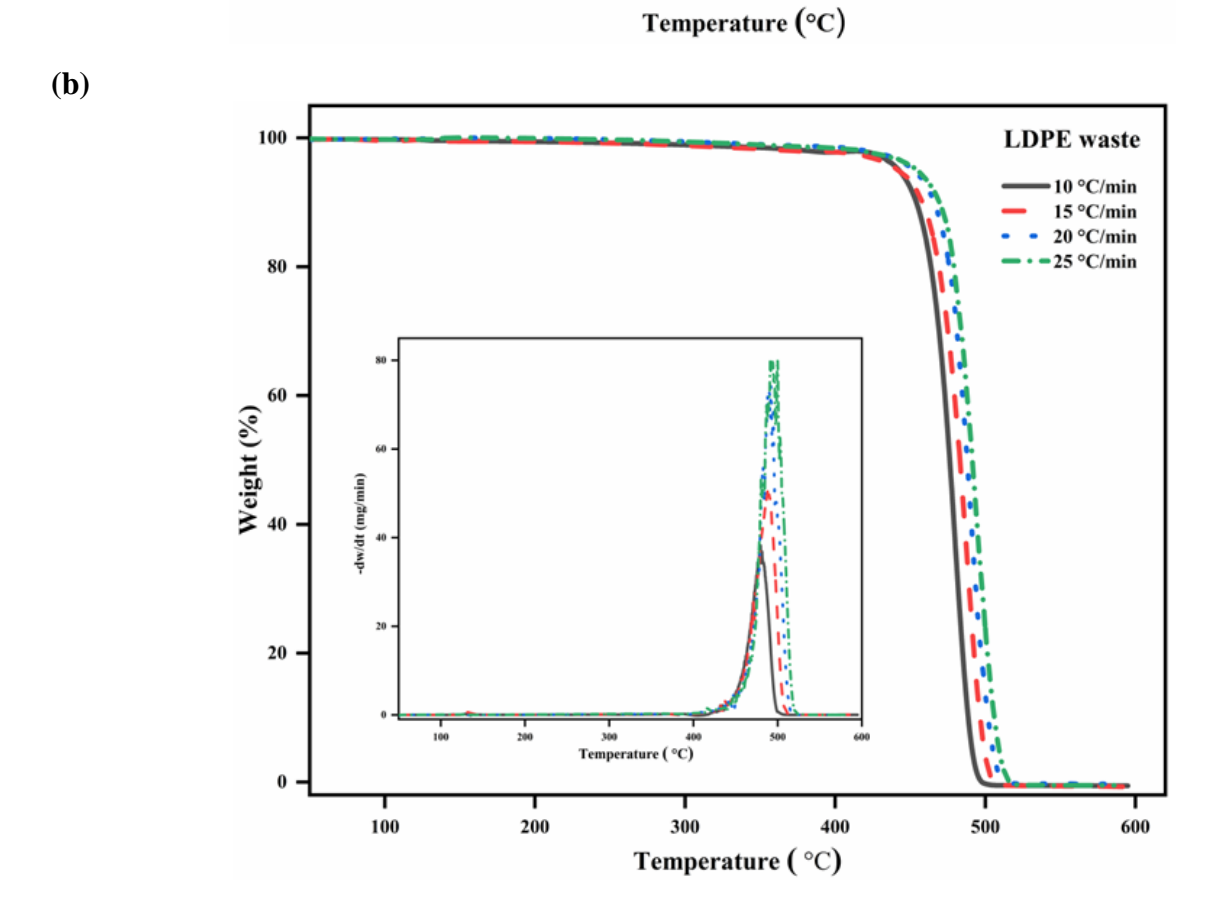
Table 4.1, shows the elemental composition obtained from ultimate analysis and the proximate analysis results for all the real-world plastic waste and their modal compounds. Higher quantities of volatile matter with lower values of ash content and fixed carbon content were observed in both the forms of the plastic. This result is designated with the production of liquid oil from plastic wastes when treated thermally under controlled heating and inert environment (Anuar Sharuddin et al., 2016). It was observed that the oxygen content in the waste forms were higher as compared with that of the modal forms.

5.2.2 Thermogravimetric (TG)/ Derivative thermogravimetric (DTG) analysis

Fig. 5.1, depicts the TG and DTG curves of LDPE, HDPE, PP and PS wastes at four different heating rates; 10, 15, 20 and 25 °C/min respectively. The TG curves for all of the wastes showed similar pattern concluding that the thermal degradation occurs in a single stage for all the plastic wastes. Subsequently, obtaining single peak in DTG curves of all the waste samples confirmed the single stage thermal degradation process. Despite of having different degree of polymerisation and monomers, showing same thermal degradation pattern was because of having chemical structure built with similar chemical bonds (Aboulkas et al., 2010; Xu et al., 2018).

Although the TG curve showed the similar trend but the maximum weight loss temperature (T_{max}) , the maximum weight loss and the temperature interval of thermal degradation process of each of the plastic waste varied at four heating rates. Table 5.1, shows the aforementioned temperatures and maximum weight loss for different plastic wastes at four heating rates. The temperature interval of thermal degradation and T_{max} for HDPE waste at 10, 15, 20 and 25 °C⋅min⁻¹ were 388 – 481 and 475, 397 – 502 and 479, 404 - 508 and 485, and 425 - 514 and 497 respectively. Similarly, temperature interval of thermal degradation and T_{max} for LDPE waste at 10, 15, 20 and 25 $^{\circ}\text{C}\cdot\text{min}^{-1}$ were 280 - 498 and 477, 309 - 505 and 484, 425 - 509 and 488, and 435 - 513 and 491 respectively. For PP waste, the temperature interval of thermal degradation and T_{max} at 10, 15, 20 and 25 °C·min⁻¹ were 365 - 477 and 456, 387 - 484 and 461, 349 - 492 and 466, and 352 - 487 and 471 respectively. And for PS waste, temperature interval of thermal degradation and T_{max} at 10, 15, 20 and 25 °C·min⁻¹ were 255 - 425 and 409, 246 - 458 and 417, 279 - 463 and 423, and 250 - 450 and 430 respectively. From all the TG curves of the wastes, it was observed that there was a delay in the maximum weight loss temperature on increasing the heating rates. Subsequently, showing that on increasing the heating rate there was a delay in the thermal degradation reaction. Also, in case of HDPE, PP and LDPE wastes, the maximum weight loss was observed at 15 °C·min⁻¹ heating rate. However, the maximum weight loss of PS waste occurred at 10 °C·min⁻¹. Whereas, it is comparable with the weight loss occurred at 15 °C·min⁻¹.





(c)

(**d**)

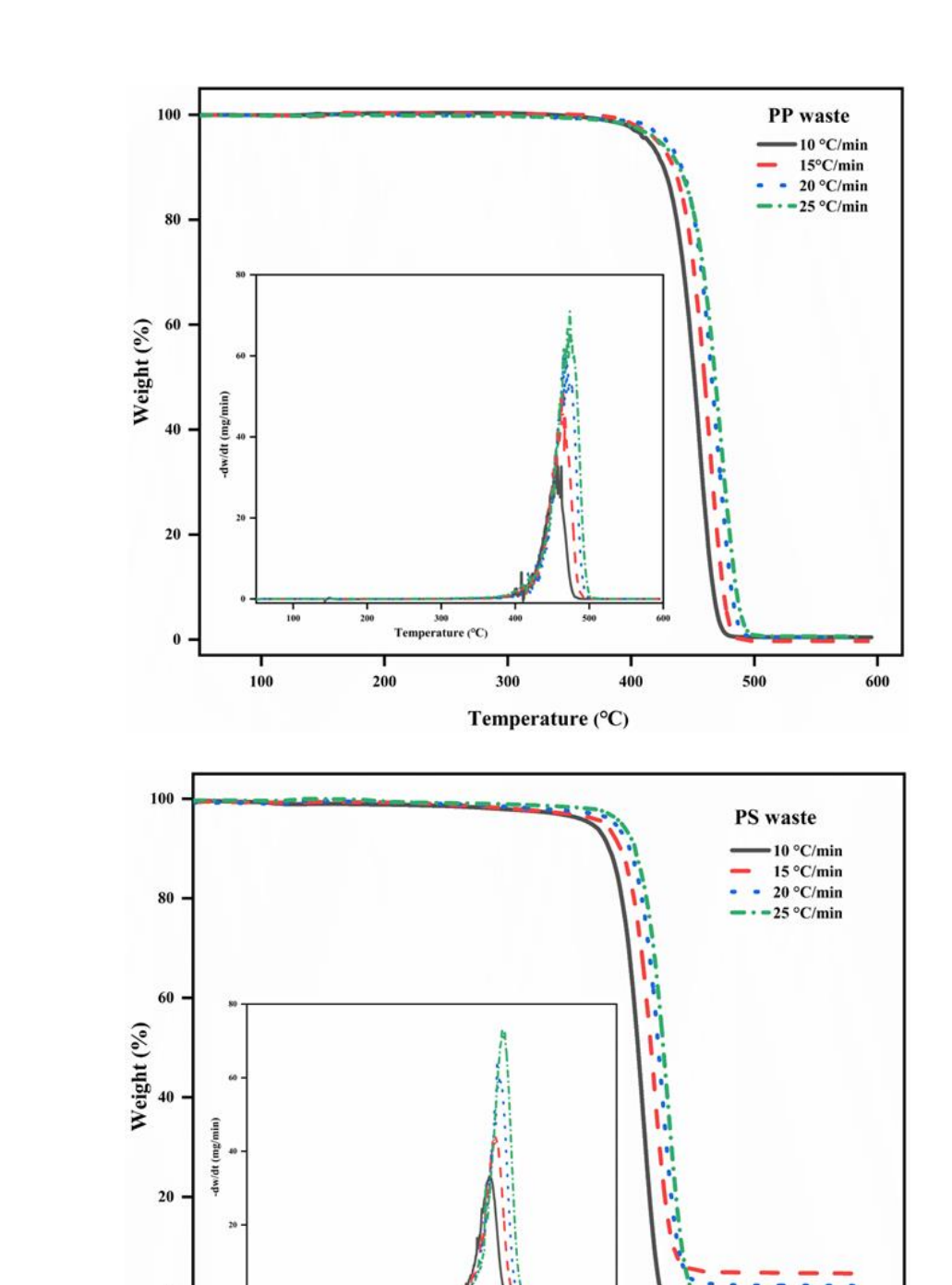


Figure 5.1 TG/DTG curves of (a)HDPE, (b)LDPE, (c)PP, and (d)PS waste at different heating rates

Temperature (°C)

300

400

500

360 400 Temperature (°C)

200

100

Table 5.1 Thermal degradation interval, maximum weight loss temperature (T_{max}) and maximum weight loss at different heating rates for HPDE, PP, LDPE, and PS waste.

| Waste Sample | β | Thermal degradation | Tmax | Weight Loss | |
|--------------|----------|---------------------|---------------|-------------|--|
| | (°C/min) | interval (°C) | (° C) | (wt. %) | |
| HDPE | 10 | 388 – 481 | 475 | 95.2 | |
| | 15 | 397 - 502 | 479 | 99.2 | |
| | 20 | 404 - 508 | 485 | 94.5 | |
| | 25 | 425 - 514 | 497 | 95.6 | |
| PP | 10 | 365 - 477 | 456 | 95.0 | |
| | 15 | 387 - 484 | 461 | 99.4 | |
| | 20 | 349 - 492 | 466 | 98.9 | |
| | 25 | 352 - 487 | 471 | 93.0 | |
| LDPE | 10 | 280 - 498 | 477 | 99.0 | |
| | 15 | 309 - 505 | 484 | 99.7 | |
| | 20 | 425 - 509 | 488 | 98.9 | |
| | 25 | 435 - 513 | 491 | 98.8 | |
| PS | 10 | 255 - 425 | 409 | 99.4 | |
| | 15 | 246 - 458 | 417 | 98.9 | |
| | 20 | 279 - 463 | 423 | 96.6 | |
| | 25 | 250 - 450 | 430 | 99.1 | |

The DTG curves shown in Fig. 5.1, also displayed the offsetting of the curves to the higher temperatures with increase in heating rates. Also, a lateral shift in the T_{max} was observed from the DTG curves, and it can be evident from Table 2. However, for HDPE wastes, the DTG curves for the heating rate of 10 and 15 °C·min⁻¹ had followed the same pattern of offsetting to higher temperatures on increasing the heating rate. But on further increase of the heating rate from 15 to 20 °C·min⁻¹, the DTG curve shifted to lower temperature. Although the height of the peak was increasing with increasing heating rates. Thereafter, on further increasing of the heating rate from 20 to 25 °C·min⁻¹, the peak decomposition temperature increased to higher temperature. In all of the DTG curves of different plastic wastes, it was observed that, thermal degradation interval were expanding on increasing the heating rates hence resulting in broader peaks, and further higher temperatures were required to attain the same degree of conversion (Dwivedi et al., 2021).

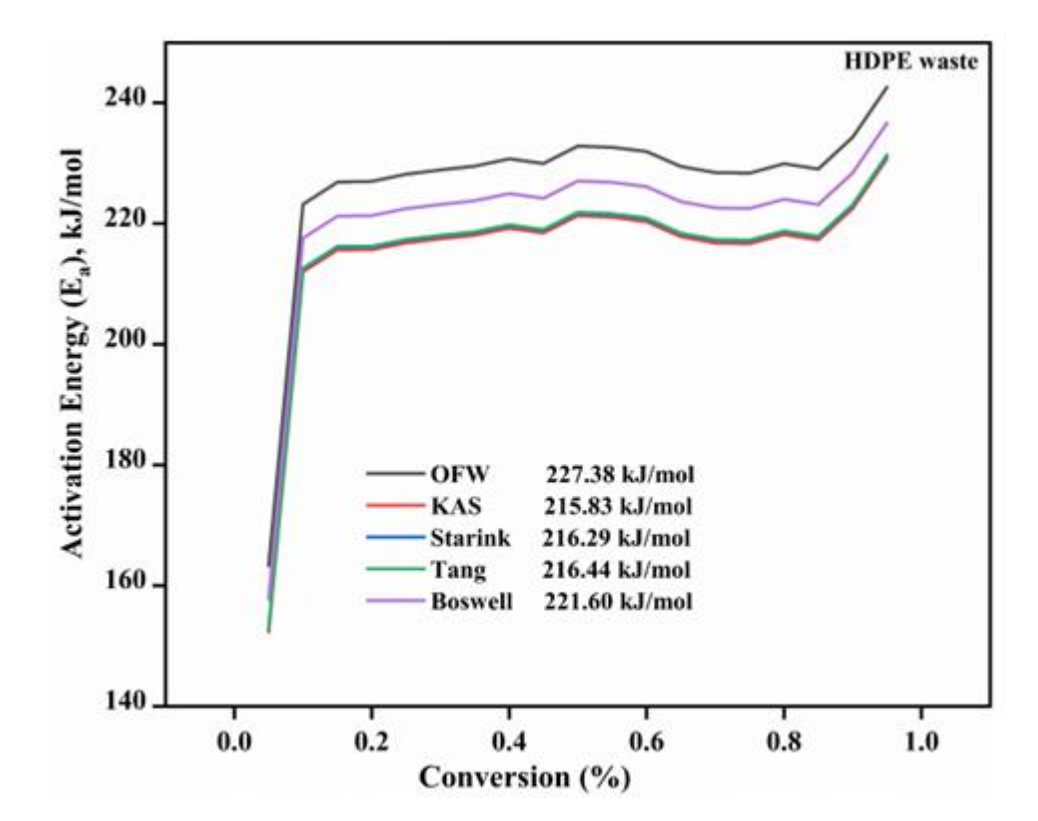
This phenomenon of peak broadening and peak offsetting had gathered attention of various research

groups, and obtained scattered set of arguments from them. Most of the researchers observed that the thermal lag during the thermogravimetric experiment and heat transfer limiting property of plastic polymer are the two significant reasons for this phenomenon (Al-Salem et al., 2017). At higher heating rates, it was observed that the furnace temperature and sample temperature in the thermogravimetric holder differs largely, and this in turn causes the existing thermal lag (Khedri and Elyasi, 2016; Kunwar et al., 2016). Also, the heat transfer into the reacting solid surface becomes more difficult at higher heating rates. Whereas a few researchers had reported that the change in the reaction mechanism during the thermal degradation at varying heating rate can be a suitable reason for the phenomenon (V et al., 1985; Wu et al., 1993).

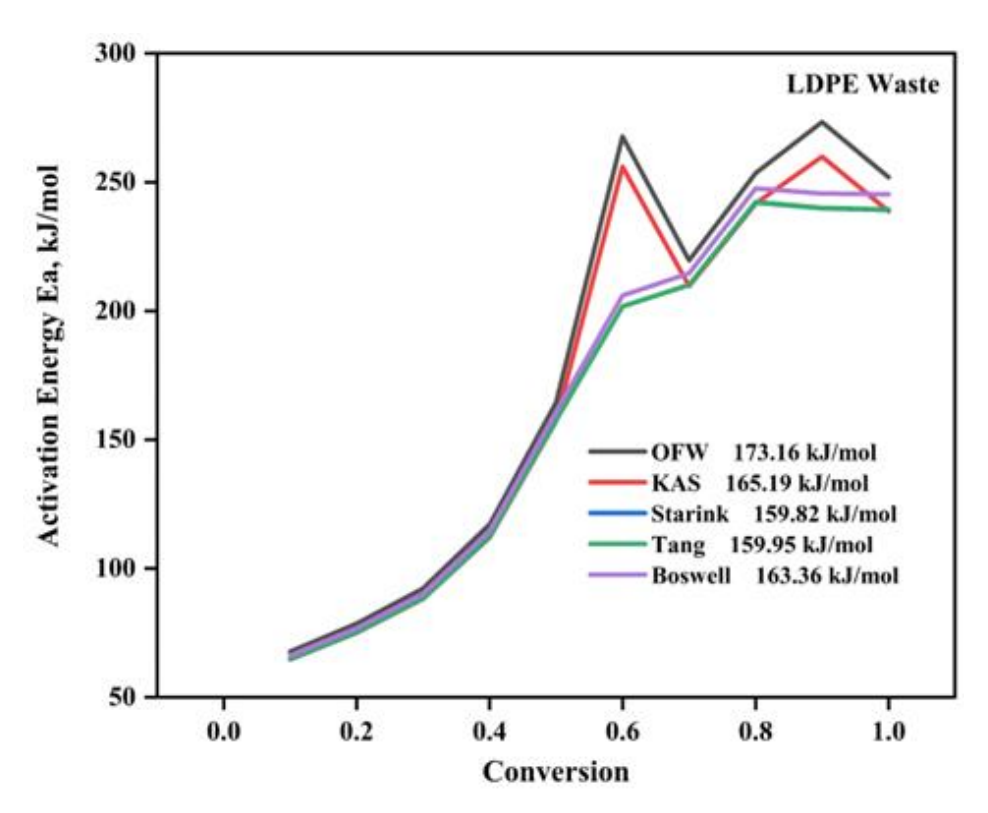
5.2.3 Kinetic parameters estimation using isoconversional methods

To evaluate the various kinetic parameters from obtained TGA data at different degree of conversion, the following five isoconversional/model-free methods; OFW, KAS, Starink, Tang and Boswell method were used. Initially, the left-hand side (LHS) of equations (8), (9), (10), (11) and (12) were plotted against 1/T. Thereby, the individual slope based on linear fitting equations were used to evaluate the E_{α} values. The evaluated E_{α} for α values ranging from 0.05 to 0.95 of different plastic wastes is displayed in Fig. 2. The evaluated values of the E_{α} obtained were ranging; 215.83 - 227.38 kJ·mol⁻¹, 33.91- 66.82 kJ·mol⁻¹, 159.83 - 171.72 kJ·mol⁻¹, and 149.59 - 160.48 kJ·mol⁻¹ for HDPE, LDPE, PP and PS respectively. Fig. 5.2, shows that all the five models displayed similar kind of trend of dependency of E_{α} on the degree of α . For HDPE and PS, initially at very lower α values, the E_{α} increased exponentially. Further there were fluctuations in the E_{α} values for α range 0.2 – 0.6. There was a gradual decrease in E_{α} values from 0.6 – 0.8 range of α . Towards the end of the thermal degradation of HDPE, the E_{α} values again showed an increasing trend, whereas that for PS continued decreasing further.

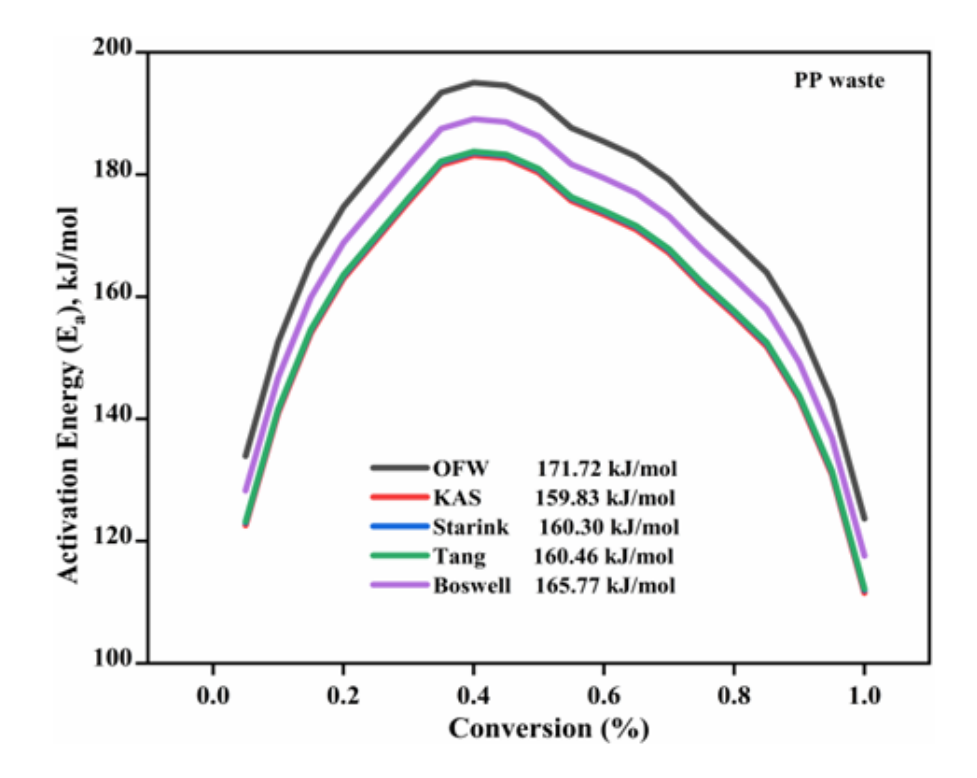




(b)









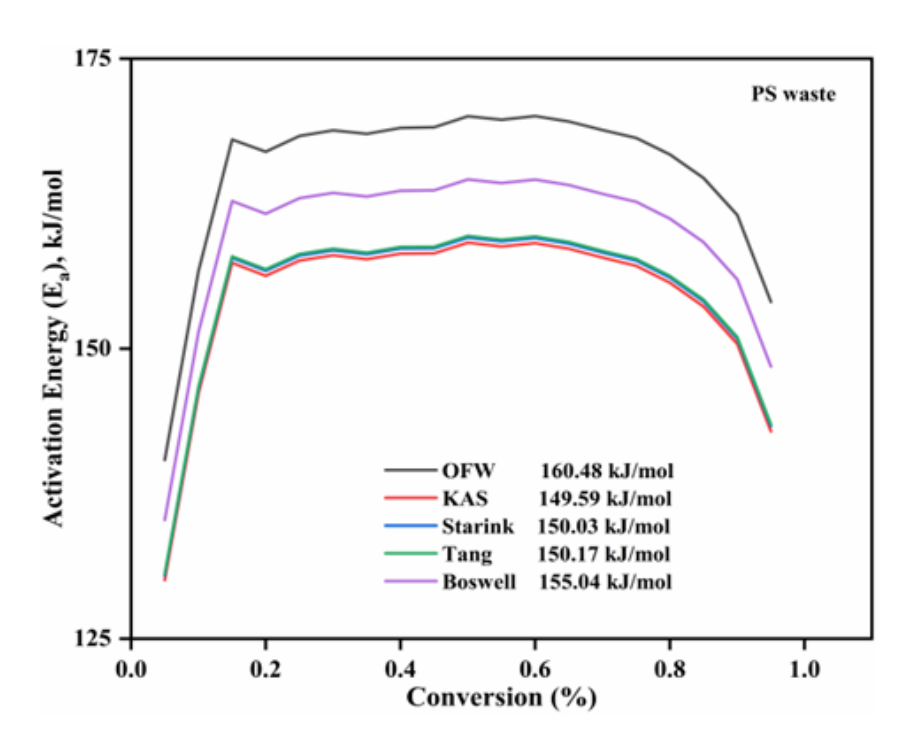


Figure 5.2 The calculated values of activation energies for (a) HDPE, (b) LDPE, (c) PP, and (d)

PS plastic wastes obtained from model-free methods

For PP waste, there was gradual increase of E_{α} values up to $\alpha=0.39$, followed by a gradual decrease continuously towards the end of the degradation process. The LDPE degradation process showed gradual increase in E_{α} values initially up to $\alpha=0.5$. Later, there was an increase in E_{α} values, however this increase was much steeper in OFW and KAS methods. Further the E_{α} values decreased and again the OFW and KAS showed a sudden decrease. Towards the end of the degradation the OFW and KAS methods followed the same trend as before, whereas the Starink, Tang and Boswell methods showed a constant value of E_{α} values. Generally, this irregular trend of E_{α} values contributes to the complex nature of thermal degradation reaction of plastic wastes (Ma et al., 2015). Researchers found that reaction schemes such as; chain end scission, molecular rearrangement and other reaction mechanisms contributes to this complex nature (Ma et al., 2015). The plastic waste degradation followed the following order: PS < PP < LDPE< HDPE based on their E_{α} values.

According to Fig. 2, the mean values of E_{α} obtained by OFW, KAS, Starink, Tang and Boswell method were; 227.35, 215.83, 216.29, 216.44 and 221.60 kJ·mol⁻¹ for HDPE, 171.72, 159.83, 160.30, 160.46, and 165.77 kJ·mol⁻¹ for PP, were 160.45, 149.59, 150.03, 150.17 and 155.04 kJ·mol⁻¹ for PS and 173.16, 165.19, 159.82, 159.95 and 163.36 for LDPE. A great consistency was seen among mean E_{α} values of all wastes evaluated from different methods. Whereas, the various differences among the mean values of E_{α} were because of the approximations used by models and factors like; heating rate, the source of materials and experimental apparatus (Hu et al., 2016).

The overall activation energy values of all four materials differ due to their molecular structures. During thermal treatment, the polyolefins; LDPE, HDPE and PP decompose into smaller hydrocarbons of various kinds (J.D. Peterson, et al., 2001). Thermal stability of polyolefins strongly affected by branching. In PP every other carbon atom in the main polymer chain is a tertiary carbon, which provide more weak links for the starting of the degradation reaction. Degradation of both PE and PP occur via random scission followed by radical transfer process. An increase in effective activation energy with the progress of reaction for PE (LDPE and HDPE) and PP is caused by shift of the rate limiting step from initiation to the degradation initiated by the random scission. The degradation of plastics involves the breaking of the bonds between individual atoms forming the polymer chain. The breaking of C-C bond (~350 kJ/mol) requires higher activation energy and the degradation occurs above 400 °C temperature. But the degradation starts easily because of thermally labile bonds (weak links like branching and head-to-head links) inherent with the polymer chain. This explains the low activation

energy at the beginning of the process (S. Vyazovkin, et al., 2006).

5.2.4 Model-fitting methods

5.2.4.1 Coats-Redfern Method

To determine the $f(\alpha)$, Coats–Redfern method is widely ("© 1964 Nature Publishing Group," 1964; Hu et al., 2016). It was proposed by Coats and Redfern, expressed in equation (13). Table 5.2, shows the E_{α} for all $g(\alpha)$ evaluated at 15 °C·min⁻¹ for the same degree of α as used by the model-free methods. Since the maximum weight loss degradation had happened at 15 °C·min⁻¹, hence E_{α} values at this heating rate only are tabulated. From the tabulated values, $E_{\alpha} = 260 \text{ kJ.mol}^{-1}$ that corelates with the E_{α} values obtained from model free methods, thereby suggesting that R3 mechanism was the most suitable for HDPE degradation. Criado method was used to further confirm the $f(\alpha)$. Similarly, the best suitable $g(\alpha)$ for other wastes obtained were A3, A2 and R2 for PP, PS and LDPE respectively. The E_{α} obtained for PP, PS and LDPE wastes from Coats-Redfern method were 166.38, 144.47 and 167.13 kJ.mol⁻¹ respectively, as compared with $E_{\alpha} = 165.77$, 149.59, and 165.19 kJ.mol⁻¹ obtained from Boswell, KAS and KAS (isoconversional methods) respectively. The reliability of the obtained $g(\alpha)$ by using Coats-Redfern method was confirmed by the value of correlation coefficient (R^2). Mostly the R^2 values were above 0.9 for all $g(\alpha)$. Moreover, different $g(\alpha)$ showed great fluctuations in E_{α} , which proves that not all the $g(\alpha)$ is suitable for the particular sample.

Table 5.2 The evaluated values of Ea for LDPE, PS, PP and HDPE at 15 °C·min-1 by Coats-Redfern method.

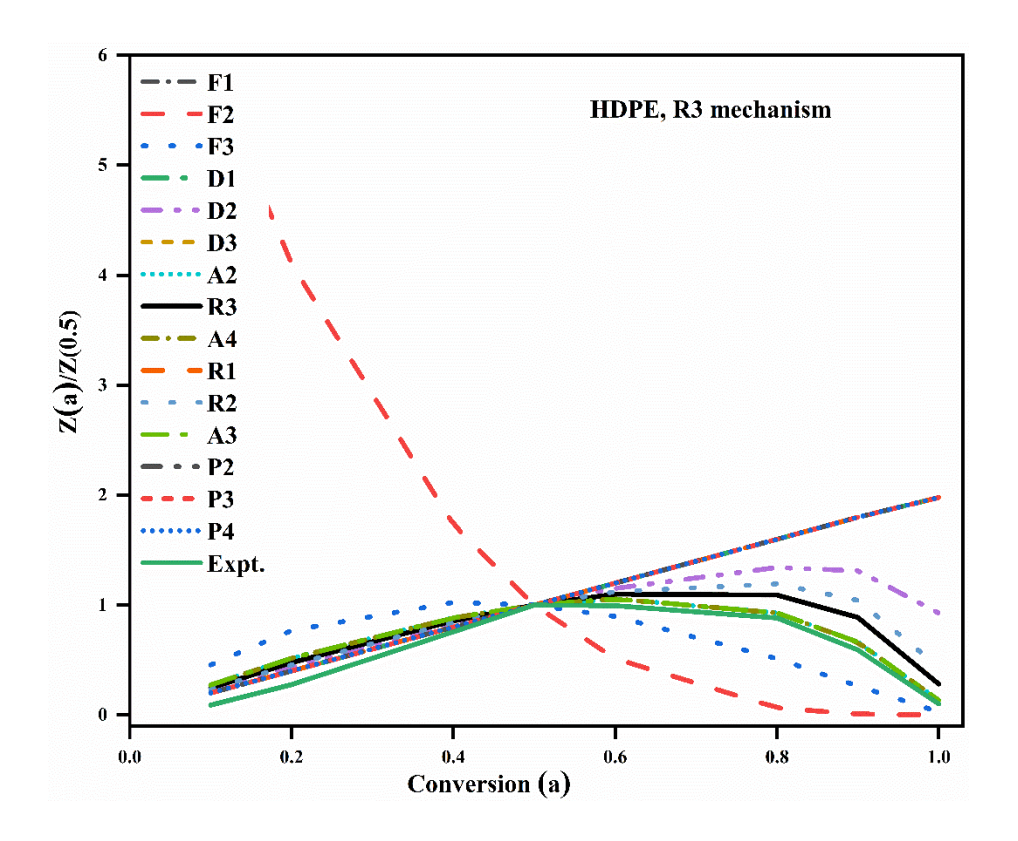
| Model | LDPE | | PS | PP | | HDPE | | |
|------------|---------------------------|----------------|---------------------------|----------------|---------------------------|----------------|---------------------------|----------------|
| | 15 (°C/min) | | | | | | | |
| | $\mathbf{E}_{\pmb{lpha}}$ | \mathbb{R}^2 | $\mathbf{E}_{\pmb{lpha}}$ | \mathbb{R}^2 | $\mathbf{E}_{\pmb{lpha}}$ | \mathbb{R}^2 | $\mathbf{E}_{\pmb{lpha}}$ | \mathbb{R}^2 |
| | (kJ/mol) | value | (kJ/mol) | value | (kJ/mol) | value | (kJ/mol) | value |
| F 1 | 419.05 | 0.9677 | 260.40 | 0.9682 | 345.16 | 0.9786 | 319.23 | 0.9914 |
| F2 | -709.53 | 0.5175 | -266.72 | 0.7790 | -293.60 | 0.6382 | -286.87 | 0.6302 |
| F3 | 1556.56 | 0.5842 | 636.51 | 0.8955 | 742.41 | 0.7798 | 714.40 | 0.7724 |

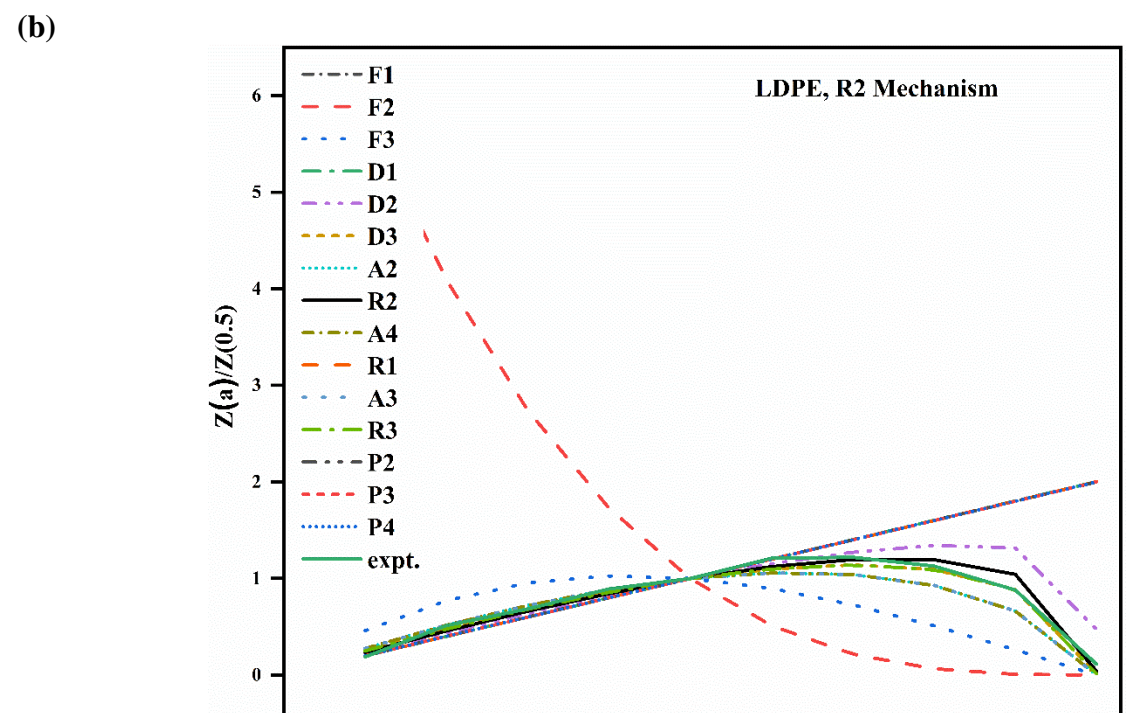
| D1 | 481.14 | 0.9542 | 353.60 | 0.8705 | 491.29 | 0.9762 | 450.46 | 0.9672 |
|-----------|--------|--------|--------|--------|--------|--------|--------|--------|
| D2 | 548.66 | 0.9762 | 394.56 | 0.8981 | 543.46 | 0.9843 | 498.49 | 0.9815 |
| D3 | 668.37 | 0.9989 | 456.84 | 0.9389 | 617.44 | 0.9883 | 568.24 | 0.9945 |
| A2 | 203.25 | 0.9658 | 144.47 | 0.9651 | 106.79 | 0.9771 | 153.58 | 0.9908 |
| A3 | 131.32 | 0.9638 | 79.16 | 0.9615 | 166.38 | 0.9755 | 98.36 | 0.9901 |
| A4 | 95.35 | 0.9616 | 56.51 | 0.9575 | 77.00 | 0.9737 | 70.76 | 0.9894 |
| R1 | 234.30 | 0.9517 | 171.07 | 0.8625 | 239.45 | 0.9749 | 219.20 | 0.9653 |
| R2 | 167.13 | 0.9989 | 207.21 | 0.9170 | 284.24 | 0.9876 | 278.09 | 0.9898 |
| R3 | 157.91 | 0.9922 | 222.69 | 0.9357 | 302.53 | 0.9878 | 260.79 | 0.9942 |
| P2 | 110.87 | 0.9462 | 79.81 | 0.8445 | 113.53 | 0.9721 | 103.57 | 0.9610 |
| P3 | 69.73 | 0.9397 | 49.39 | 0.8230 | 71.56 | 0.9688 | 65.02 | 0.9560 |
| P4 | 49.16 | 0.9320 | 34.18 | 0.7974 | 50.57 | 0.9649 | 45.75 | 0.9501 |

5.2.4.2 Master plots of Criado Method to determine the reaction mechanism

Coats-Redfern equation suggests that if a correct $g(\alpha)$ is selected for the reaction then a linear plot of $\ln (g(\alpha)/T^2)$ versus 1/T with high R^2 value will be obtained (Dubdub and Al-yaari, 2020). Hence, only Coats-Redfern method is not enough and unable to kinetics assessment of reactions (Criado, 1978). Therefore, employment of Criado method is very important, as it can be additional to Coats-Redfern method and provides more information about the reaction kinetics. From fig. 5.3, it was observed that the most suitable $f(\alpha)$ for HDPE, LDPE, PP and PS obtained from overlapping of the experimental curves over theoretical curves were R3, R2, A3 and A2 respectively. The obtained $f(\alpha)$ for LDPE and HDPE were similar to the $f(\alpha)$ obtained by other researchers (Das and Tiwari, 2017; Xu et al., 2018). However, the $f(\alpha)$ obtained for PP varied from the other studies. This change maybe due to the heterogeneity in the composition of the PP. Therefore, further investigation is needed for determining the best suitable $f(\alpha)$ for the thermal degradation of plastic waste irrespective of the many factors influencing the kinetic parameters.

(a)





0.4 Conversion (a) 0.6

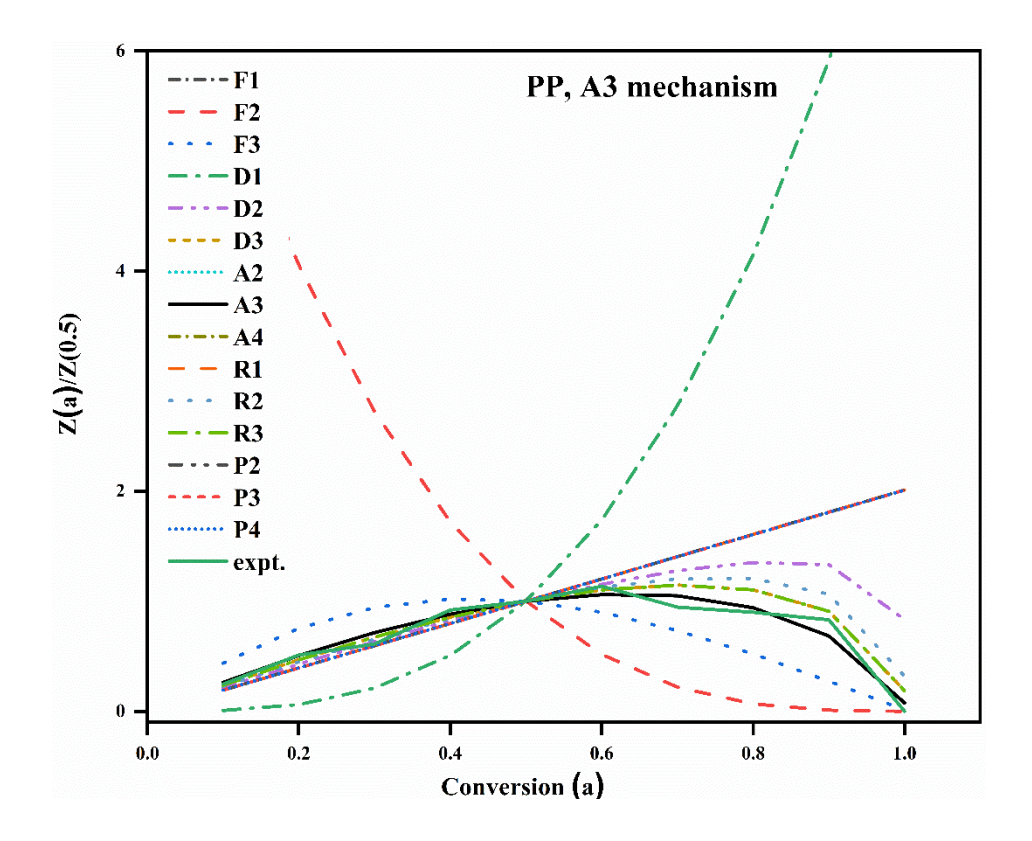
0.8

1.0

(c)

0.0

0.2



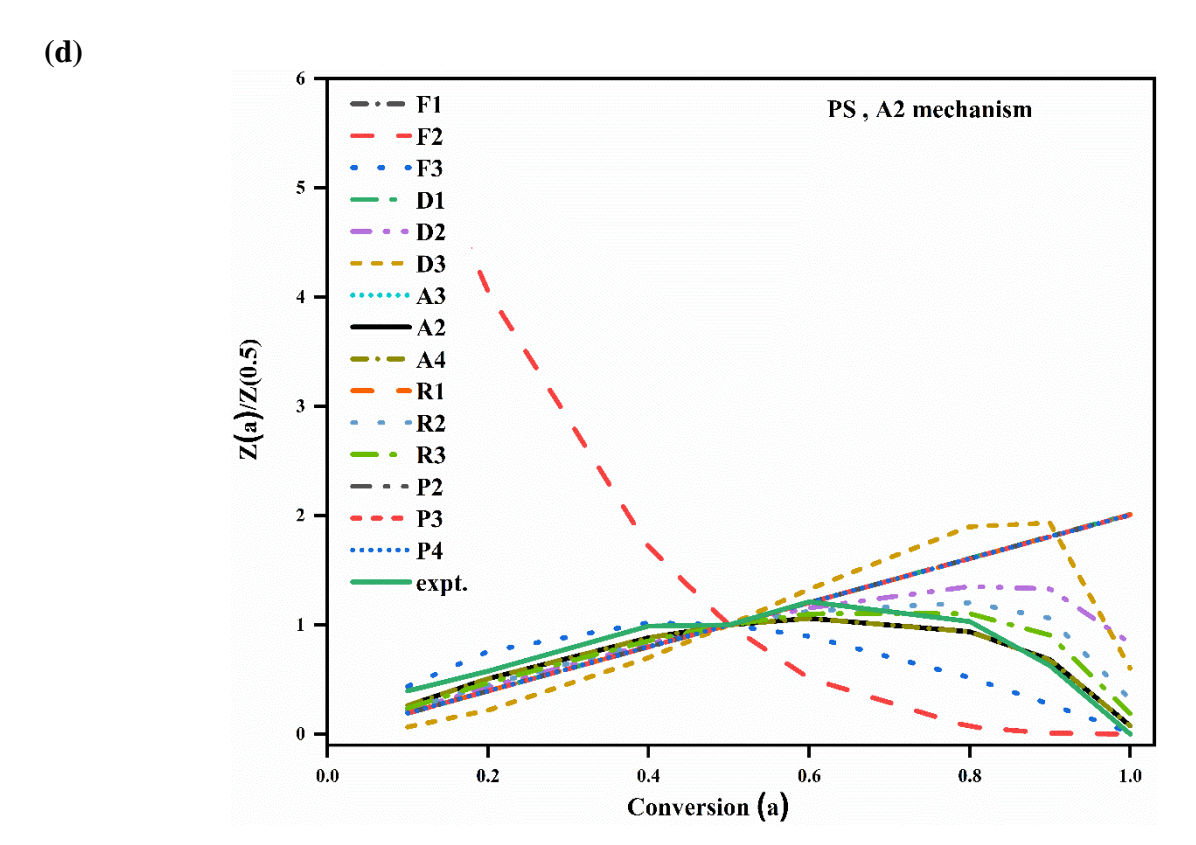


Figure 5.3 Determination of reaction mechanism for (a) HDPE, (b) LDPE, (c) PP, and (d) PS wastes from master plots of Criado method

5.3 Conclusion

The kinetic analysis of HDPE, LDPE, PP and PS wastes were studied by TGA at heating rates 10, 15, 20 and 25 °C/min. The thermal degradation of all these plastic wastes was observed to be of a single stage. TG/DTG curves showed lateral shift in maximum weight loss temperature and peak broadening towards higher temperature at higher heating rates. Estimated values of E_{α} computed from five isoconversional methods were 159.83–171.72 kJ·mol⁻¹ for PP, 215.83 - 227.38 kJ·mol⁻¹ for HDPE, 159.82 to 173.16 kJ.mol⁻¹ for LDPE and 149.59 – 160.48 kJ·mol⁻¹ for PS, respectively. According to E_{α} values, the ease of thermal degradation of wastes followed the order as follows; PS < PP < LDPE < HDPE. Furthermore, method-fitting methods provided the $f(\alpha)$ of all the plastic wastes and these were R3(contracting cylinder), R2 (contracting sphere), A3 (3D nucleation) and A2 (2D nucleation) for HDPE, LDPE, PP, and PS respectively. Since heterogeneity is a critical parameter of assessing plastic wastes, it's effect on kinetic analysis of thermal degradation process of plastic is still an interesting area to study. Ongoing work will further focus on investigating thermal pyrolysis of the these real-waste plastic wastes at different heating rates and their product distribution and properties.

5.4 References

- [1] Aboulkas, A., El harfi, K., El Bouadili, A., 2010. Thermal degradation behaviors of polyethylene and polypropylene. Part I: Pyrolysis kinetics and mechanisms. Energy Convers. Manag. 51, 1363–1369. https://doi.org/10.1016/j.enconman.2009.12.017
- [2] Al-Salem, S.M., Antelava, A., Constantinou, A., Manos, G., Dutta, A., 2017. A review on thermal and catalytic pyrolysis of plastic solid waste (PSW). J. Environ. Manage. 197, 177–198. https://doi.org/10.1016/j.jenvman.2017.03.084
- [3] Al-Salem, S.M., Lettieri, P., Baeyens, J., 2009. Recycling and recovery routes of plastic solid waste (PSW): A review. Waste Manag. 29, 2625–2643. https://doi.org/10.1016/j.wasman.2009.06.004
- [4] Khawam, A. (2007). Application of solid-state kinetics to desolvation reactions. The University of Iowa.
- [5] Criado, J.M., 1978. Kinetic analysis of DTG data from master curves. Thermochim. Acta 24, 186–189. https://doi.org/10.1016/0040-6031(78)85151-X
- [6] Das, P., Tiwari, P., 2017. Thermal degradation kinetics of plastics and model selection. Thermochim. Acta 654, 191–202. https://doi.org/10.1016/j.tca.2017.06.001
- [7] Dubdub, I., & Al-Yaari, M. (2020). Pyrolysis of mixed plastic waste: I. kinetic study. *Materials*, 13(21), 4912.
- [8] Dwivedi, U., Naik, S.N., Pant, K.K., 2021. High quality liquid fuel production from waste plastics via two-step cracking route in a bottom-up approach using bi-functional Fe/HZSM-5 catalyst. Waste Manag. 132, 151–161. https://doi.org/10.1016/j.wasman.2021.07.024
- [9] Hu, M., Chen, Z., Wang, S., Guo, D., Ma, C., Zhou, Y., Chen, J., Laghari, M., Fazal, S., Xiao, B., Zhang, B., Ma, S., 2016. Thermogravimetric kinetics of lignocellulosic biomass slow pyrolysis using distributed activation energy model, Fraser-Suzuki deconvolution, and isoconversional method. Energy Convers. Manag. 118, 1–11. https://doi.org/10.1016/j.enconman.2016.03.058
- [10] Khedri, S., Elyasi, S., 2016. Kinetic analysis for thermal cracking of HDPE: A new isoconversional approach. Polym. Degrad. Stab. 129, 306–318. https://doi.org/10.1016/j.polymdegradstab.2016.05.011

- [11] Kremer, I., Tomić, T., Katančić, Z., Hrnjak-Murgić, Z., Erceg, M., Schneider, D.R., 2021. Catalytic decomposition and kinetic study of mixed plastic waste. Clean Technol. Environ. Policy 23, 811–827. https://doi.org/10.1007/s10098-020-01930-y
- [12] Kunwar, B., Cheng, H.N., Chandrashekaran, S.R., Sharma, B.K., 2016. Plastics to fuel: a review. Renew. Sustain. Energy Rev. 54, 421–428. https://doi.org/10.1016/j.rser.2015.10.015
- [13] Luiz, J., Alves, F., Constantino, J., Francisco, V., Francisco, R., Venicio, W., Galdino, D.A., Felix, R., Sena, D., 2019. Biomass and Bioenergy Kinetics and thermodynamics parameters evaluation of pyrolysis of invasive aquatic macrophytes to determine their bioenergy potentials. Biomass and Bioenergy 121, 28–40. https://doi.org/10.1016/j.biombioe.2018.12.015
- [14] Ma, Z., Chen, D., Gu, J., Bao, B., Zhang, Q., 2015. Determination of pyrolysis characteristics and kinetics of palm kernel shell using TGA-FTIR and model-free integral methods. Energy Convers. Manag. 89, 251–259. https://doi.org/10.1016/j.enconman.2014.09.074
- [15] Nisar, J., Ali, G., Shah, A., Iqbal, M., Ali, R., Anwar, F., Ullah, R., Salim, M., 2019. Fuel production from waste polystyrene via pyrolysis: Kinetics and products distribution. Waste Manag. 88, 236–247. https://doi.org/10.1016/j.wasman.2019.03.035
- [16] Özsin, G., Eren, A., 2019. TGA / MS / FT-IR study for kinetic evaluation and evolved gas analysis of a biomass / PVC co-pyrolysis process. Energy Convers. Manag. 182, 143–153. https://doi.org/10.1016/j.enconman.2018.12.060
- [17] Qin, L., Han, J., Zhao, B., Wang, Y., Chen, W., Xing, F., 2018. Thermal degradation of medical plastic waste by in-situ FTIR, TG-MS and TG-GC/MS coupled analyses. J. Anal. Appl. Pyrolysis. https://doi.org/10.1016/j.jaap.2018.10.012
- [18] Šimon, P. (2004). Isoconversional methods. *Journal of Thermal Analysis and Calorimetry*, 76, 123-132.
- [19] Sbirrazzuoli, N., Vincent, L., Mija, A., Guigo, N., 2009. Chemometrics and Intelligent Laboratory Systems Integral, differential and advanced isoconversional methods Complex mechanisms and isothermal predicted conversion time curves. Chemom. Intell. Lab. Syst. 96, 219–226. https://doi.org/10.1016/j.chemolab.2009.02.002
- [20] Senneca, O., Chirone, R., Masi, S., & Salatino, P. (2002). A thermogravimetric study

- of nonfossil solid fuels. 1. Inert pyrolysis. *Energy & fuels*, 16(3), 653-660.
- [21] Mookherjee, S., Ray, H. S., & Mukherjee, A. (1985). Thermogravimetric studies on the reduction of hematite ore fines by a surrounding layer of coal or char fines: Part 2. Non-isothermal kinetic studies. *Thermochimica acta*, 95(1), 247-256.
- [22] Vyazovkin, S., & Wight, C. A. (1999). Model-free and model-fitting approaches to kinetic analysis of isothermal and nonisothermal data. *Thermochimica acta*, *340*, 53-68.
- [23] Wu, C. H., Chang, C. Y., Hor, J. L., Shih, S. M., Chen, L. W., & Chang, F. W. (1993). On the thermal treatment of plastic mixtures of MSW: pyrolysis kinetics. *Waste Management*, 13(3), 221-235.
- [24] Xu, F., Wang, B., Yang, D., Hao, J., Qiao, Y., Tian, Y., 2018. Thermal degradation of typical plastics under high heating rate conditions by TG-FTIR: Pyrolysis behaviors and kinetic analysis. Energy Convers. Manag. 171, 1106–1115. https://doi.org/10.1016/j.enconman.2018.06.047
- [25] Yao, D., Yang, H., Chen, H., Williams, P.T., 2018. Co-precipitation, impregnation and so-gel preparation of Ni catalysts for pyrolysis-catalytic steam reforming of waste plastics. Appl. Catal. B Environ. 239, 565–577. https://doi.org/10.1016/j.apcatb.2018.07.075
- [26] J.D. Peterson, S. Vyazovkin, C.A. Wight, Kinetics of the thermal and thermo-oxidative degradation of polystyrene, polyethylene and poly(propylene), Macromol. Chem. Phys. 202 (2001) 775–784.
- [27] S. Vyazovkin, N. Sbirrazzuoli, Isoconversional kinetic analysis of thermally stimulated processes in polymers, Macromol. Rapid Commun. 27 (2006) 1515–1532.

6.1 Introduction

The catalytic pyrolysis of real-world plastic wastes with synthesized hierarchical ZSM-5 can produce aromatic rich fuel grade liquid oil. In the present work the synthesis of hierarchical ZSM-5 catalyst by using single organic template i.e., 10% tetra propylammonium hydroxide (TPAOH) resulting in dual porosity framework has been explored in depth. The presence of both mesopores and micropores in the hierarchical ZSM-5 catalyst have exhibited remarkable selectivity and increase in the yield of producing higher quality liquid oil. The results indicate that presence of catalyst has exceptionally lowered the reaction temperature in the range of 400- 430 °C, required for the pyrolysis of different plastic wastes. Also, the obtained liquid oils have comparable fuel properties with that of kerosene and diesel.

6.2. Results and discussion

6.2.1. Raw material characterizations

This section provides a detailed discussion on elemental analysis and FT-IR spectroscopy of raw material characterizations.

6.2.1.1 Proximate and ultimate (elemental) analysis

Table 4.1 shows the results of the ultimate analysis and proximate of different types of plastic wastes. The proximate analysis shows that PS waste contained the maximum volatile matter (99.96 wt. %) and minimum fixed carbon (0.04 wt. %) content as compared with others. However, HDPE, PP, and LDPE contained (96.08, 3.92), (95.57, 4.43) and (93.00, 7.00) wt. % of volatile matter and fixed carbon content respectively. It was observed from ultimate analysis that all the wastes contained considerable amount of the oxygen content in it. Hence, the obtained liquid oil contains oxygen derived components in it, further demanding the oil upgrading techniques.

6.2.1.2 FT-IR

Fig. 6.1 shows the FT-IR inferograms on transmission of the IR radiation of four plastic wastes, representing different chemical functionalities present in it (Chércoles Asensio et al., 2009; Guidelli et al., 2011; I. Noda et al., 2007; Smith, 2018; Tennakoon et al., 2020).

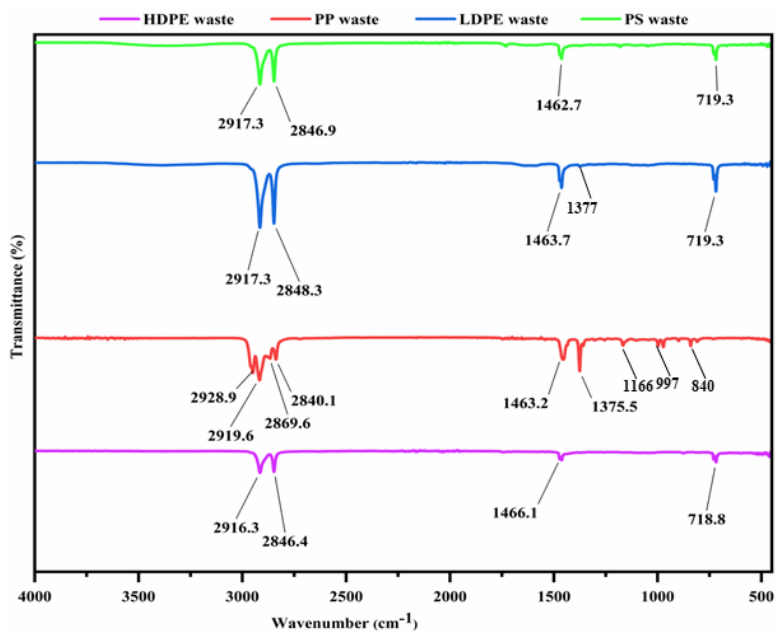


Figure 6.1 FT-IR spectrum of HDPE, PP, LDPE, and PS plastic wastes (raw materials)

From fig. 6.1, it is observed that in HDPE spectrum, the peak at 1466.1 cm⁻¹ is a confirmation of the denser form of polyethylene (PE) (Jung et al., 2018; Smith, 2021). Since the side chains are absent in HDPE, therefore the peaks at 2916.3 cm⁻¹ (asymmetric C-H stretch), 2846.4 cm⁻¹ (symmetric C-H stretch) and 719 cm⁻¹ corresponding to the methylene (-CH₂) group vibrations further confirms the HDPE form of PE (Das and Tiwari, 2018b; Jung et al., 2018). Similarly, the LDPE spectrum also contains methylene (-CH₂) group vibrations at peaks; 2917.3 cm⁻¹, 2848 cm⁻¹, 1463.7 cm⁻¹ and 719.3 cm⁻¹. However, differentiating between HDPE and LDPE is a challenging task, but due the presence of various side chains in LDPE, peak at 1377 cm⁻¹ confirms the presence of methyl (-CH₃) bending deformation (Chércoles Asensio et al., 2009; Yu et al., 2021). The peak at 1166 cm⁻¹ and 997 cm⁻¹ shows the characteristic peak of PP that represents its helix structure (Abdel-Hamid, 2005). The peaks at 2928.9 and 2919.6 cm⁻¹ corresponds to the asymmetric, whereas those at 2869.6 and 2840.1 cm⁻¹ are the symmetric stretching vibration of CH₃ and CH₂ groups (Abdel-Hamid, 2005; Yu, 2021). The peaks at 1463.2 and 1375.5 cm⁻¹ corresponds to symmetric and asymmetric scissoring vibrations of

the methyl group in PP. Similarly, PS also has asymmetric and symmetric stretching vibration of aliphatic CH₃ and CH₂ groups at 2917.3 and 2846.9 cm⁻¹ respectively, methylene (-CH₂) group vibration at 1462.7 and 719.3 cm⁻¹ (Wu et al., 2001).

6.2.2 Catalyst characterizations

6.2.2.1 Scanning electron microscope (SEM)

Fig. 6.2 shows the surface morphology of hierarchical ZSM-5. The presence of hierarchical mesoporosity and rough surface is clearly visible in fig. 7.2 (a) (Wang et al., 2010). The surface roughness results after the removal of the template (Krisnandi et al., 2015; Wang et al., 2010). At higher magnification in fig. 7.2 (b & c), the hierarchical mesoporosity is present along with uniform pentasil shaped crystals looking like coffin and sharp needles (Feng et al., 2009; Mohamed et al., 2005). This pentasil structure characterizes a typical ZSM-5 particle (Mohamed et al., 2005; Wang et al., 2010; Xue et al., 2012). In addition, N₂ adsorption results further confirms the hierarchical ZSM-5 structure.

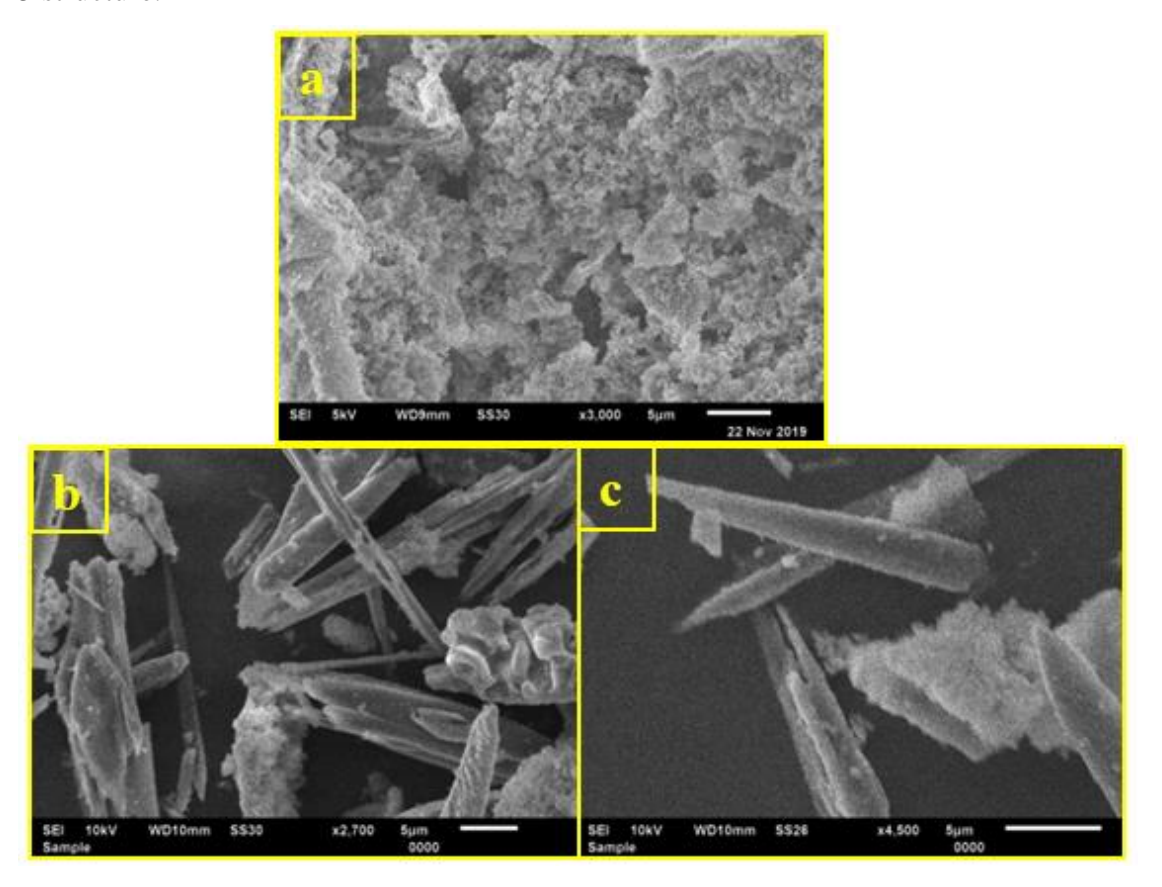


Figure 6.2 SEM images showing the surface morphology of the synthesized hierarchical ZSM-5 catalyst

6.2.2.2 X-ray diffraction (XRD)

The XRD pattern of the synthesized hierarchical ZSM-5 shown in the fig. 6.3, is in good agreement with literature (Biriaei, 2021; Feng et al., 2009; Mohamed et al., 2005; Ren et al., 2012; Wang et al., 2010; Xu et al., 2008; Zahara et al., 2023). The characteristic peaks were obtained at $2\theta = 7-9^{\circ}$ (2 peaks) and $2\theta = 22-25^{\circ}$ (3 peaks). The presence of characteristic crystalline phase (MFI structure) of the catalyst is established by the presence of the 6 planes i.e., (101), (020), (301), (501), (303) and (133) corresponding to various diffraction peaks at $2\theta = 7.93$, 8.77, 14.75, 23.05, 23.92 and 24.51 respectively (Anekwe et al., 2024; Michael et al., n.d.; Peng et al., 2019; Yang et al., 2019). Furthermore, the narrow and sharp nature of these peaks proves the high degree of crystallinity (Reding et al., 2003; Rohayati et al., 2017; Zahara et al., 2023).

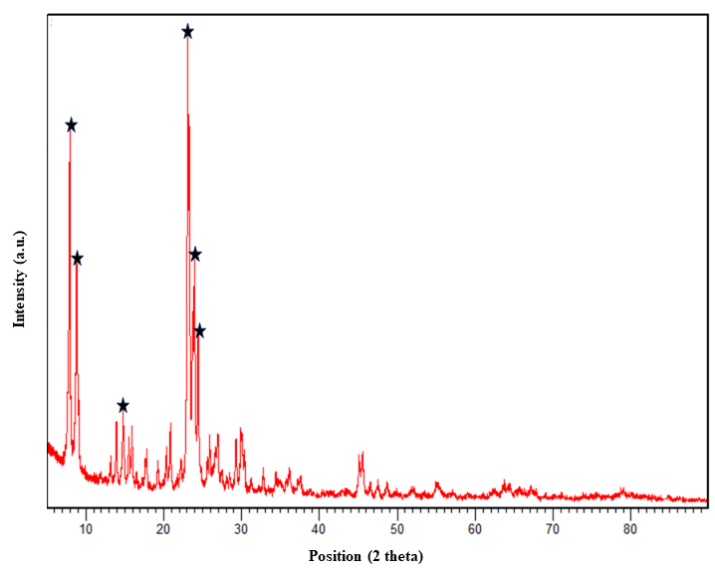


Figure 6.3 XRD pattern of the synthesized hierarchical ZSM-5 catalyst

6.2.2.3 FT-IR

Fig. 6.4 presents the FT-IR spectra of the synthesized hierarchical ZSM-5 in 499 to 4000 cm⁻¹ wavenumbers range. The peak at 546 cm⁻¹ marks the presence of double 5-ring units of pentasil zeolite framework (Anekwe et al., 2024; Sabarish and Unnikrishnan, 2020; Tao et al., 2013) in agreement of the SEM results. The sharp peak at 1072.22 cm⁻¹ corresponds to the internal symmetric stretching of the tetrahedrons (Si–O–Si linkage) (Anekwe et al., 2024; Liu et al., 2011). The catalyst framework-

sensitive (T-O band, here T= Si or Al) region of IR is represented by peaks at 1113.81 cm⁻¹ and 1218.09 cm⁻¹ corresponding to internal and external asymmetric stretching of siliceous materials respectively. The water adsorbed in the cavities of catalyst framework, attributes to the peak at 1630.58 cm⁻¹. The stretching frequency of silanol (Si–O–H) bond of the catalyst is shown by the peak at 3600 cm⁻¹.

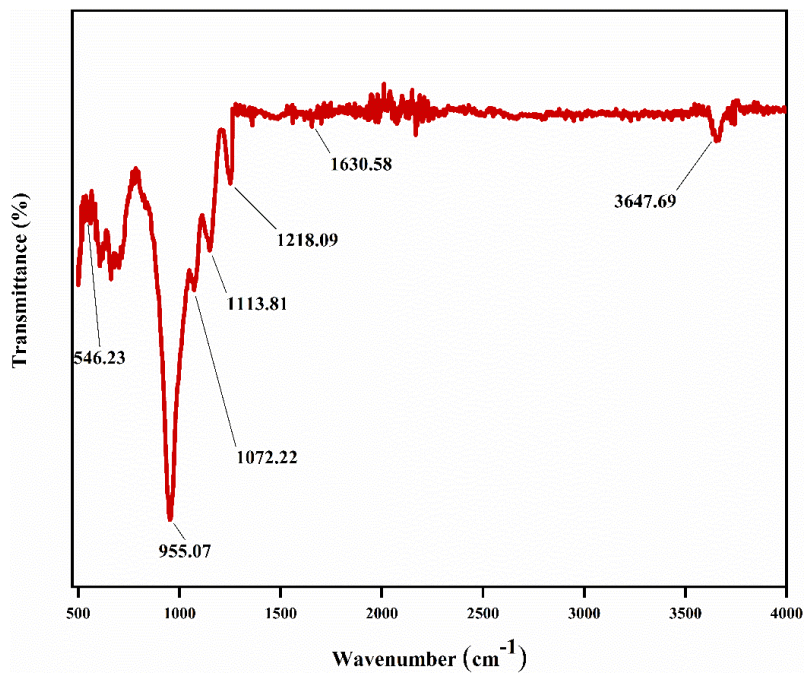


Figure 6.4 FT-IR spectra of synthesized hierarchical ZSM-5 catalyst

6.2.2.4 N₂ adsorption-desorption

Fig. 6.5 depicts the N_2 sorption isotherms of the synthesized hierarchical ZSM-5 catalyst. The broad hysteresis loop of N_2 adsorption-desorption isotherms indicate a type IV isotherm (Pyra et al., 2021). It is observed that the primary adsorption is in the range of $P/P_0 = 0.0 - 0.02$ (relative pressure), showcasing the characteristic presence of micropores. Additionally, the presence of mesopores is confirmed by the hysteresis loop occurring at $P/P_0 = 0.4 - 0.9$. Thus, the N_2 sorption isotherms confirm the presence of dual porosities in the catalyst. Table 6.1 shows the result of BET surface area analysis and textural properties of the catalyst. The pore size distribution of the catalyst is shown in the fig. 6.5 inset graph. Although the total surface area obtained was 295 m²/g, a little less as compared with the literature, however the presence of dual porosity was evident from presence of two different types of pore diameters.

Table 6.1 Textural properties of the synthesized hierarchical ZSM-5 catalyst

| Catalyst | Total S _{BET} | Total volume | Avg. Pore dia. | | | | |
|----------|-----------------------------|----------------------|-------------------------------------|--|--|--|--|
| | $(\mathbf{m}^2/\mathbf{g})$ | (cm ³ /g) | (nm) | | | | |
| ZSM-5 | 295 | 0.38 | 1.49 (micropore) & 32.48 (mesopore) | | | | |

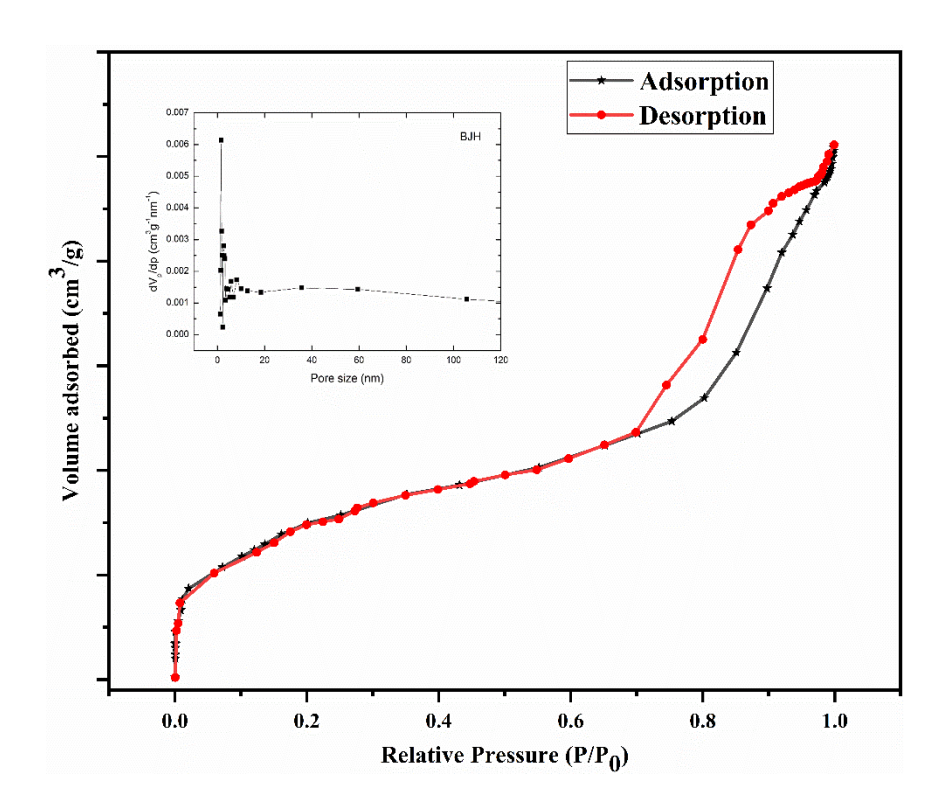


Figure 6.5 Nitrogen adsorption-desorption isotherm for synthesized hierarchical ZSM-5 with inset

BJH pore size distribution result

6.2.3 Catalytic cracking test and product analysis

The synthesized hierarchical ZSM-5 was used for the catalytic cracking of the different plastic wastes. Fig. 6.6 shows the thermal degradation temperature range of the various plastic wastes at a heating rate of 15 °C/min with the DTG curves in the inset graph. It was observed that the degradation temperature increased as PS < PP < LDPE < HDPE in the temperature range of 430-500 °C. 95-99 % weight loss was observed in this temperature range.

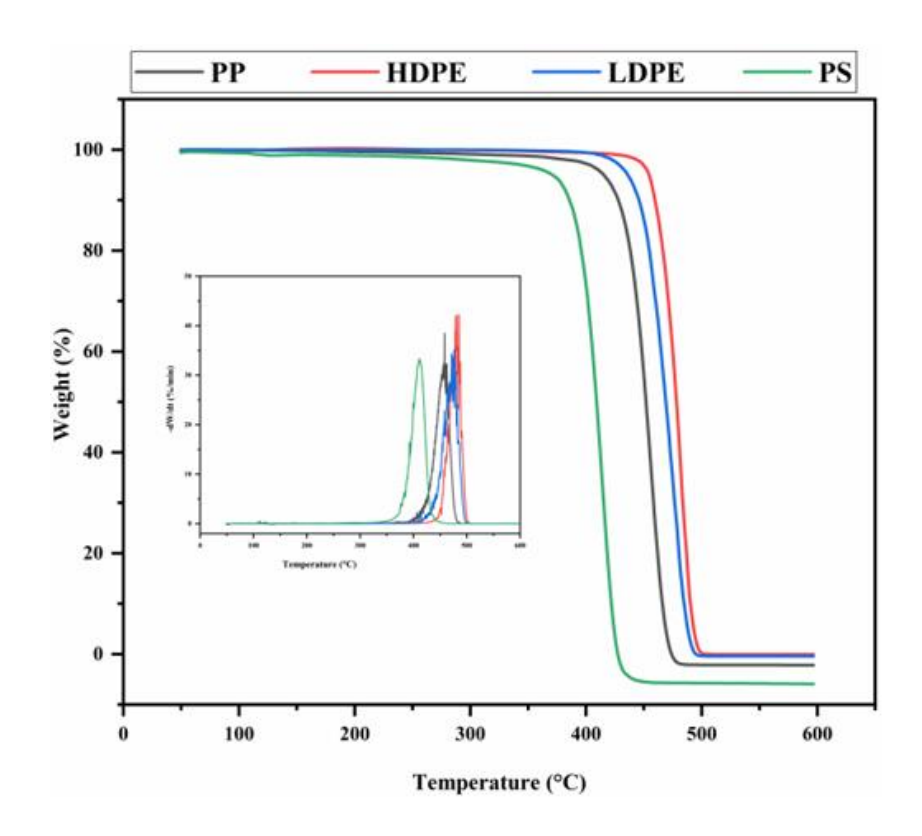


Figure 6.6 The thermal degradation trends of PP, HDPE, LDPE, and PS along with their inset DTG curves

However, it was observed that higher temperatures favored higher gas yields (Al-Salem et al., 2017; Calero et al., 2023; Dwivedi et al., 2021; Maqsood et al., 2021). Hence after few sets of test runs, the reaction temperature range was reduced to 400 – 430 °C in agreement with various literature (Al-Salem et al., 2017; Calero et al., 2023; Dwivedi et al., 2021; Maqsood et al., 2021). This lower range of cracking temperature is due to the presence of the catalyst ZSM-5. Hence as compared with the previous study dealing with the thermal cracking of the same wastes using same reactor set up (Subhashini and Mondal, 2023), it was evident that use of the catalyst had achieved higher desired product distribution at lower temperatures with the same heating rate. The product distribution obtained from the catalytic cracking of the plastic waste is shown in fig. 6.7. The use of catalyst had favored higher liquid oil yield. The wt. % of the liquid oil obtained from PP, HDPE, LDPE, and PS were 45%, 54%, 59%, and 63%. This varying liquid oil yield validates effect of elemental composition on the products yield (Al-Salem et al., 2017; Barbarias et al., 2018; Rehan et al., 2017).

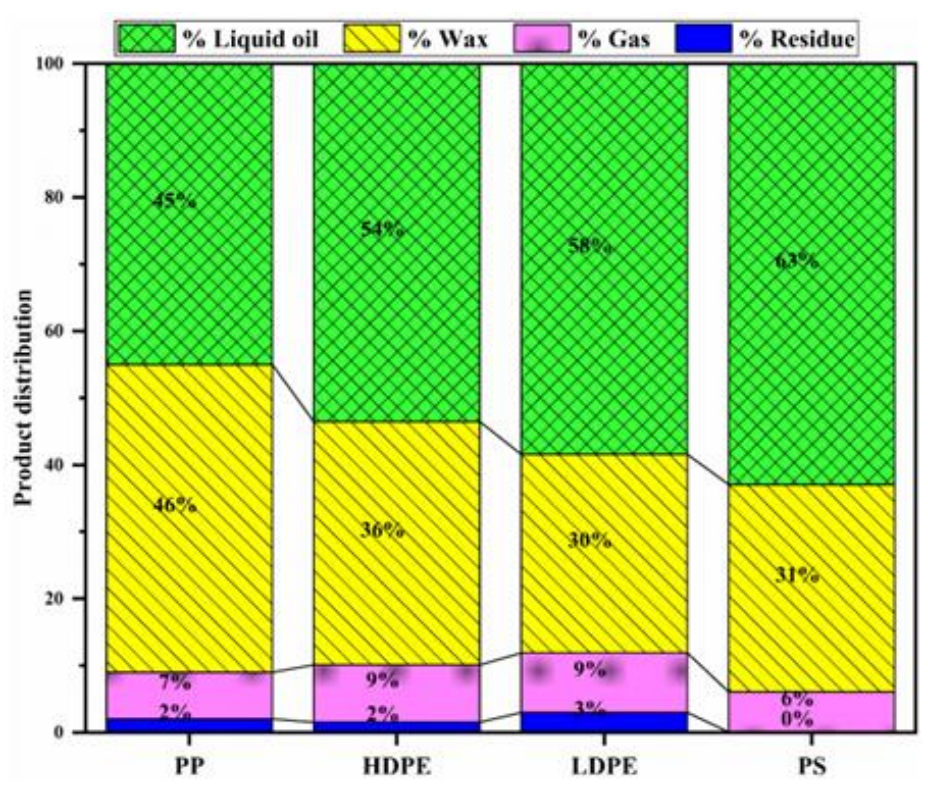


Figure 6.7 Product distribution of catalytic process of different plastic wastes

PS produced the maximum oil of 63 wt. %. Since the volatile matter content was maximum in PS waste hence it favored maximum liquid oil yield. Fig. 6.8 evident a remarkable increase in the yield of liquid oil produced from catalytic pyrolysis of different wastes. In case of PP, HDPE and LDPE, the percentage yield of liquid oil almost got doubled i.e., 24%, 37%, and 43.9% respectively as compared to that obtained in thermal pyrolysis. Whereas, the PS wastes observed an increment of 9.6% in the liquid oil yield. In case of percentage yield of wax, a downtrend is observed in catalytic pyrolysis of all the plastic wastes. A decline of 15%, 26.3%, 30.8% and 9.9% is observed in the % wax yield obtained from catalytic pyrolysis of PP, HDPE, LDPE, and PS wastes respectively. A similar downtrend is observed in the percentage yield of residue (9%, 11.5%, 10.9% and 0% in PP, HDPE, LDPE, and PS respectively) in catalytic pyrolysis of plastic wastes. These results support the

performance of the catalyst in aiding the cracking of larger molecules into smaller molecules and favoring the liquid oil yield. Therefore, the hierarchical nature of the synthesized catalyst provided the mesoporous sized active sites for the cracking of larger molecules and enhancing the catalytic efficiency. However, the %gas yield remained almost same for PP waste in both type of pyrolysis but decreased for both HDPE and LDPE waste by 0.2% and 1.2% respectively, and increased for PS waste by 0.4% catalytic pyrolysis.

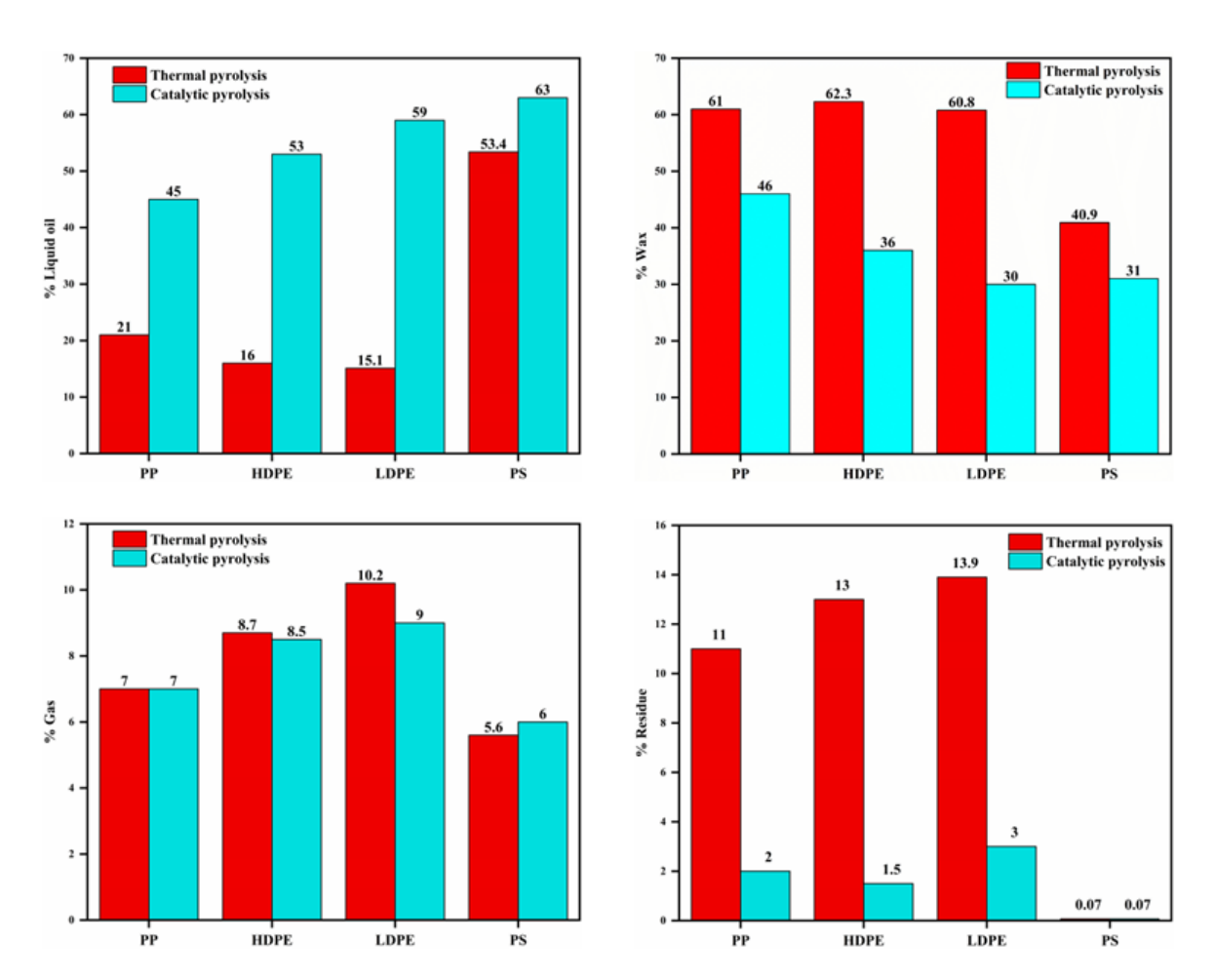


Fig. 6.8 Showing the comparative analysis of percentage yield (by weight) of the liquid oil, wax, gas, and residue in catalytic and thermal pyrolysis of different plastic wastes.

The liquid oil obtained had comparable viscosity and higher heating values (HHV) comparable with

that of the commercial fuels. 2.19, 5.23, 3.25, and 1.08 (mPa·s) are the viscosities and 35.15, 47.23, 41.25, and 33.15 (MJ/Kg) are the HHV of oil obtained from PP, HDPE, LDPE, and PS respectively. The HDPE oil had the highest viscosity and HHV value, validating the elemental composition. The composition of liquid oil had mixture of aromatic compounds, olefins, paraffins, aldehyde compounds, ketones. Table 6.2 shows a few components present in oil obtained from different plastic wastes.

Table 6.2 Different compounds constituting the composition of PP oil, HDPE oil, LDPE oil, and PS oil.

| | | HDPE oil | | LDPE oil | | PP oil | | |
|---------------------------|--------------------------------|---------------------------|----------|----------------------|----------|-------------------|-----------|--|
| Compound name | Chemical | Compound name | Chemical | Compound name | Chemical | Compound name | Chemical | |
| | Formula | | Formula | | Formula | | Formula | |
| Toluene | C_7H_8 | 1,3,5,7-Cyclooctatetraene | C8H8 | 2-Pentanone | C6H12O2 | Toluene | C7H8 | |
| | CII | | | | | 2,4-Dimethyl-1- | C7H14 | |
| Ethylbenzene | C_8H_{10} | 10-Methyl-octadecene | C19H38 | 1,13-Tetradecadiene | C14H26 | heptene | C/H14 | |
| 1,3,5,7 Cyclooctatetraene | C_8H_8 | 1-Decene | C10H20 | 1,15-Pentadecanediol | C15H32O2 | p-Xylene | C8H10 | |
| | $C_{10}H_{8}$ | | | 1,3,5,7- | | 1,3,5,7- | Collo | |
| Naphthalene | | 1-Docosene | C22H44 | Cyclooctatetraene | C8H8 | Cyclooctatetraene | C8H8 | |
| Biphenyl | $C_{14}H_{14}$ | 1-Eicosanol | C20H42O | 11-Hexadecen-1-ol | C16H32O | Benzene | C9H10 | |
| Diphenylmethane | (C_6H_5) ₂ CH_2 | 1-Heptadecene | C17H34 | 1-Decene | C10H20 | Phenprobamate | C10H13NO2 | |
| Benzene | C_6H_6 | 1-Tetracosene | C24H48 | 1-Nonadecene | C19H38 | Carbonic acid | C23H44O3 | |
| 1,2diphenylcyclopropane | $C_{15}H_{14}$ | 1-Tetradecene | C12H10 | 1-Nonene | C9H18 | 1H-Indene | С9Н8 | |
| 1H-Indene,2-phenyl- | $C_{15}H_{12}$ | 1-Tridecanethiol | C13H28S | 1-Pentadecene | C15H30 | Azulene | C10H8 | |
| Naphthalene,1-phenyl- | $C_{16}H_{12}$ | 1-Tridecene | C13H26 | 1-Tetradecene | C14H28 | Heptanol | C7H16O | |
| m-Terphenyl | $C_{18}H_{14}$ | 3-Methylphenylacetylene | С9Н8 | 1-Tridecene | C13H26 | Naphthalene | C11H10 | |
| Cyclohexane | C_6H_{12} | 5-Eicosene | C20H40 | 1-Undecene | C11H22 | 1-Tetradecene | C14H28 | |
| Hexadecane | $C_{17}H_{36}$ | Acenaphthylene | C12H8 | Azulene | C10H8 | Acenaphthylene | C12H8 | |
| n-Heptadecanol-1 | $C_{17}H_{36}O$ | Azulene | C10H8 | Butanoic acid | C13H18O2 | 1,3,5-Triazine | C3H3N3 | |
| Heptadecane | $C_{17}H_{36}$ | Benzene, (1-methyl) | C10H10 | Carbonic acid | C23H44O3 | 1-Decanol | C10H22O | |
| 1,19-Eicosadiene | $C_{20}H_{38}$ | Benzene | C9H10 | Cyclododecane | C14H28 | Phenanthrene | C10H14 | |

The FT-IR and GCMS results confirm the presence of the characteristic functional groups and composition of liquid oil. Fig. 6.9 (a) and (b) shows the FT-IR and GCMS results of the liquid oil. From fig. 6.9(a), the FT-IR spectrum of PP oil displayed the presence of alkanes (C–H stretching) at 3019.015 cm⁻¹, carbon dioxide (O=C=O stretching) at 2315 cm⁻¹, aromatic compounds (C-H bending) at 2042 cm⁻¹ and alkene disubstituted (cis) (C=C bending) at 662 cm⁻¹ wavenumbers respectively. The HDPE oil was mainly comprised of the alkanes (C–H stretching) at 2922 and 2853 cm⁻¹, alkanes (C–H bending) at 1467 cm⁻¹ and 1,2,3 trisubstituted (C-H bending) at 907 cm⁻¹ wavenumbers respectively.

Similarly, LDPE oils were dominated with alkanes (C–H stretching) at 2921.62 and 2854.13 cm⁻¹, alkanes (C–H bending) at 1469 cm⁻¹ and 1,2,3 trisubstituted (C-H bending) such as esters, ethers, carboxylic acids, and alcohols at 910 cm⁻¹ wavenumbers respectively. The PS oil was comprised of alkane (C-H stretching), thiol (S-H stretching), amine (N-H bending), carboxylic acid (O-H bending), ester (C=O stretching) and alkene (monosubstituted) (C=O bending) at 2861, 2590, 1585, 1420, 1151 and 991 cm⁻¹ wavenumbers respectively. The results were found consistent when compared with the results of GC-MS.

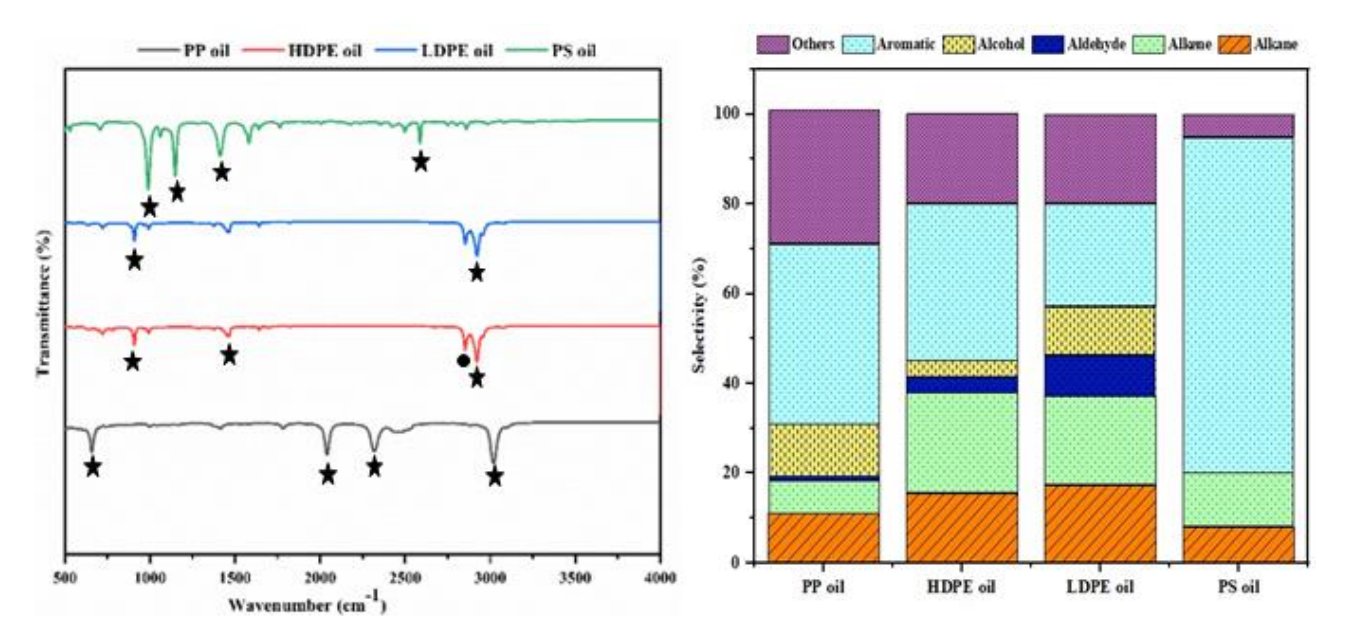


Figure 6.9 (a) FT-IR of liquid oil and (b) liquid oil composition obtained from GCMS results

Fig. 6.9(b) depicts the hydrocarbon distribution in different liquid oil products obtained from GC-MS results. Since the main objective of this study was to enhance the selectivity of aromatic components in the obtained liquid oil, therefore the GC-MS result confirmed the increase in the aromatic components. The aromatic components in PP, HDPE, LDPE, and PS oil were 40%, 35%, 23% and 75% respectively. The maximum aromatic components were obtained in the PS oil. Alkane and alkene components followed the aromatics in all the obtained oils. The liquid oils obtained from PP, HDPE, LDPE, and PS contained 10.98%, 15.54%, 17.28%, and 7.97% of alkanes and 7.06%, 22.48%, 20%, and 12.01% of alkenes respectively. Alcohols constituted a good share in the PP, HDPE, and LDPE oil of 11.93%, 3.56% and 10.82% respectively. Another main constituent in liquid oils from PP, HDPE, and LDPE were aldehydes. 1.04%, 3.54% and 9.13% of aldehydes constituted the PP, HDPE, and LDPE oil respectively. However, the PS oil was devoid of alcohols and aldehydes. Other groups

such as amines, carboxylic acids, ketones, etc. in trace amounts were present in all the liquid oils. Hence the performance of the synthesized catalyst had shown comparable product yield as compared with that of the similar commercially available catalysts. Table 6.3 lists a few results of the similar catalysts used by several researchers in their studies.

Table 6.3 Comparison of product distribution obtained from catalytic cracking of waste plastics

| Catalyst | Plastics | Operating conditions | Product | t distrib | Investigation | | |
|--------------|------------------|---------------------------|------------|-----------|---------------|-----------------------|--|
| | | | %) | | | | |
| | | | Liquid | Gas | Residue | | |
| HZSM-5 | LDPE | 425 °C, Fixed-bed tubular | 15- 25 | - | - | Uemichi et al., | |
| | | flow reactor | | | | (1998) | |
| HZSM-5 | HDPE | 500 °C, conical spouted | 48- 58 | - | - | Elordi et al., (2009) | |
| | | bed reactor | | | | | |
| HZSM-5 | PE | 460 °C, 30 min retention | 55 | 40 | 5 | de Marco I et al., | |
| | | time | | | | (2009) | |
| ZSM-5 | PE, PP, PS, PET, | 450 °C | 56.9 | 40.4 | 3.2 | Lopez et al. (2012) | |
| | PVC | | | | | | |
| ZSM-5 | HDPE | 500 °C | 83.5 | - | - | Ratnasari D K et al., | |
| | | | | | | (2017) | |
| Hierarchical | PP, HDPE, | 400 - 430 °C | 45- 63 | 6-9 | 2- 0.07 | Present study | |
| ZSM-5 | LDPE, and PS | | | | | | |

6.3 Conclusion

The present work investigated the performance of the synthesized hierarchical ZSM-5 catalyst in the conversion of real-world plastic wastes (PP, HDPE, LDPE, and PS) into higher quality fuel grade hydrocarbons via catalytic pyrolysis in a fixed-bed reactor. Although, zeolites are the most widely used and suitable catalysts in the catalytic pyrolysis of the plastic waste due their intrinsic properties like thermal stability at higher temperatures, flexible frameworks, uniform and small pore size and providing higher active surface area but these smaller pores create diffusion limitation for macromolecules. Therefore, in our study, we attempted to incorporate dual porosity i.e. presence of micropores and mesopores in the framework of the catalyst. To achieve this, hierarchical ZSM-5 catalyst was successfully synthesized using 10% TPAOH template, characterized and employed in the

ZSM-5 catalyst had favoured selective and remarkable increase in the yield of fuel grade liquid oil from different plastic wastes at lower reaction temperatures in the range of 400- 430 °C. The higher surface area, pore volume and the dual porosity of the catalyst helped in cracking and diffusion of the larger molecules through their active sites. Also, the catalyst provided a lower energy pathway with lower activation energy for the catalytic pyrolysis process resulting in lower reaction temperatures as compared with thermal pyrolysis process. A remarkable increase of 24%, 37%, 43.9% and 9.6%, in the percentage yield of liquid oil was obtained from catalytic pyrolysis of PP, HDPE, LDPE, and PS wastes respectively as compared with that of the thermal pyrolysis. The lower reaction temperature and higher liquid oil yield validated the catalytic efficiency of the catalyst. Also, the obtained liquid oils had comparable fuel properties like viscosity and HHV with that of commercial fuels. Therefore, the obtained liquid oils can be an appealing and promising alternative to commercial fuels after undergoing further purification processes. The use of ZSM-5 had produced high quality liquid oil with more selectivity towards aromatic compounds and C₆-C₂₀ hydrocarbons. Therefore, catalytic pyrolysis provides a more desired route to obtain higher liquid oil production at lower temperatures.

6.4 References:

- [1] R. Chércoles Asensio, M. San Andrés Moya, J. M. De La Roja, and M. Gómez, "Analytical characterization of polymers used in conservation and restoration by ATR-FTIR spectroscopy," *Anal. Bioanal. Chem.*, vol. 395, no. 7, pp. 2081–2096, 2009, doi: 10.1007/s00216-009-3201-2.
- [2] A. Tennakoon *et al.*, "Catalytic upcycling of high-density polyethylene via a processive mechanism," *Nat. Catal.*, vol. 3, no. 11, pp. 893–901, 2020, doi: 10.1038/s41929-020-00519-4.
- [3] E. J. Guidelli, A. P. Ramos, M. E. D. Zaniquelli, and O. Baffa, "Green synthesis of colloidal silver nanoparticles using natural rubber latex extracted from Hevea brasiliensis," *Spectrochim. Acta Part A Mol. Biomol. Spectrosc.*, vol. 82, no. 1, pp. 140–145, 2011, doi: 10.1016/j.saa.2011.07.024.
- [4] I. Noda, A. E. Dowrey, C. Marcott, J. L. Haynes, and C. Marcott, "Group Frequency Assignments for Major Infrared Bands Observed in Common Synthetic Polymers BT Physical Properties of Polymers Handbook," *New York*, pp. 395–406, 2007, [Online]. Available: https://doi.org/10.1007/978-0-387-69002-5_22.
- [5] B. Smith, "Infrared spectral interpretation: A systematic approach," *Infrared Spectr. Interpret. A Syst. Approach*, pp. 1–304, 2018, doi: 10.1201/9780203750841.
- [6] B. C. Smith, "The Infrared Spectra of Polymers II: Polyethylene," *Spectroscopy*, pp. 24–29, 2021, doi: 10.56530/spectroscopy.xp7081p7.
- [7] M. R. Jung *et al.*, "Validation of ATR FT-IR to identify polymers of plastic marine debris, including those ingested by marine organisms," *Mar. Pollut. Bull.*, vol. 127, no. November 2017, pp. 704–716, 2018, doi: 10.1016/j.marpolbul.2017.12.061.
- [8] P. Das and P. Tiwari, "Resources, Conservation & Recycling Valorization of packaging plastic waste by slow pyrolysis," *Resour. Conserv. Recycl.*, vol. 128, no. September 2017, pp. 69–77, 2018, doi: 10.1016/j.resconrec.2017.09.025.
- [9] D. Yu, H. Hui, G. Ding, N. Dong, and S. Li, "Enhancement of aromatics production from catalytic co-pyrolysis of walnut shell and LDPE via a two-step approach," *J. Anal. Appl. Pyrolysis*, vol. 157, no. April, p. 105216, 2021, doi: 10.1016/j.jaap.2021.105216.

- [10] H. M. Abdel-Hamid, "Effect of electron beam irradiation on polypropylene films-dielectric and FT-IR studies," *Solid. State. Electron.*, vol. 49, no. 7, pp. 1163–1167, 2005, doi: 10.1016/j.sse.2005.03.025.
- [11] D. Yu, "Composite Pyrolysis of Biomass and Plastic for High-quality Fuel Oil over HZSM-5," *Am. J. Chem. Eng.*, vol. 9, no. 2, p. 39, 2021, doi: 10.11648/j.ajche.20210902.12.
- [12] H. Der Wu, S. C. Wu, I. Der Wu, and F. C. Chang, "Novel determination of the crystallinity of syndiotactic polystyrene using FTIR spectrum," *Polymer (Guildf)*., vol. 42, no. 10, pp. 4719–4725, 2001, doi: 10.1016/S0032-3861(00)00849-1.
- [13] Y. K. Krisnandi, B. A. P. Putra, M. Bahtiar, Zahara, I. Abdullah, and R. F. Howe, "Partial Oxidation of Methane to Methanol over Heterogeneous Catalyst Co/ZSM-5," *Procedia Chem.*, vol. 14, pp. 508–515, 2015, doi:10.1016/j.proche.2015.03.068.
- [14] H. Feng, C. Li, and H. Shan, "In-situ synthesis and catalytic activity of ZSM-5 zeolite," *Appl. Clay Sci.*, vol. 42, no. 3–4, pp. 439–445, 2009, doi: 10.1016/j.clay.2008.05.004.
- [15] R. M. Mohamed, H. M. Aly, M. F. El-Shahat, and I. A. Ibrahim, "Effect of the silica sources on the crystallinity of nanosized ZSM-5 zeolite," *Microporous Mesoporous Mater.*, vol. 79, no. 1–3, pp. 7–12, 2005, doi: 10.1016/j.micromeso.2004.10.031.
- T. Xue, L. Chen, Y. M. Wang, and M. Y. He, "Seed-induced synthesis of mesoporous ZSM-5 aggregates using tetrapropylammonium hydroxide as single template," *Microporous Mesoporous Mater.*, vol. 156, pp. 97–105, 2012, doi: 10.1016/j.micromeso.2012.02.022.
- [17] F. Xu *et al.*, "Rapid tuning of ZSM-5 crystal size by using polyethylene glycol or colloidal silicalite-1 seed," *Microporous Mesoporous Mater.*, vol. 163, pp. 192–200, 2012, doi: 10.1016/j.micromeso.2012.07.030.
- [18] R. Biriaei, "Synthesis of mesoporous ZSM-5 zeolites and their application in furan deoxy ge nation," 2021.
- [19] L. Xu *et al.*, "Synthesis, characterization of hierarchical ZSM-5 zeolite catalyst and its catalytic performance for phenol tert-butylation reaction," *Catal. Commun.*, vol. 9, no. 6, pp. 1272–1276, 2008, doi: 10.1016/j.catcom.2007.11.018.
- [20] N. Ren, J. Bronić, B. Subotić, Y. M. Song, X. C. Lv, and Y. Tang, "Controllable and SDA-free synthesis of sub-micrometer sized zeolite ZSM-5. Part 2: Influence of sodium ions and ageing of the reaction mixture on the chemical composition, crystallinity and particulate

- properties of the products," *Microporous Mesoporous Mater.*, vol. 147, no. 1, pp. 229–241, 2012, doi: 10.1016/j.micromeso.2011.06.022.
- [21] Z. Zahara, W. Wibowo, D. A. Nurani, D. U. C. Rahayu, and H. Haerudin, "Synthesis and Characterization of Hierarchical ZSM-5," vol. 020088, no. 2018, 2023.
- [22] I. M. S. Anekwe *et al.*, "Stability, deactivation and regeneration study of a newly developed HZSM-5 and Ni-doped HZSM-5 zeolite catalysts for ethanol-to-hydrocarbon conversion," *Catal. Commun.*, vol. 186, p. 106802, 2024, doi: 10.1016/j.catcom.2023.106802.
- [23] Anekwe, I. M. S., Oboirien, B., & Isa, Y. M. "Synthesis and characterisation of a novel mesoporous zsm-5 zeolite catalyst for the conversion of bioethanol to aromatics and c5+ hydrocarbons".
- [24] M. Yang *et al.*, "Conversion of lignin into light olefins and aromatics over Fe/ZSM-5 catalytic fast pyrolysis: Significance of Fe contents and temperature," *J. Anal. Appl. Pyrolysis*, vol. 137, no. November 2018, pp. 259–265, 2019, doi: 10.1016/j.jaap.2018.12.003.
- [25] Y. Peng *et al.*, "Fe-ZSM-5 supported palladium nanoparticles as an efficient catalyst for toluene abatement," *Catal. Today*, vol. 332, no. April 2018, pp. 195–200, 2019, doi: 10.1016/j.cattod.2018.05.032.
- [26] G. Reding, T. Mäurer, and B. Kraushaar-Czarnetzki, "Comparing synthesis routes to nano-crystalline zeolite ZSM-5," *Microporous Mesoporous Mater.*, vol. 57, no. 1, pp. 83–92, 2003, doi: 10.1016/S1387-1811(02)00558-9.
- [27] H. Tao *et al.*, "Space-confined synthesis of nanorod oriented-assembled hierarchical MFI zeolite microspheres," *J. Mater. Chem. A*, vol. 1, no. 44, pp. 13821–13827, 2013, doi: 10.1039/c3ta12989f.
- [28] R. Sabarish and G. Unnikrishnan, "A novel anionic surfactant as template for the development of hierarchical ZSM-5 zeolite and its catalytic performance," *J. Porous Mater.*, vol. 27, no. 3, pp. 691–700, 2020, doi: 10.1007/s10934-019-00852-5.
- [29] G. Liu, F. Xiangli, W. Wei, S. Liu, and W. Jin, "Improved performance of PDMS/ceramic composite pervaporation membranes by ZSM-5 homogeneously dispersed in PDMS via a surface graft/coating approach," *Chem. Eng. J.*, vol. 174, no. 2–3, pp. 495–503, 2011, doi: 10.1016/j.cej.2011.06.004.

- [30] A. H. Mukaromah, T. Ariyadil, I. H. Azizah, and Mifbakhuddin, "Characterization of ZSM-5 Zeolite Membrane Synthesis Results with 304-200 Gauze Supports with Pretreatment variations," vol. 410, no. Imcete 2019, pp. 272–276, 2020, doi: 10.2991/assehr.k.200303.066.
- [31] S. M. Al-Salem, A. Antelava, A. Constantinou, G. Manos, and A. Dutta, "A review on thermal and catalytic pyrolysis of plastic solid waste (PSW)," *J. Environ. Manage.*, vol. 197, no. 1408, pp. 177–198, 2017, doi: 10.1016/j.jenvman.2017.03.084.
- [32] M. Calero, R. R. Solís, M. J. Muñoz-Batista, A. Pérez, G. Blázquez, and M. Ángeles Martín-Lara, "Oil and gas production from the pyrolytic transformation of recycled plastic waste: An integral study by polymer families," *Chem. Eng. Sci.*, vol. 271, p. 118569, 2023, doi: 10.1016/j.ces.2023.118569.
- [33] U. Dwivedi, S. N. Naik, and K. K. Pant, "High quality liquid fuel production from waste plastics via two-step cracking route in a bottom-up approach using bi-functional Fe/HZSM-5 catalyst," *Waste Manag.*, vol. 132, no. July, pp. 151–161, 2021, doi: 10.1016/j.wasman.2021.07.024.
- [34] T. Maqsood, J. Dai, Y. Zhang, M. Guang, and B. Li, "Pyrolysis of plastic species: A review of resources and products," *J. Anal. Appl. Pyrolysis*, vol. 159, no. August, p. 105295, 2021, doi: 10.1016/j.jaap.2021.105295.
- [35] I. Barbarias, G. Lopez, M. Artetxe, A. Arregi, J. Bilbao, and M. Olazar, "Valorisation of different waste plastics by pyrolysis and in-line catalytic steam reforming for hydrogen production," *Energy Convers. Manag.*, vol. 156, no. November 2017, pp. 575–584, 2018, doi: 10.1016/j.enconman.2017.11.048.
- [36] K. Pyra, K. A. Tarach, and K. Góra-Marek, "Towards a greater olefin share in polypropylene cracking Amorphous mesoporous aluminosilicate competes with zeolites," *Appl. Catal. B Environ.*, vol. 297, no. May, 2021, doi: 10.1016/j.apcatb.2021.120408.
- [37] M. Rehan *et al.*, "Effect of zeolite catalysts on pyrolysis liquid oil," *Int. Biodeterior*. *Biodegrad.*, vol. 119, pp. 162–175, 2017, doi: 10.1016/j.ibiod.2016.11.015.
- [38] Krisnandi, Y. K., Nurani, D. A., Agnes, A., Pertiwi, R., Antra, N. F., Anggraeni, A. R., ... & Howe, R. F. (2019). Hierarchical MnOx/ZSM-5 as heterogeneous catalysts in conversion of delignified rice husk to levulinic acid. *Indonesian Journal of Chemistry*.
- [39] Elordi G, Olazar M, Lopez G, Amutio M, Artetxe M, Aguado R, Bilbao J.Catalytic

- pyrolysis of HDPE in continuous mode over zeolite catalysts in a conical spouted bed reactor .J Anal Appl Pyrolysis 2009; 85(1-2): 345-51.
- [40] Uemichi Y, Nakamura J, Itoh T, Sugioka M, Garforth A A, Dwyer J. Conversion of polyethylene into gasoline-range fuels by two-stage catalytic degradation using silica–alumina and HZSM-5 zeolite. Ind Eng Chem Res 1998; 38(2): 385–90.
- [41] de Marco I, Caballero B M, López A, Laresgoiti M F, Torres A, Chomón M J. Pyrolysis of the rejects of a waste packaging separation and classification plant. J Anal Appl Pyrolysis 2009; 85: 384–91.
- [42] Ratnasari DK, Nahil MA, Williams PT. Catalytic pyrolysis of waste plastics using staged catalysis for production of gasoline range hydrocarbon oils. J Anal Appl Pyrolysis 2017;124:631–7

7.1 Conclusions

Plastic is a cheap, petro-derived, and hydrocarbon rich source of energy. Managing and minimizing the huge heaps of plastic waste has been one of the most critical problems for environmentalists and researchers. Pyrolysis technology outdoes all the plastic waste management techniques and appears to be the most promising technique for converting plastic waste into fuel, platform chemicals and energy rich resources. Plastics mostly being synthetic polymers possess higher degree of heterogeneity in their chemical composition. This nature of plastics contributes to the complexity of the pyrolytic behavior. Therefore, to understand the kinetics of the pyrolysis process of the real-world plastic waste, a comprehensive study should be done by considering each of the significant parameters such as; process and operating conditions as well as physicochemical properties. Hence, it is very important to perceive the effect of each parameter on pyrolytic behavior of the real-world plastic waste as it influences the desired product distribution greatly. Although the thermal pyrolysis process successfully converts the real-world plastic waste into fuel grade liquid oil at optimum operating parameters, but the catalytic pyrolysis process provides a much lower energy route to obtain better yield of the desired products. In this study, the real-world plastic wastes were provided with heat treatment at a rate of 15 °Cmin⁻¹ to attain a temperature range of 450-480 °C in a fixed-bed reactor for achieving desired product distribution via slow thermal pyrolysis process. It was observed that slow thermal pyrolysis mode helped in the effective conversion of real-world plastic waste into considerable yield of aromatic rich liquid oil and wax without the use of any catalyst. Hence, the significance of reactor dimensions in attaining the proper temperature distribution within the reactor was evident in this work. The obtained liquid oil was composed of aromatics and had comparable viscosity and HHV values with that of diesel and kerosene oil.

The kinetic study was done to get an insight into the complexity of the plastic pyrolysis process. Therefore, different plastic wastes HDPE, LDPE, PP, and PS were investigated using thermogravimetric analysis. It was observed that all the plastic wastes followed a similar degradation trend irrespective of their composition heterogeneity. However, there was a remarkable difference in the trend of utilizing the activation energy in each of the plastic waste. Effective kinetic modelling was studied to evaluate the kinetic triplets by using five isoconversional methods i.e., OFW, KAS, Starink,

Boswell and Tang and two model fitting methods i.e., Coats Redfern and Criado method.

Further, a hierarchical ZSM-5 catalyst having dual porosity i.e., mesopore and micropore, in its framework was synthesized using single organic template to study the effect of catalyst in the conversion of real-world plastic waste into aromatic rich fuel grade liquid oil. The same reactor set-up was used for the experiments, and it was observed that even at slower heating rates of the pyrolysis the catalytic pyrolysis further reduced the required reaction temperature for the effective plastic cracking. Thereby providing an alternate lower energy route for achieving higher selectivity and yield of the desired product. The dual porosity nature of the catalyst enhanced the selective product distribution and lowered the reaction temperature to 400-430 °C in comparison with 450-480 °C of the thermal pyrolysis. A remarkable increase of 24%, 37%, 43.9% and 9.6%, in the percentage yield of the liquid oil obtained from catalytic pyrolysis of PP, HDPE, LDPE, and PS wastes respectively was obtained as compared with that obtained from the thermal pyrolysis. The fuel properties of the liquid oils were also comparable and leads to a positive direction towards providing a sustainable alternative for fossil fuels.

7.2 Recommendation for future work

Based on the investigations done in the present work, following recommendations are provided for the future work:

- Since, the size of the raw material plays a very crucial role in the pyrolysis process, therefore
 achieving the uniform temperature distribution inside the fixed-bed reactor becomes very
 challenging. Hence, pyrolysis process in a fluidized-bed reactor can provide more insight into
 various operating parameters and product distribution.
- The prospect of combined approach of employing computational methods based on machine learning cab be explored to study the kinetic behavior of plastic pyrolysis process to overcome this complexity.
- MOFs can be explored for performing catalytic pyrolysis process of plastic wastes for even more selective product distribution.
- The possibilities of obtaining CNTs from the residues obtained during the process can be explored.
- For scaling up of the process, a pilot plant study and its techno-economic assessment can

provide essential insights into the various challenges and adaptations required to be addressed at industrial scale.

Addressing these research gaps can further provide significant observations and contribute in advancing and development of more reliable and effective the plastic pyrolysis process, which can convert the plastic waste into energy resource.

List of Publications

Journal Publications

❖ Subhashini & Mondal, T. (2023). "Experimental investigation on slow thermal pyrolysis of real-world plastic wastes in a fixed bed reactor to obtain aromatic rich fuel grade liquid oil." *Journal of Environmental Management*, 344, 118680.

DOI: 10.1016/j.jenvman.2023.118680

❖ Subhashini & T. Mondal, "Probing the influence of synthesized hierarchical ZSM-5 catalyst in ex-situ catalytic conversion of real-world plastic waste into aromatic rich liquid oil." *Journal of the Energy Institute (Elsevier)*, 117, 101853.

DOI: doi.org/10.1016/j.joei.2024.101853

- ❖ Subhashini & T. Mondal, "Potential deviation in kinetics and degradation mechanism of real-world plastic waste thermal pyrolysis due to their composition heterogeneity."

 Canadian Journal of Chemical Engineering (Under review)
- ❖ Subhashini & T. Mondal, "Thermal pyrolysis of plastic waste into fuel." ACS Books (Under review)

Conference presentation

- ❖ Poster presentation entitled "Catalytic pyrolysis of single-use plastic waste over hierarchical zeolite to obtain fuel grade hydrocarbons" at 15th European Congress on Catalysis (EUROPA CAT 2023) Prague, Czeck Republic, (27th Aug − 1st Sept 2023).
- ❖ An oral presentation entitled "Kinetic study of thermal pyrolysis of real-world plastic waste" at 4th International Conference on Waste Management (RECYCLE 2023) IIT Guwahati, (18th 19th May 2023).

Awarded "Best Paper Award"

- ❖ An oral presentation entitled "Catalytic pyrolysis of plastic waste over synthesized HZSM-5 to obtain fuel grade hydrocarbons" at 7th International Conference on Sustainable Energy and Environmental Challenges (SEEC 2022) IIT BHU, Varanasi, (16th − 18th December 2022)
- ❖ An oral presentation entitled "Conversion of plastic waste into gasoline range hydrocarbons using synthetic zeolite catalyst" at International Conference on Reaction Engineering (ICRE 2021) NIT Raipur, (07th − 08th May 2021).

Biodata

Subhashini

Education:

Master of Engineering: Chemical Engineering from Dr. SSB UICET, Panjab University, Chandigarh, Punjab, India (2017). CGPA: 8.2/10

Bachelor of Engineering: Chemical Engineering from Sant Longowal Institute of Engineering and Technology Sangrur, Punjab, India (2015). CGPA: 8.75/10

Diploma of Engineering: Chemical Engineering Sant Longowal Institute of Engineering and Technology, Sangrur, Punjab, India (2012). CGPA: 8.9/10

Work experience:

Assistant Professor (Adhoc): Chemical Engineering, DAV University Jalandhar, Punjab, India (September 2018- January 2018)

Research Intern: Sant Longowal Institute of Engineering and Technology, Sangrur, Punjab, India (January 2018- June 2018)

Research interest:

- Plastic waste management
- Pyrolysis
- ► Heterogeneous catalysis
- Material synthesis
- > Waste to energy

Technical skills:

Handling and analysing the data using the following sophisticated analytical instruments:

- > FTIR with ATR assembly
- XRD (room temperature and high temperature with inert and ambient atmosphere)
- > RAMAN Spectroscopy
- > TGA

Softwares: Origin, Xpert-plus highscore, DWSIM, MS Office etc.

AWARDS / HONOURS / Memberships:

- Awarded as Best Paper Presentation in "4th International Conference on Waste Management (RECYCLE 2023)."
- Won best player of the tournament and 1st prize for Table Tennis (women) in "IYSC 2022".
- ➤ Won 1st prize in Badminton (Women) in "IYSC 2021", "IYSC 2019" & "AAROHAN 2019".